THE NATIONAL ACADEMIES PRESS

Integral Steel Box-Beam Pier Caps

BUY THIS BOOK

FIND RELATED TITLES

AUTHORS

L F Greimann; D Davis; R E Abendroth; S Sritharan; W G Wassef; J R Vander Werff; J Redmond; Transportation Research Board

NCHRP REPORT 527

Integral Steel Box-Beam Pier Caps

WAGDY G. WASSEF
DUSTIN DAVIS
Modjeski and Masters, Inc.
Harrisburg, PA

AND

SRI SRITHARAN
JUSTIN R. VANDER WERFF
ROBERT E. ABENDROTH
JULI REDMOND
LOWELL F. GREIMANN
Iowa State University
Ames, IA

TRANSPORTATION RESEARCH BOARD

WASHINGTON, D.C.
2004
www.TRB.org

NATIONAL COOPERATIVE HIGHWAY RESEARCH PROGRAM

Systematic, well-designed research provides the most effective approach to the solution of many problems facing highway administrators and engineers. Often, highway problems are of local interest and can best be studied by highway departments individually or in cooperation with their state universities and others. However, the accelerating growth of highway transportation develops increasingly complex problems of wide interest to highway authorities. These problems are best studied through a coordinated program of cooperative research.

In recognition of these needs, the highway administrators of the American Association of State Highway and Transportation Officials initiated in 1962 an objective national highway research program employing modern scientific techniques. This program is supported on a continuing basis by funds from participating member states of the Association and it receives the full cooperation and support of the Federal Highway Administration, United States Department of Transportation.

The Transportation Research Board of the National Academies was requested by the Association to administer the research program because of the Board's recognized objectivity and understanding of modern research practices. The Board is uniquely suited for this purpose as it maintains an extensive committee structure from which authorities on any highway transportation subject may be drawn; it possesses avenues of communications and cooperation with federal, state and local governmental agencies, universities, and industry; its relationship to the National Research Council is an insurance of objectivity; it maintains a full-time research correlation staff of specialists in highway transportation matters to bring the findings of research directly to those who are in a position to use them.

The program is developed on the basis of research needs identified by chief administrators of the highway and transportation departments and by committees of AASHTO. Each year, specific areas of research needs to be included in the program are proposed to the National Research Council and the Board by the American Association of State Highway and Transportation Officials. Research projects to fulfill these needs are defined by the Board, and qualified research agencies are selected from those that have submitted proposals. Administration and surveillance of research contracts are the responsibilities of the National Research Council and the Transportation Research Board.

The needs for highway research are many, and the National Cooperative Highway Research Program can make significant contributions to the solution of highway transportation problems of mutual concern to many responsible groups. The program, however, is intended to complement rather than to substitute for or duplicate other highway research programs.

Note: The Transportation Research Board of the National Academies, the National Research Council, the Federal Highway Administration, the American Association of State Highway and Transportation Officials, and the individual states participating in the National Cooperative Highway Research Program do not endorse products or manufacturers. Trade or manufacturers' names appear herein solely because they are considered essential to the object of this report.

NOTICE

The project that is the subject of this report was a part of the National Cooperative Highway Research Program conducted by the Transportation Research Board with the approval of the Governing Board of the National Research Council. Such approval reflects the Governing Board's judgment that the program concerned is of national importance and appropriate with respect to both the purposes and resources of the National Research Council.

The members of the technical committee selected to monitor this project and to review this report were chosen for recognized scholarly competence and with due consideration for the balance of disciplines appropriate to the project. The opinions and conclusions expressed or implied are those of the research agency that performed the research, and, while they have been accepted as appropriate by the technical committee, they are not necessarily those of the Transportation Research Board, the National Research Council, the American Association of State Highway and Transportation Officials, or the Federal Highway Administration, U.S. Department of Transportation.

Each report is reviewed and accepted for publication by the technical committee according to procedures established and monitored by the Transportation Research Board Executive Committee and the Governing Board of the National Research Council.

THE NATIONAL ACADEMIES
Advisers to the Nation on Science, Engineering, and Medicine

The **National Academy of Sciences** is a private, nonprofit, self-perpetuating society of distinguished scholars engaged in scientific and engineering research, dedicated to the furtherance of science and technology and to their use for the general welfare. On the authority of the charter granted to it by the Congress in 1863, the Academy has a mandate that requires it to advise the federal government on scientific and technical matters. Dr. Bruce M. Alberts is president of the National Academy of Sciences.

The **National Academy of Engineering** was established in 1964, under the charter of the National Academy of Sciences, as a parallel organization of outstanding engineers. It is autonomous in its administration and in the selection of its members, sharing with the National Academy of Sciences the responsibility for advising the federal government. The National Academy of Engineering also sponsors engineering programs aimed at meeting national needs, encourages education and research, and recognizes the superior achievements of engineers. Dr. William A. Wulf is president of the National Academy of Engineering.

The **Institute of Medicine** was established in 1970 by the National Academy of Sciences to secure the services of eminent members of appropriate professions in the examination of policy matters pertaining to the health of the public. The Institute acts under the responsibility given to the National Academy of Sciences by its congressional charter to be an adviser to the federal government and, on its own initiative, to identify issues of medical care, research, and education. Dr. Harvey V. Fineberg is president of the Institute of Medicine.

The **National Research Council** was organized by the National Academy of Sciences in 1916 to associate the broad community of science and technology with the Academy's purposes of furthering knowledge and advising the federal government. Functioning in accordance with general policies determined by the Academy, the Council has become the principal operating agency of both the National Academy of Sciences and the National Academy of Engineering in providing services to the government, the public, and the scientific and engineering communities. The Council is administered jointly by both the Academies and the Institute of Medicine. Dr. Bruce M. Alberts and Dr. William A. Wulf are chair and vice chair, respectively, of the National Research Council.

The **Transportation Research Board** is a division of the National Research Council, which serves the National Academy of Sciences and the National Academy of Engineering. The Board's mission is to promote innovation and progress in transportation through research. In an objective and interdisciplinary setting, the Board facilitates the sharing of information on transportation practice and policy by researchers and practitioners; stimulates research and offers research management services that promote technical excellence; provides expert advice on transportation policy and programs; and disseminates research results broadly and encourages their implementation. The Board's varied activities annually engage more than 5,000 engineers, scientists, and other transportation researchers and practitioners from the public and private sectors and academia, all of whom contribute their expertise in the public interest. The program is supported by state transportation departments, federal agencies including the component administrations of the U.S. Department of Transportation, and other organizations and individuals interested in the development of transportation. **www.TRB.org**

www.national-academies.org

FOREWORD

By David B. Beal
Staff Officer
Transportation Research
Board

This report contains the findings of research to develop recommended details, design methodologies, and specifications for integral connections of steel superstructures to concrete intermediate piers. An example illustrating the design of the connection of the cap beam to the girders and column is also included. The material in this report will be of immediate interest to bridge designers.

An integral connection provides some degree of continuity between the substructure and adjacent superstructure spans. Simple-span girders made integral with the concrete substructure provide continuity for live load and may reduce fabrication and erection costs. Continuous girders made integral with the concrete substructure can enhance seismic performance and increase underclearance.

Steel highway bridges have traditionally been designed as two separate systems: the substructure and the superstructure. As such, the connection between the two has typically relied on a system consisting of anchor bolts and bearings. Although such systems simplify the design process by uncoupling the computations related to the substructure and superstructure, there are cost, weight, and performance disadvantages.

A composite steel girder bridge superstructure weighs substantially less than a concrete superstructure. This reduction of mass in the superstructure reduces the bridge's seismic susceptibility. Nevertheless, the mass of large concrete bent caps or hammerhead piers used to support the superstructure can offset the reduced weight of the steel. Integral construction eliminates this mass, increases clearance, and provides improved aesthetics.

In many cases, concrete bridge superstructures are constructed integrally with the substructure. Thus, the entire structure is treated as one system to resist loads, and lateral loads are distributed to adjacent piers, resulting in more economical foundations. Similar economies are possible in steel bridges by integrally connecting steel superstructures to concrete substructures. To gain these potential advantages, bridge engineers need design guidance based on the best information currently available.

The objective of this project was to develop recommended details, design methodologies, and specifications for integral connections of steel superstructures to concrete substructures. The report's recommendations are based on experimental verification of the effectiveness of the integral connection. Specifications and connection details to achieve the full benefits of continuity are recommended based on the physical testing and analysis.

The research was performed by Modjeski and Masters, Inc., with the assistance of Iowa State University. The report fully documents the research leading to the recommended details and specifications. A detailed design example is included. Accompanying CRP-CD-47 contains detailed information on the laboratory testing program.

CONTENTS

INTEGRAL STEEL BOX-BEAM PIER CAPS

SUMMARY   Conventional I-girder bridge superstructures usually are supported on bearings placed on the bridge substructure. The bearings are designed to support the vertical reaction of the bridge girders and may also be designed to restrain the horizontal movements of the bridge. The bearings are usually detailed to allow the superstructure to rotate at pier locations. The superstructures and substructures of conventional bridges essentially are designed as separate systems.

Unlike conventional bridges, an integral connection between the superstructure and substructure provides some degree of continuity between the two systems, thus enhancing the seismic performance of the structure. In addition, the elevation of the bottom of the integral pier cap may be the same as that of the bottom of girders. This reduces the need to elevate the bridge approaches to provide adequate clearance under the bridge while orienting the pier caps in a direction perpendicular to the girders. This orientation is preferred as it eliminates the problems associated with sharp skew angles.

This report presents the details and results of the work on the use of integral connections for steel I-girder bridge superstructures connected integrally to concrete substructures. This work was conducted under NCHRP Project 12-54.

A questionnaire on past use and performance of integral pier caps was used to study the state of the practice of integral connections. The questionnaire was sent to all AASHTO members, domestic researchers, and domestic and international bridge designers. In addition to the questionnaire, an extensive literature search was performed to identify and review relevant past research.

Analyzing the response to the questionnaire and the results of the literature search allowed the research team to identify the issues related to the design and construction of the integral connections, to identify the connection systems used in the past and the reasons for selecting these systems, and to develop several new systems that were potential candidates for this study. In total, 14 connection configurations were examined.

Selection criteria were developed to determine the most viable systems. The selection criteria were based on the expected economy, constructability, and expected performance of each system. The system selected for final study consists of a steel box-beam pier cap connected integrally with a steel I-girder superstructure and a single-column reinforced concrete pier. The integral connection between the column and the

pier cap was accomplished by extending the column longitudinal reinforcement through holes in the bottom flange of the pier cap into the pier cap compartment directly above the column. This compartment is bounded by the four sides of the box-beam pier cap and two interior diaphragms of the box-beam. The compartment was filled with concrete which transfers the load from the pier cap to the column reinforcement.

Analytical and experimental studies were conducted to validate the selected connection system. A bridge with two equal spans, each 30.5 m (100 ft) long, was selected as the basis for these studies. Throughout this report, this bridge is referred to as "the prototype bridge."

The experimental studies were accomplished by testing two, one-third-scale models of the pier region of the prototype bridge. The two test specimens were similar except that the depth of the girders, and consequently the depth of the pier cap, was deeper in the first specimen than in the second one. The deeper girders of the first specimen allowed the full development of the column longitudinal bars within the depth of the pier cap. The shallower depth of the girders in the second specimen was not sufficient for the full development of the column longitudinal reinforcement within the depth of the pier cap and, thus, mechanical connections were used to provide the required additional anchorage for the column reinforcement. The mechanical connections were provided by threading the ends of the column longitudinal reinforcement and installing nuts embedded in the concrete in the integral connection region.

The analytical studies were conducted on finite element models of both the prototype bridge and the test specimens. The analytical studies of the prototype bridge were used to validate the applicability of some of the existing design provisions, which originally were developed for girders supported on conventional bearings, to girders of structures with integral connections.

The analytical studies on the test specimen computer model were used to determine the anticipated forces acting on different components of the laboratory specimens and to validate the modeling technique by comparing the analytical results with the laboratory results.

Observation from testing of the first test specimen under cyclic loading revealed that the specimen behaved as expected under lateral loading (i.e., a plastic hinge was formed in the column adjacent to the cap beam). The superstructure behaved elastically throughout the entire test, also in accordance with the intent of the design. As expected, flexural cracking of the column occurred at loads below the predicted yield of the column longitudinal reinforcement. Defining the displacement ductility, μ_D, as the ratio between the maximum displacement during a load cycle during the test divided by the displacement required to cause the yield of the column longitudinal reinforcement, concrete spalling at the column-to-cap beam connection began to occur at displacement ductility $\mu_\Delta = 1.5$. At ductility $\mu_\Delta = 4.0$, several column longitudinal bars were visible, with a few showing indications of buckling. At ductility $\mu_\Delta = 6.0$, the three extreme column longitudinal bars on each side of the column fractured. The buckling is believed to have been caused by loss of confinement because of interaction effects between the steel cap beam and concrete column.

The second test specimen also displayed satisfactory seismic performance, exhibiting the formation of a plastic hinge in the column adjacent to the cap beam and showing elastic behavior of the superstructure. Early stages of the test revealed similar behavior to the first test specimen. Increased cracking was observed in the slab as could be expected for the more flexible superstructure in the second specimen. The primary difference in results in the second test specimen was the failure mechanism of the longitudinal bars, which appeared to lose anchorage in the connection region and fractured the mechanical connections.

The test specimens were also tested under low-level loads to simulate service loads. The results from this testing were compared with the results of the analytical model of the pier region to validate the analytical modeling techniques used.

The results of the analytical and experimental studies were used to finalize the details of the integral connections and to develop design methodologies, specifications, commentary, and a detailed design example based on the proposed specifications.

CHAPTER **1**

INTRODUCTION AND RESEARCH APPROACH

1.1 INTRODUCTION

Conventional girder bridge superstructures usually are supported on bearings placed on the bridge substructure. The bearings are designed to support the vertical reaction of the bridge girders and may also be designed to restrain the horizontal movements of the bridge. The bearings are usually detailed to allow the superstructure to rotate at pier locations. The superstructures and substructures of conventional bridges are essentially designed as separate systems.

Unlike conventional bridges, an integral connection between the superstructure and substructure provides some degree of continuity between the two systems. The elevation of the bottom of the integral pier cap may be the same as that of the bottom of girders. Moments, in addition to vertical and horizontal forces, are transferred from the superstructure to the substructure.

In past applications, integral connections of steel bridge structures were typically used on bridges crossing over other highways or railway tracks at sharp skew angles. The use of integral connections allowed the pier cap bottom elevation to be the same as the elevation of the bottom of the girders. This allowed orienting the pier cap in the direction perpendicular to the girders without causing the pier cap to reduce the overhead clearance of the lower highway or railroad. This orientation of the pier cap eliminated the problems associated with orienting the pier cap at a sharp skew, which would be required if a conventional pier cap were used. The use of the integral pier cap also eliminated the need to raise the elevation of the bridge and bridge approaches to maintain underclearance while orienting conventional pier caps perpendicular to the girders. Integral connections were also used to enhance seismic performance of bridge structures. Figure 1 depicts a concrete bridge pier connected integrally to a steel superstructure.

Past research on integral connections was essentially conducted on concrete structures. The use of integral connections on concrete bridges helped in reducing the mass of concrete bridges and, thus, improved their seismic performance.

A composite steel girder bridge superstructure weighs substantially less than a concrete superstructure. This reduction of mass in the superstructure reduces the seismic susceptibility of bridge structures. Nevertheless, steel superstructures placed on top of large concrete drop bent caps or hammerhead piers can result in unnecessary mass, offsetting the ben-

efits from the reduced weight of the steel. Integral construction reduces this mass and, with close attention to detailing, provides improved aesthetics.

This report presents the details and results of the work on the use of integral connections between steel I-girder bridge superstructures and concrete substructures. This work was conducted under NCHRP Project 12-54.

Past use of integral pier connections for steel bridge structures was reviewed to determine the best approach to this investigation. The reasons that led to using integral connections in the past (type of construction, pier configurations, and the performance of integral pier bridges) were documented. In addition, research on integral connections for concrete structures was reviewed and summarized.

Several integral pier cap connections were developed and reviewed by bridge designers and steel bridge fabricators. Concepts for the connections between the girders and the integral pier caps were also developed. The review of the expected performance of different concepts resulted in recommending five connection concepts for further development and detailing. One concept representing I-girder superstructure supported on a box-beam integral pier cap and a reinforced-concrete single-column pier was recommended for detailed analytical and experimental validation.

1.2 PROBLEM STATEMENT
AND RESEARCH OBJECTIVE

The objective of was to develop recommended details, design methodologies, and specifications for integral connections of steel superstructures to concrete substructures. The recommended specifications were to be in a form suitable for consideration by the AASHTO Highway Subcommittee on Bridges and Structures (HSCOBS). The stated objective was further narrowed to exclude integral abutments and only include integral connections between steel superstructures and concrete intermediate piers or bents.

1.3 SCOPE OF THE STUDY

The scope of the study was generally determined by the tasks identified in the RFP as the tasks anticipated to be encompassed by the research. The task description, copied from the RFP, is provided below.

Figure 1.   Concrete pier cap connected integrally to steel I-girder superstructure.

Task 1. Review relevant domestic and foreign practice, performance data, research findings, cost comparisons, and other information related to integral connections. This information shall be assembled from technical literature and from unpublished experiences of engineers, bridge owners, steel suppliers, fabricators, and others. Information on field performance is of particular interest.

Task 2. Identify integral connection concepts that enhance bridge performance and economy.

Task 3. Based on review and assessment of the findings in Task 1 as well as new concepts generated by the research team in Task 2, recommend concepts to be fully developed, validated, and detailed.

Task 4. Prepare a detailed work plan for the remainder of the project that includes a description of the proposed processes for validating the effectiveness of the integral connection concepts. Estimates of the cost to evaluate each concept shall be provided.

Task 5. Submit an interim report to document Tasks 1 through 4 for review by the NCHRP panel.

Task 6. In accordance with the approved work plan, conduct analytical and/or experimental work to validate the integral connections approved by the project panel for further development.

Task 7. Based upon the results of Task 6, further develop and finalize integral connections that will enhance performance, economy, and construction ease.

Task 8. Develop recommended methodologies, specifications, commentary, and design examples.

Task 9. Submit a final report describing the entire research project. Include the recommended methodologies, specifica-

tions with commentary, the design examples, and the recommended integral connection details as appendices.

In addition to the inherent limitations of the study tasks, as the work progressed, other limitations to the scope were dictated by the type of connection and type of substructures selected for further study and by the characteristics of the structures analyzed. The system selected for detailed studies and laboratory testing consists of a straight (non-curved) I-girder superstructure connected rigidly to a steel box-beam pier cap that is, in turn, connected integrally to a reinforced concrete single-column pier. All studies assumed that the column is at mid-width of the bridge and that the bridge is not skewed. Studying this system implies that the following types of structures and structural components were not directly studied:

- Curved structures,
- Multi-column substructures,
- Single-column piers with the column not at mid-width of the bridge,
- Superstructure girders other than I-girders,
- Pier caps other than steel box-beam pier caps, and
- Skewed superstructures.

Throughout the work, engineering judgment was used, to the extent possible, to extrapolate the research results to cover these types of structures that were not directly covered in the study.

1.4 RESEARCH APPROACH

To accomplish the stated objectives of the research and to cover the work on the tasks of the project, the following approach was followed:

- To gather information on past use and performance of integral pier caps, a questionnaire was prepared and was sent to all AASHTO voting and nonvoting members (i.e., DOTs in all states and Canadian provinces, as well as other quasi-governmental authorities such as turnpike authorities). A slightly modified questionnaire was sent to domestic researchers and bridge designers and international bridge designers. The response to the questionnaire was used to study the state of the practice of integral connections.

  In addition to the questionnaire, an extensive literature search was performed to identify and review relevant past research.

- To identify integral connection concepts that are potential candidates for this study, the research team studied the

connection concepts used in the past and developed several other systems. In total, 14 systems were examined.

- Selection criteria were developed to assist in selecting a system for detailed studies. The selection criteria were based on the expected economy, constructability, and expected performance of the 14 systems considered. Several practicing engineers participated in this process and the average of the scores was recorded. The system with the highest score was selected for further study and was approved by the project Technical Panel.
- Analytical and experimental studies were conducted to validate the system approved by the project technical panel for further development. A two-span bridge was selected as the basis for these studies. Throughout this report, this bridge is referred to as "the prototype bridge."

The experimental studies were accomplished by testing two, one-third-scale models of the pier region of the prototype bridge. The specimens were tested under low-level loads to simulate the performance under simulated service conditions and under cyclic loads to simulate performance during seismic events. Load, strain, displacement, and rotation measurements were recorded throughout the tests.

The analytical studies were conducted on finite element models of both the prototype bridge and the test specimens. The analytical studies of the prototype bridge were used to validate the applicability of some of the existing design provisions, which were originally developed for girders supported on conventional bearings, to girders of structures with integral connections. The analytical studies on the test specimen computer model were used to determine the anticipated forces acting on different components of the laboratory specimens and to validate the modeling technique by comparing the analytical results with the laboratory results.

The results of the analytical and experimental studies were used to finalize the details of the integral connections and to develop design methodologies, specifications, commentary, and a detailed design example based on the proposed specifications.

CHAPTER **2**

FINDINGS

2.1 STATE-OF-THE-ART SUMMARY

Two different approaches to collecting data on the state of the art of integral connections were studied. First, the state of practice was studied through the questionnaire on past use of integral connections. Second, the state of research was studied through the literature search. The summary of the results of these studies is presented below. The details of the state of practice and the literature search are presented in Appendixes A and B, respectively (which are included on the accompanying CD-ROM).

2.1.1 State of Practice

The questionnaire on past use of integral connections was sent to all AASHTO voting and nonvoting members (i.e., DOTs in all states and Canadian provinces, and quasi-governmental authorities such as turnpike authorities).

In addition, the questionnaire was slightly modified and sent to domestic researchers and bridge designers and international bridge designers. The modifications were intended to allow the person responding to comment on the performance of bridges he or she did not design but is familiar with, provide contact information on the designer of bridges with integral pier caps, or forward the questionnaire to the bridge designer. The modified questionnaire was sent to 30 domestic bridge designers and 20 international bridge designers in 12 countries (i.e., Japan, France, the United Kingdom, Canada, Switzerland, Denmark, Poland, Portugal, Germany, Austria, Spain, and Egypt).

In addition to the questionnaire, information was solicited from the American Iron and Steel Institute (AISI), the American Institute of Steel Construction (AISC), and the National Steel Bridge Alliance (NSBA). Also, the manufacturers of prestressing systems were asked to provide information on the bridges where their systems were used to post-tension concrete integral pier caps.

In total, 111 copies of the questionnaire were sent out. A total of 67 responses were received. The breakdown of the responses is given in Appendix A (provided on the accompanying CD-ROM). Among the responses, 11 state DOTs indicated past use of integral pier caps. However, two of these responses indicated that the pier caps were integral with the superstructure but were supported on bearings (not integral

with the substructures). Among the responses from domestic practicing engineers, six indicated designing bridges with integral pier caps in the past. Only one of the responses received from abroad indicated past use of integral pier caps.

The analyses of the responses to the questionnaire are provided in Appendix A. The main conclusions from the responses to the questionnaire were as follows:

- The main reason for using integral pier caps in the past has been to increase underclearance and to avoid placing the pier caps at a sharp skew (94 percent of the cases). Enhancing seismic performance was cited in 33 percent of the cases.
- The total number of bridges with integral pier caps reported in the responses is 59 (i.e., 47 bridges reported by state DOTs and 12 bridges reported by domestic practicing engineers; however, some bridges may have been reported in both groups).
- Plate girders were used in the superstructures of most bridges with integral pier caps.
- Most integral pier caps (76 percent) are supported on single-column piers, 8 percent are supported on multi-column piers, and the type of piers was not defined for the remaining bridges.
- Most integral pier caps (90 percent) are made of concrete. The remaining pier caps are made of steel.
- No accurate cost data were available. The respondents estimated that the weight of the steel was decreased by 5 to 10 percent and the cost of fabrication and the cost of erection both increased 5 to 10 percent. However, in one case it was estimated that the use of integral pier caps eliminated the need to raise the approach roadway elevation leading to an estimated savings of $250,000 for each 305 mm (12 in.) difference in elevation.
- In most cases, the forces acting on the superstructure and the substructures were calculated taking into account the frame action between the superstructure and substructure. In a few cases the frame action was ignored in designing the superstructure or in designing both the superstructure and the substructure.
- In general, past performance of integral pier cap bridges appears to be satisfactory. Deck cracking transverse to the girders is the most cited problem. However, it was concluded that this type of cracking does not seem to be

caused by the integral connection as it also has been reported for conventional bridges. Many of the bridges reported in the responses are new bridges and, hence, long-term performance data were not available.

- The difficulties faced during construction of integral pier cap bridges included the congestion of reinforcement at the columns-to-pier-cap joint and the need for a substantial temporary shoring system.

See Appendix A for more detailed analyses of the questionnaire responses.

2.1.2 Summary of Literature Review

A comprehensive literature review was performed as part of the NCHRP 12-54 Project. Over the course of the project, other newer relevant articles and reports were reviewed and added to the documentation.

At the time of the literature study, some critical aspects of the prototype structure to be used in the NCHRP 12-54 Project were not finalized. These included the type of cap beam (i.e., steel versus concrete), type of concrete bent (i.e., single column versus multiple column), and the critical loading direction (i.e., transverse, longitudinal, or both). In fact, information obtained from the literature review was used in deciding that the research of the NCHRP Project 12-54 should focus on the longitudinal direction seismic response of a prototype bridge with a single-column concrete bent and a steel cap beam. Consequently, the literature review generally focused on past research and past use of integral pier bridges in both seismic and non-seismic regions.

Most of the research materials relevant to seismic applications of integral column bridges were found to be based on research sponsored by the California Department of Transportation (Caltrans) following the 1989 Loma Prieta Earthquake. This event demonstrated that integral connections of concrete bridges in California were not sufficiently designed and detailed to permit bridges to experience ductile seismic response. As a result of damage to the cap beam-to-column integral connections, several bridges experienced significant damage, including collapse, in the Loma Prieta Earthquake (3,4). Throughout the 1990s, researchers at the San Diego and Berkeley campuses of the University of California conducted vigorous experimental seismic research on various aspects of concrete box-girder bridges with integral concrete columns. This particular bridge type was singled out because of its widespread application in California. The research effort, which was generally initiated to characterize the behavior of existing structural members, investigated retrofit techniques, repair methods and improved design methods for columns, cap beams, foundations, and cap beam-to-column integral connections.

Of particular interest to the investigation undertaken in the NCHRP 12-54 project were the alternative methods studied at the University of California at San Diego (UCSD) for designing cap beam-to-column concrete integral joints for

seismic response in the longitudinal and transverse directions. Using simplified strut-and-tie models to represent the joint force conditions, these methods established efficient reinforcement details suitable for integral box-girder concrete bridge joints. The investigation of alternative design methods included large-scale experimental tests and detailed analytical studies (4–10), which are summarized in Appendix B (provided on the accompanying CD-ROM).

Despite common application in non-seismic regions and in some seismic regions such as in Washington State, precast concrete girders have seldom been used in California. The limited use of precast girders in California was attributed to the lack of design methods and past experimental research confirming satisfactory seismic behavior. Consequently, the Precast Concrete Manufacturers Association of California (PCMAC) and Caltrans sponsored a research program at UCSD to investigate the seismic response of precast spliced-girder bridges with integral piers (11). Similar to the previous UCSD studies, cast-in-place columns and cap beams as well as cast-in-place integral connections between the cap beam and column were used in this research project. However, the soffit slab, which was assumed to be assisting the joint force transfer in the previous box girder studies, did not exist in the precast, spliced-girder bridge. Using both the bulb-tee and bathtub precast girders, the project demonstrated that the integral precast splice-girder bridge system without soffit slab can be constructed cost-effectively to produce satisfactory seismic response.

A logical next step in the seismic bridge design advancement was the investigation of the integral bridge system with concrete columns and a steel superstructure, because the use of steel members in the superstructure can provide additional benefits over those realized with the precast concrete girder system (12). Although such a design is the subject of the NCHRP 12-54 Project, Caltrans initiated a similar investigation at UCSD around the same time that NCHRP 12-54 was approved for research. Using the prototype structure from the precast spliced-girder research project, the UCSD study examined an integral steel girder bridge system with a concrete cap beam (13,14) whereas the NCHRP Project 12-54 has investigated the use of steel girders supported on, and connected integrally to, steel box-beam pier caps. The pier caps are assumed to be supported on reinforced concrete columns. The connection between the columns and the pier cap is accomplished by extending the column longitudinal reinforcement through holes in the bottom flange of the box-beam pier cap. The compartment of the box-beam pier cap directly above a column is then filled with concrete to anchor the column reinforcement.

The UCSD study included several component tests representing the integral connection region, which included a concrete cap beam, two interior girders, and a support block modeling the concrete column. The loads were applied directly to the girders with the main objective of investigating the connection between the steel girder and the concrete cap beam. Two girder parameters were investigated in the component tests, namely girders with web stiffeners in the cap-beam

region and girders without web stiffeners. Two conditions for the cap beam were also considered—a conventional reinforced concrete cap beam and a post-tensioned cap beam. Four component tests were conducted under longitudinal seismic loading to investigate several possible combinations of the above-mentioned parameters. Based on the test results, an integral bridge system composed of stiffened steel girders and a post-tensioned cap beam was selected for system level investigation.

The system test was conducted at 40-percent scale and showed that the proposed integral bridge system with stiffened girders and post-tensioned cap beams would provide ductile seismic response. In the test unit, the plastic hinge was fully developed in the column while the superstructure exhibited essentially elastic response.

Concrete box-girder bridges and precast concrete and steel girder bridges designed generally with post-tensioned pier caps were the subjects of these articles, most of which discuss the application of integral pier bridges in non-seismic regions. Review of these articles made it apparent that integral pier concrete bridges have gained increasing popularity both in the United States and overseas since the mid-1970s. At present, several state DOTs use the integral pier concept for new bridges. Given the benefits of steel girder integral pier bridges in seismic regions, an investigation of this bridge concept with emphasis on seismic issues was needed.

2.2 FEASIBLE INTEGRAL PIER CONCEPTS

To identify integral connection concepts for this study, the research team studied the connection concepts used in the past and developed several other systems. In total, 14 different pier cap systems were examined. The attributes of each pier cap system were determined, and the systems were grouped based on the number of columns per pier, type of girders, the need for shoring during construction, and the pier cap material. In addition, two main types, concrete and steel, of the integral connections were examined. A detailed description of all systems examined and their attributes is provided in Appendix C (provided on the accompanying CD-ROM).

Criteria were developed to assist in selecting a system for further detailed studies. These selection criteria were based on listing several desirable features and giving each of the 14 systems considered a score for each feature. Some of the features considered were related to construction and others were related to the long-term performance and economy of the system. Several practicing engineers participated in the selection process and the scores were averaged.

The systems with highest score were as follows:

- Steel I-girders on single-column piers and post-tensioned concrete pier cap,
- Steel I-girders on multi-column piers with columns located under each girder, and
- Steel I-girders on single-column piers and steel box-beam pier cap.

The first of the three systems was not selected in order not to duplicate the work started at UCSD (see Section 2.1.2 above). The second system was excluded because multi-column piers have not been used in the past and also because the results of studying the connection of a single-column pier to the superstructure can be applied to the design of the connection of the columns of a multi-column pier. The third system was selected for further study.

The details of the selection process are presented in Appendix C (provided on the accompanying CD-ROM).

2.3 PROTOTYPE BRIDGE CONFIGURATION AND DESIGN

Following is a summary of the description of the prototype bridge and its design. More details on the prototype bridge are provided in Appendix D (provided on the accompanying CD-ROM).

2.3.1 Configuration

A continuous, two-span bridge with a single-column reinforced-concrete intermediate pier, steel box-beam pier cap, and steel girders as shown in Figure 2 was selected as the prototype bridge. The prototype contains an integral connection between the column and the pier cap and integral connections between the girders and pier cap and is simply supported at the abutments. Each span of the prototype bridge was 30.5 m (100 ft.). The column height measured from the bottom of the pier cap to the top of the footing was taken as 12.2 m (40 ft.). The bridge was assumed to have four girders spaced at 3.050 m (10 ft.).

A compartment centered above the column and bounded by the two box-beam webs and internal diaphragms aligned with the interior girder was assumed to be filled with concrete. The column longitudinal bars were assumed to pass through holes in the bottom flange of the pier cap and to be anchored in the concrete inside the cap. Shear studs welded to the inside of the pier cap were assumed to transfer the column forces from the concrete inside the cap to the cap itself.

2.3.2 Design

The bridge superstructure and substructure components were designed in accordance with the 1998 *AASHTO LRFD Bridge Design Specifications* (*1*). In addition to traffic loads, the bridge was designed for seismic loads as a bridge in Seismic Zone 4, assuming a ground acceleration of 0.4 g.

The seismic design of the prototype structure was based on two criteria: (1) the 1998 AASHTO-LRFD provisions as representative of typical design procedure and (2) the ATC-32 recommendations in consideration of current seismic design philosophy. In addition, it was decided that a minimum reinforcement ratio of 2 percent would be considered in order to

200 mm (8 in.)
concrete deck

30.5 m
(100 ft)

30.5 m
(100 ft)

Steel girder

Steel cap beam
2290 mm x 1680 mm
(7.5 ft x 5.5 ft)

12.2 m
(40 ft)

Reinforced concrete column
1830 mm (6 ft) diameter

(a) Longitudinal Elevation

200 mm (8 in.)
concrete deck

Cap beam

Steel plate girders
@ 3050 mm (10 ft)
on center

Reinforced concrete column
1830 mm (6 ft) diameter

(b) Transverse elevation
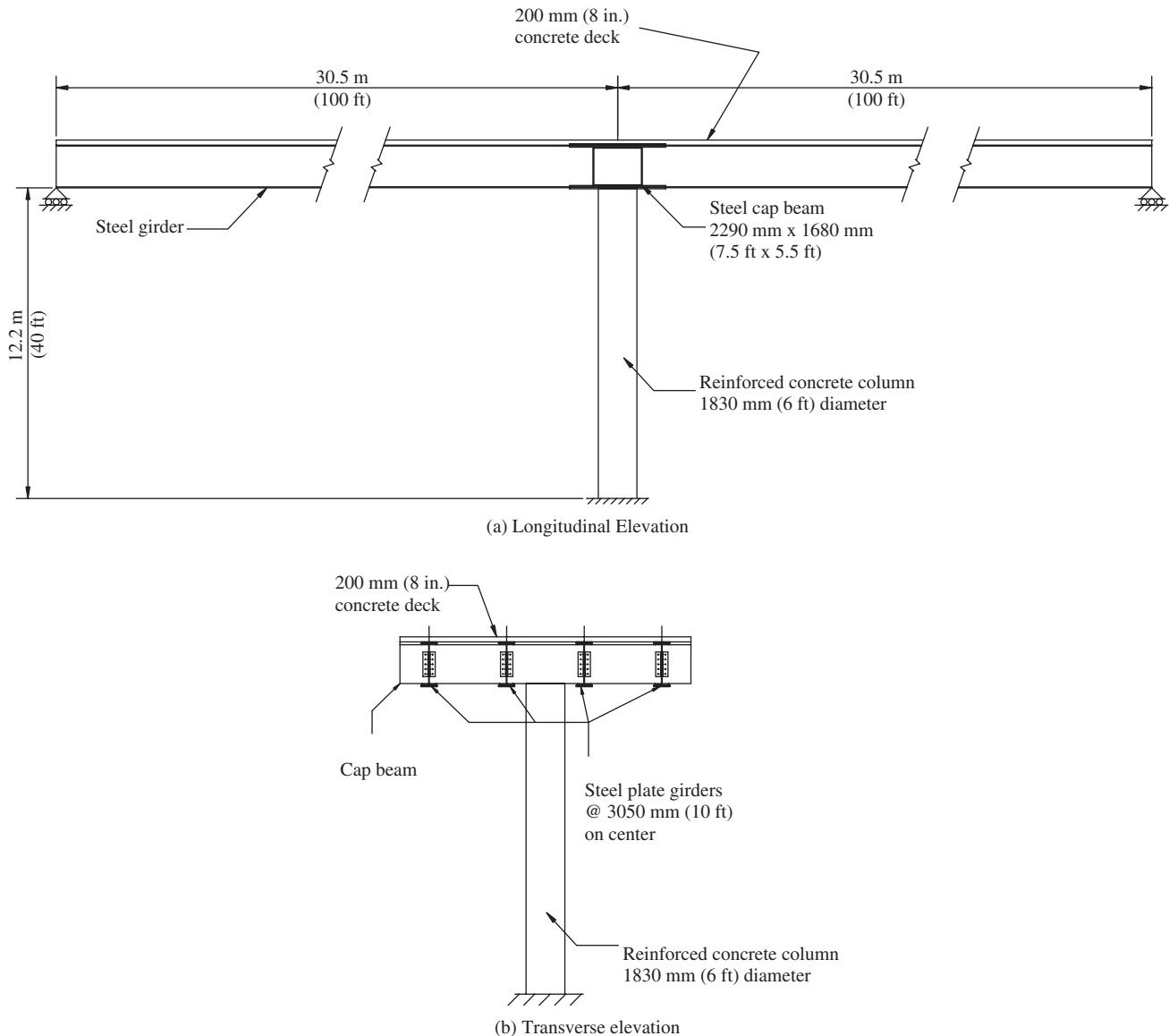
Figure 2.   Prototype bridge.

ensure that a sufficient demand would be placed on the connection region to illustrate the connection performance under high loads. The minimum reinforcement ratio was determined to govern the design, and the corresponding required volumetric ratio of transverse reinforcement was calculated as 0.00727.

2.4 TEST SPECIMEN CONFIGURATION AND TESTING

2.4.1 Test Specimen Configuration

Two one-third-scale test specimens were constructed and tested in the Iowa State University Structures Laboratory. The two specimens are referred to throughout this report as SPC1 and SPC2. The specimens were used to evaluate the lateral distribution of load between steel girders and the corresponding torsional demand on the cap beam and to verify the accuracy of the analytical models used to analyze the test specimens. Testing of these specimens also provided data to evaluate the effectiveness of the design details for the integral connection between the reinforced concrete column and the steel box-beam pier cap. Test specimen SPC1 was tested in October 2001. Specimen SPC2 was designed based on results and observations of SPC1 and was tested in September 2002.

Both test specimens were one-third-scale models of the center portion of the two-span prototype bridge (Figure 3). The general test configuration selected is shown in Figure 4. This configuration was based on the scaled prototype dimensions and the laboratory fixture requirements. With a length of 6.1 m (20 ft.) and a width of 3.76 m (12 ft, 4 in.), both specimens modeled the center 18.3 m (60 ft.) of the prototype
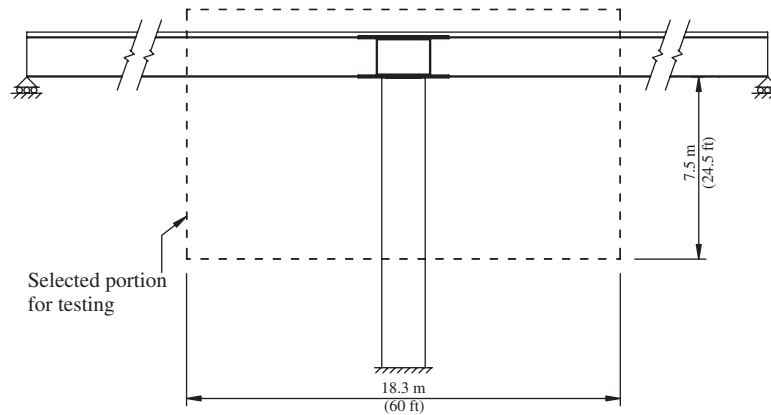
Figure 3.   Modeled portion of the prototype bridge.

bridge. The specimens were constructed and tested in an inverted position, and the girder ends were simply supported.

The column in each specimen was first subjected to low-level loads to simulate service loads. Then, the column was subjected to cyclic loading to simulate the effects of earthquake loads on the corresponding prototype structure, specif-

ically, the overall seismic performance of the structure and the performance of the connection details of the pier cap-to-column connection and the pier cap-to-girder connection regions.

2.4.2 Design Details

For the specimen column diameter of 2 ft., the required reinforcement ratio of 2 percent resulted in longitudinal steel of 20 reinforcing bars, 19 mm (¾ in.) in diameter. The resulting design for the plastic hinge region, to provide the required volumetric ratio, was a #10 (#3) spiral with a pitch of 63 mm (2.5 in.). The clear concrete cover provided outside the longitudinal reinforcement was 1 in., as shown in Figure 5a for SPC1. The connection region in SPC2 differed slightly, as shown in Figure 5b, because of the use of mechanical anchorage for the column longitudinal bars. A moment-curvature analysis was performed to predict the behavior of the plastic hinge region of the column. The same column design was used for both SPC1 and SPC2.

In specimen SPC1, 610×101 (W24 × 68) rolled shapes were used for the four girders. The girders were decreased to 460×60 (W18 × 40) rolled shapes in SPC2.

The 610 mm (24 in.) depth of SPC1 girders corresponds to a depth of 1,830 mm (72 in.) for the prototype bridge. This is larger than the typical girder depth for bridges with spans comparable to the prototype bridge. This depth was selected to provide adequate development length for the column longitudinal bars inside the connection region of the test specimen. For SPC2, the 457 mm (18 in.) girder depth corresponds to 1,370 mm (54 in.) in the prototype bridge. This depth is representative of actual bridges of span comparable to that of the prototype bridge. The depth of the connection region in SPC2 was not sufficient to fully develop the column longitudinal bars inside the connection region. The ends of the column bars were threaded and mechanical anchorage, in the form of nuts threaded at the column bar ends, was added to provide full anchorage for these bars.

Grillage model analyses were performed to predict the force-displacement responses of SPC1 and SPC2. A nonlinear
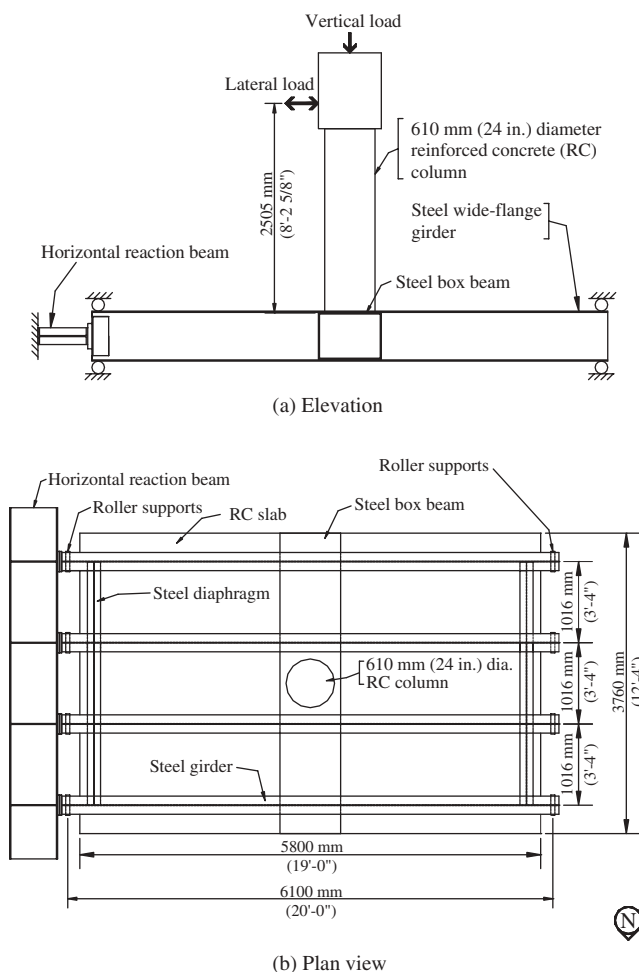
Figure 4.   General configuration of the test specimen.

12

Load

Gauged short bars

Gauged long bars

#10 (#3) spiral

Section X-X

#10 (#3) spiral @ 65 mm (2.5 in.)

20 - #19 (#6) longitudinal bars

20 - 16x68 mm (5/8 x 2 11/16 in.) shear studs
135 mm (5 5/16 in.) vertical spacing
138 mm (5 7/16 in.) horizontal spacing
Located on vertical cap plate

#10 (#3) spiral @ 90 mm (3.5 in.)

16x106 mm (5/8 x 4 3/16 in.) shear studs
W610x101 (W24 x 68) girder

13x80 mm (1/2 x 3 1/8 in.) shear studs

Cap beam
760x560x13 mm
(30 x 22 x 1/2 in.)

13x80 mm (1/2 x 3 1/8 in.) shear studs

Slab reinforcement
#10 (#3) bar
@ 100 mm (4 in.) c-to-c
both directions

Deck, 67 mm (2 5/8 in.) thick

13x54 (1/2 x 2 1/8 in.) shear studs

(a) SPC1

Load

Bars without mechanical
anchorage

#10 (#3) spiral

Section X-X

20 - 16x70 mm (5/8 x 2 11/16 in.) shear studs
135 mm (5 5/16 in.) vertical spacing
100 mm (3 15/16 in.) horizontal spacing
Located on vertical cap plate

#10 (#3) spiral @ 90 mm (3.5 in.)

#10 (#3) spiral @ 63 mm (2.5 in.)

20 - #19 (#6) longitudinal bars

16x106 mm (5/8 x 4 3/16 in.) shear studs

W460x60 (W18x40) girder

13x80 mm (1/2 x 3 1/8 in.) shear studs

Cap beam
760x410x10 mm
(30 x 16 1/8 x 3/8 in.)

13x80 mm (1/2 x 3 1/8 in.) shear studs

Cap beam $\mathbb{P}$

10 mm (3/8 in.) washer $\mathbb{P}$

16 mm (5/8 in.) nut

Longitudinal bar
threaded end

Slab reinforcement
#10 (#3) bar
@ 100 mm (4 in.) c-to-c
both directions

70 mm (2 5/8 in.) deck

13x54 mm (1/2 x 2 1/8 in.) shear studs

(b) SPC2

Figure 5.   Column-to-cap beam connection detail.

spring was used to model the plastic hinge region of the column. The spring's properties reflected the moment-rotation behavior developed from the moment-curvature analysis conducted for the column section.

2.4.3 Instrumentation

Load cells were used to measure the horizontal and vertical column loads applied at the free end of the specimen column. In SPC2, two load cells were added to measure interior girder support reactions.

Displacement and rotation transducers were used on SPC1 and SPC2 to monitor selected displacements and rotations. These transducers measured horizontal deflection and rotation of the column free end, relative vertical deflections of the column used to determine column curvature, vertical deflections of the specimen girders, relative horizontal girder displacements used to determine girder curvature, girder elon-

gation, cap beam dilatation, and overall horizontal specimen translation.

Strain gages were used to measure strains at selected locations in both specimens. These locations included the girders; column spiral reinforcement; column longitudinal reinforcement; slab reinforcement; and cap beam webs, flanges, diaphragms, and shear studs.

2.4.4 Seismic Load Simulation

To simulate seismic loading of the prototype, the load sequence for both specimens consisted of applying an appropriate column axial load downward to the top of the (inverted) column to simulate the prototype gravity effect. While maintaining the gravity load at a constant level, seismic effects were simulated by using a cyclic, lateral load with full reversals. To determine appropriate column axial loading, the expected shear and moment values for the prototype bridge and the test specimens were compared. Based on the results of this investigation, most of the test of SPC1 was conducted with a column axial load of 270 kN (60 kips) to produce a better prototype/specimen moment comparison, and the axial load was increased to 580 kN (130 kips) in a later stage of cyclic testing to carefully evaluate the shear transfer. The load was returned to 270 kN (60 kips) for the remainder of the test. In SPC2, a similar pattern was used except an axial load of 220 kN (50 kips) was used instead of the 270 kN (60 kips) used in SPC1. Seismic effects were simulated using a cyclic, lateral load pattern with full reversals as shown in Figure 6.

Details of the test fixture and the loading system are presented in Appendix E (provided on the accompanying CD-ROM).

2.5 TEST RESULTS

A summary of the test results is presented below. A detailed description of the test observations and measure-

ments is presented in Appendix F for SPC1 and in Appendix G for SPC2. (These appendixes are provided on the accompanying CD-ROM.)
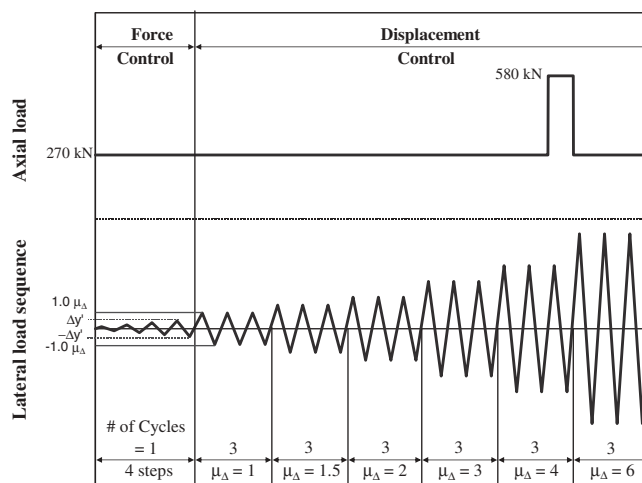
2.5.1 Seismic Test Results

General observation of SPC1 revealed that the specimen behaved as expected under lateral loading (i.e., a plastic hinge was formed in the column adjacent to the cap beam). The superstructure behaved elastically throughout the entire test, also in accordance with the intent of the design. As expected, flexural cracking of the column occurred at loads below the predicted yield of the column longitudinal reinforcement. Defining the displacement ductility, μ_D, as the ratio between the maximum displacement during a load cycle during the test divided by the displacement required to cause the yield of the column longitudinal reinforcement, concrete spalling at the column-to-cap beam connection began to occur at displacement ductility $\mu_\Delta = 1.5$. At ductility $\mu_\Delta = 4.0$, several column longitudinal bars were visible, with a few showing indications of buckling. At ductility $\mu_\Delta = 6.0$, the three extreme column longitudinal bars on each side of the column fractured, as shown in Figure 7. The buckling is believed to have been caused by loss of confinement because of interaction effects between the steel cap beam and concrete column. The steel flange of the cap beam interrupts the concrete of the column and represents a discontinuity of the concrete. In addition, the column spiral was terminated at the flange of the cap beam and was restarted on the other side of the flange. Each end of the spiral was anchored with an additional two turns of the spiral as required by current design practices for concrete members. However, it appears that, because of the discontinuity presented by the steel cap beam flange, this anchorage is not sufficient.

Specimen SPC2 also displayed satisfactory seismic performance, exhibiting the formation of a plastic hinge in the

Figure 6. Load sequence selected for simulation of seismic effects on test specimen SPC1 (1 kN = 0.225 kips).
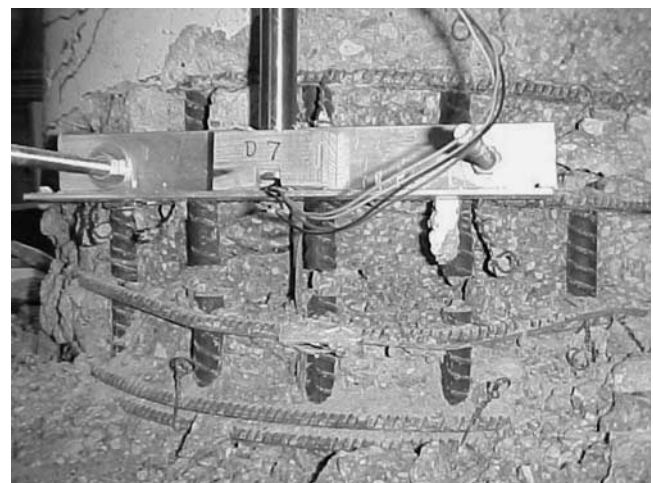
Figure 7. Fracture of column longitudinal bars at $\mu_\Delta = 6.0 \times 1$ (SPC1, column tension side while pull direction load is being applied).

column adjacent to the cap beam and showing elastic behavior of the superstructure. Early stages of the test revealed similar behavior to SPC1. Increased cracking was seen in the slab as could be expected for the more flexible superstructure in SPC2. The primary difference in results in SPC2 was the failure mechanism of the longitudinal bars, which appeared to lose anchorage in the connection region and fractured the mechanical connections. (Mechanical connections were not used in SPC1 because the increased cap beam height in SPC1 provided adequate anchorage length for the longitudinal reinforcement.) The plastic-hinge region of SPC2 following testing is shown in Figure 8.

Views of the columns from SPC1 and SPC2 following seismic testing are shown in Figures 9 and 10.

Figures 11 and 12 show the experimental load-displacement hysteresis for specimens SPC1 and SPC2, respectively. Both specimens exhibit satisfactory seismic behavior through ductility $\mu_\Delta = 4.0$ as indicated by the regular shape of the hysteresis and the gradual degradation of stiffness. In the load-displacement response for SPC1 (Figure 11), the decreased load resistance resulting from the fracture of several of the column longitudinal bars at $\mu_\Delta = 6.0$ is indicated by the lower stiffness of the last cycles in Figure 11a. SPC2 also exhibits decreased load resistance at ductility $\mu_\Delta = 6.0$ because of the

Figure 9.   Tension side of the column in the push loading direction after seismic testing (SPC1).

Figure 8.   Partial view of column at the completion of seismic testing (SPC2, tension side of the column in the pull loading direction).

fracture of the mechanical anchorage of several of the longitudinal bars as shown in Figure 12a. The predicted load-displacement relationships developed from the grillage analyses are also shown in Figures 11b and 12b. The actual column behavior is quite consistent with the predicted behavior for the initial load steps. The pull direction response of SPC2 is seen to begin to differentiate from the predicted behavior at

Figure 10. Tension side of the column in the push loading direction after seismic testing (SPC2).

tudinal bar extending through a hole in the cap beam flange into the deck are compared with the strain profiles of the opposite bar which was terminated in the connection region next to the flange near the deck (i.e., was not extended into the bridge deck). The comparison is shown for two different load steps, 0.5 F_y and $\mu_\Delta = 1.0$. Most of the load is seen to be dissipated near the column-to-cap beam interface (embedment length = 0 in.) for the smaller load step for both bars, while both bars exhibit a more linear distribution at the higher load step. The good comparison indicates that extension of the bars into the bridge deck is not necessary if adequate anchorage length is provided within the connection region.

The dilatation of the cap beam in the connection region was investigated to determine the adequacy of the steel box beam in providing confinement. This investigation revealed that, although the cap beam behaved elastically throughout the test, the dilatation began increasing more drastically at loads exceeding 1.0 F_y, indicating that the cap beam by itself would perhaps become ineffective in providing confinement at higher loads and that spiral reinforcement in the connection region is required for confinement at higher loads.

2.5.2 Simulated Service Load Testing

Four simulated service load tests were conducted as illustrated in Figure 14: SLC1, SLC2, SLC3, and SLC4 with two different support conditions (i.e., all girders supported and only exterior girders supported) and two types of loading (i.e., vertical and lateral). The primary purpose of these tests was to investigate the distribution of moments between the interior and exterior girders and to validate the analytical model by comparing the analytical results to test results.

Because of the small magnitude of loads and strains for these four load conditions, three load conditions from the seismic loading with similar support and load configurations were also used in the analysis of the girder distribution factors.

Girder strains were used to determine the experimental load distribution. Analytical models were used to predict the load distribution for loading in both the vertical and horizontal directions. Comparisons of the experimental and analytical load distributions from SPC1 and SPC2 are shown in Tables 1 and 2. The strain in the flanges of the interior and exterior girders is shown in Figure 15. The comparisons for SLC1 and SLC3 are very good for both specimens. However, in both specimens the experimental distribution for SLC2 and SLC4 revealed a significant percentage of the load being carried by the interior girders, whereas the analytical model indicates a distribution of 100 percent to the exterior girders. At least two explanations are possible. First, the experimentally based load distributions may not be accurate because of experimental errors at the low strain levels for these two tests. Second, and much more likely, the transverse stiffness of the concrete slab and end diaphragm distributed forces to the interior girders even though they were not supported. The analytical model did not account for transverse stiffness between the girders.

ductility $\mu_\Delta = 3.0$ because of slippage of the extreme bar that was not mechanically anchored.

To investigate the necessity of extending the column longitudinal bars into the bridge deck, the strains measured on the longitudinal bars in the connection region were investigated. In Figure 13, the strain profiles from SPC1 of a longi-

16
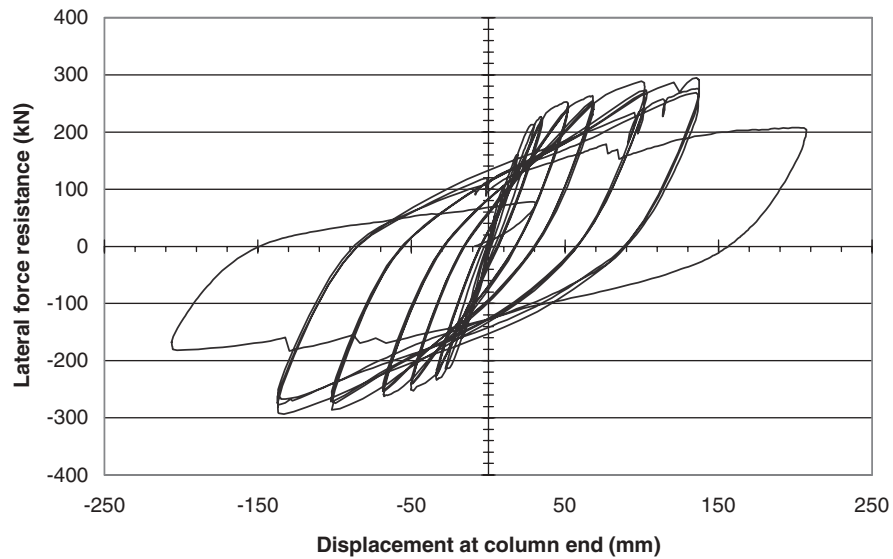
(a) Entire simulated seismic test
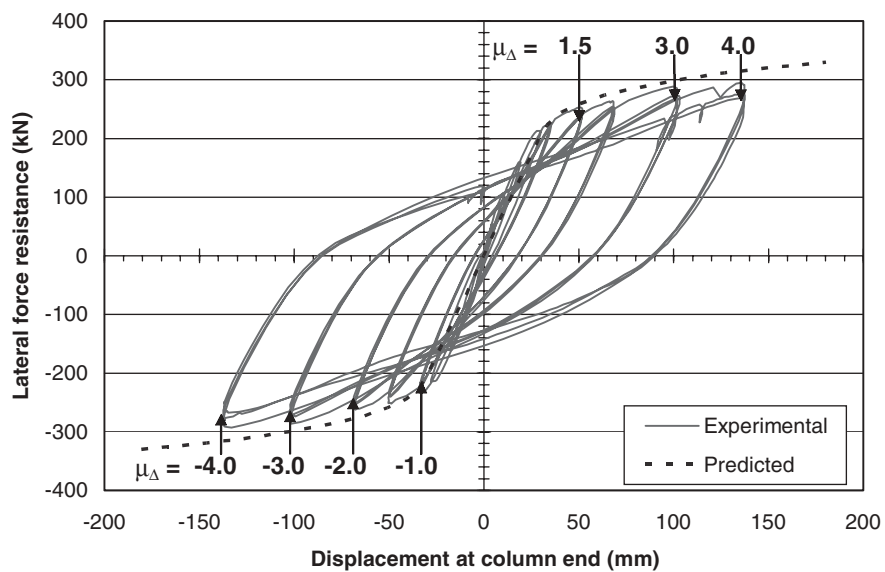
(b) Up to $\mu\Delta = 4.0$

Figure 11.   Column lateral force-displacement response of SPC1 (1 kN = 0.225 kips, 1 mm = 0.039 in.).
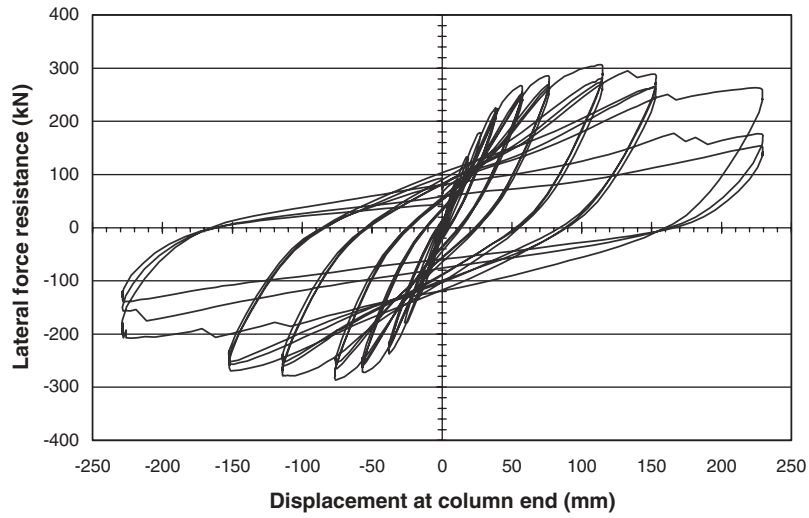
(a) Entire seismic test
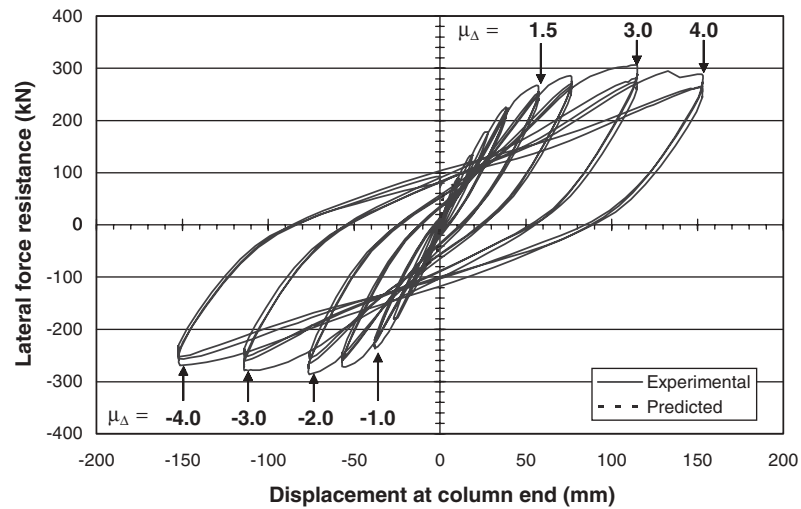
(b) Up to $\mu_\Delta = 4.0$

Figure 12. Experimental force-displacement response of SPC2 (1 kN = 0.225 kips, 1 in. = 25.4 in.).
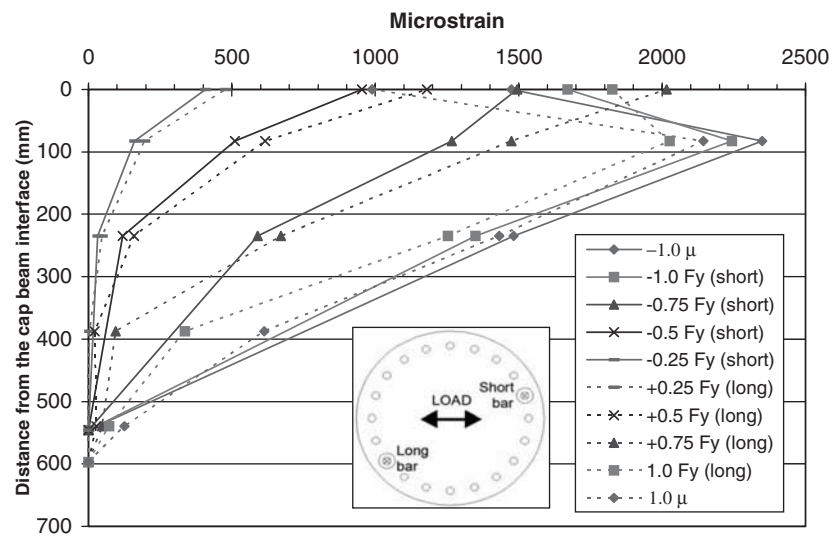
Figure 13. Tension strain profiles for the reinforcing bars (SPC1).

P = 90 kN (20 kips)

P = 90 kN (20 kips)

(a) SLC1

(b) SLC2

H = 45 kN (10 kips)

H = 45 kN (10 kips)

(c) SLC3

(d) SLC4
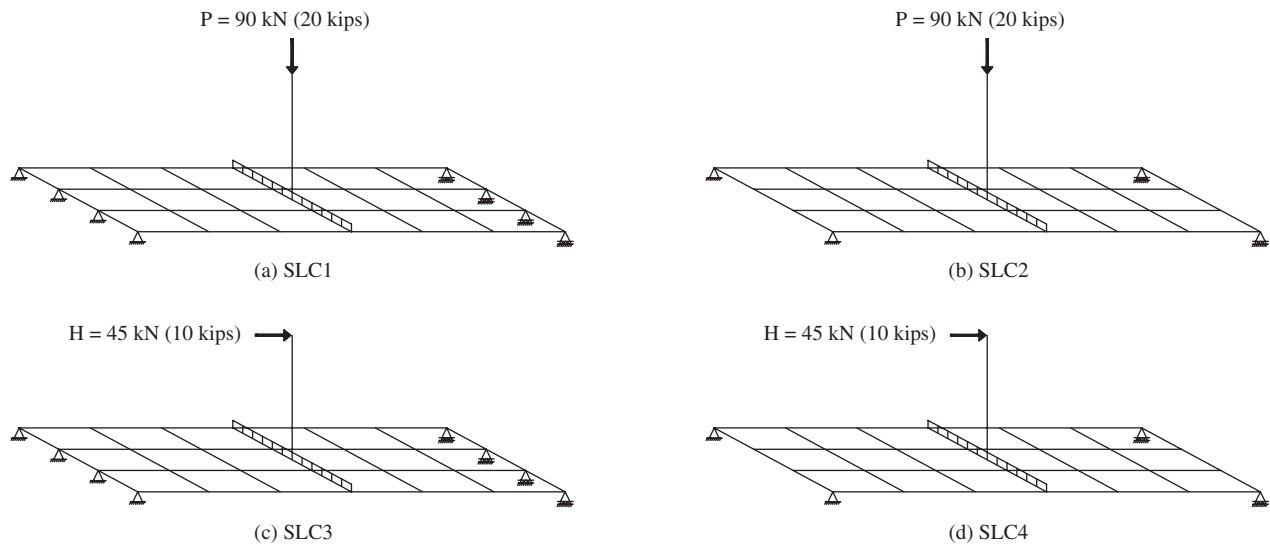
Figure 14.   Service-load test condition.

**TABLE 1   Comparison of experimental
and analytical load distributions (SPC1)**

Load Condition	Girder	Load Distributions	
		Average Experimental	Analytical
SLC1	Exterior	50%	45%
	Interior	50%	55%
SLC2	Exterior	76%	100%
	Interior	24%	0%
SLC3	Exterior	35%	28%
	Interior	65%	72%
SLC4	Exterior	72%	100%
	Interior	28%	0%

**TABLE 2   Comparison of experimental
and analytical load distributions (SPC2)**

Load Condition	Girder	Load distributions	
		Average Experimental	Analytical
SLC1	Exterior	47%	46%
	Interior	53%	54%
SLC2	Exterior	75%	100%
	Interior	25%	0%
SLC3	Exterior	32%	30%
	Interior	68%	70%
SLC4	Exterior	60%	100%
	Interior	40%	0%
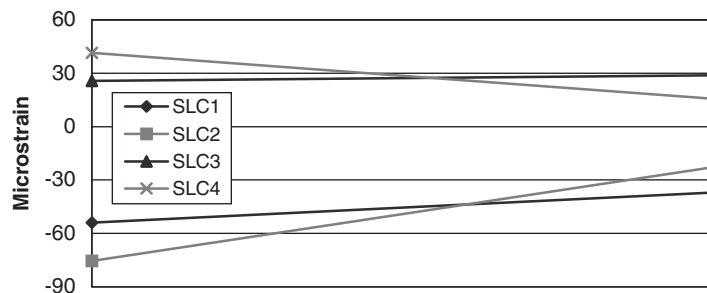
(a) Strains at gages S3 and S11 for SLC1 through SLC4

S1, S3

S9, S11

Exterior
Girder

Interior
Girder

(b) Cross-sectional view showing the relative location for strain gages S1, S3, S9, and S11

*Figure 15.   Top flange strains for the exterior and interior girders for
SLC1 through SLC4.*

CHAPTER **3**

INTERPRETATION, APPRAISAL, AND APPLICATION

The overall understanding of the behavior of integral pier connections between steel I-beam superstructures, steel box-beam pier caps, and concrete columns was gained from the questionnaire, literature survey, and results of the analytical and experimental studies. This understanding was used in determining the feasibility of the integral connections tested and in developing a design methodology for the integral pier caps. This design methodology is presented below. Proposed design provisions and commentary written in the format of the *AASHTO LRFD Bridge Design Specifications* were developed based on the proposed design methodology. The proposed design provisions and commentary are presented in Appendix H provided on the accompanying CD-ROM. A detailed design example using the proposed provisions is presented in Appendix I provided on the accompanying CD-ROM.

Some of the observations from the analytical and experimental studies were extrapolated to accommodate expected variations in geometry and site conditions that were not directly included in the studies. This extrapolation is based on the design experience of many of the research team members and sound engineering judgment.

3.1 FEASIBILITY

The experimental studies demonstrated the feasibility of connecting a concrete column integrally to a steel box-beam pier cap. They further demonstrated that the bond between the concrete placed inside a box-beam pier cap and the longitudinal column reinforcement is sufficient to develop the overstrength column moment and no further connection is required for the column reinforcement. The test results also indicated that shear connectors installed inside the box-beam pier cap are sufficient to transfer the column moments from the concrete to the pier cap.

3.2 PROPOSED DESIGN METHODOLOGY

3.2.1 Method of Analysis

Based on the analytical studies conducted as part of this project, the following observations were made:

- The maximum moments and shears in the girders calculated using a conventional line girder computer program that does not take into account the effect of the integral connection to the substructure compared well with the forces determined using a 3-dimensional finite element model of the bridge. The location of the maximum positive moments in the girders was different in the two cases; however, the shift in the maximum moment section location was relatively small to affect the design.

- The live load moments in the single column pier from the 3-dimensional model compared well with the moment calculated using a 2-dimensional frame representing the bridge in elevation. The section properties of the members representing the superstructure were taken equal to the section properties of the entire bridge cross section.

- The maximum live load torsional moment in the pier cap and the maximum live load moment at the top of the column are produced by different load cases. The maximum torsional moment is produced when opposite halves of the two spans next to the pier cap are loaded (see Figure 16a). The maximum live load column top moment is produced when the longer of the two adjacent spans is loaded (see Figure 16b). In the prototype bridge, the maximum live load torsional moment in the pier cap on either side of the column, produced from a load case similar to that shown in Figure 16a, is approximately equal to the maximum live load moment in the column at its top, produced from a load case similar to that shown in Figure 16b.

For the case of maximum torsional moments in the pier cap, the column moments and the rotation at the column top and at interior girder intersections with the pier cap are relatively small. This results in the exterior girders transferring most of the pier cap torsional moment.

The maximum seismic torsional moment in the pier cap on either side of the column may be taken equal to one-half the column overstrength moment. For a two-span bridge with two girders on either side of the column, the interior girders and the exterior girders transferred 64 and 36 percent of the torsional moment, respectively. Assuming that 40 percent of the torsional moment on either side of the column is transferred by the exterior girder and the remaining 60 percent is transferred by the first interior girder is expected to result in adequate design accuracy.

(a) Loading for Maximum Torsion

(b) Loading for Maximum Column Moment
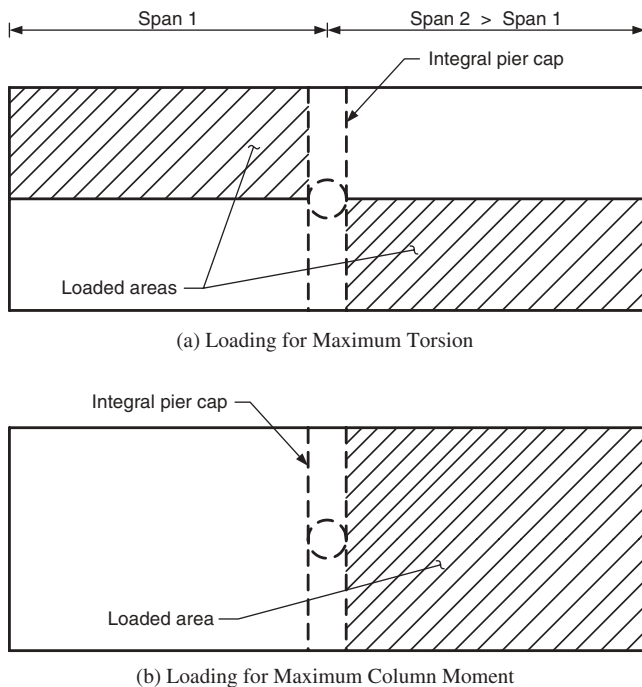
Figure 16. Live load cases for maximum pier cap torsion and maximum column moment.

For a bridge with more than two girders on either side of the column, it is rational to expect that the percentage of the torsional moment transferred by the girders is highest for the interior girder and is lowest for the exterior girder. It can also be rationally expected that the interior girder in a bridge with two girders on either side of the column transfers more moment than that in a bridge with a larger number of girders. In the absence of analytical studies on bridges with more than two girders on either side of the column, the proposed distribution, which is based on results of a bridge with two girders on either side of the column, is expected to yield conservative results for bridges with more girders.

Based on these observations, and considering the limitation of the study, the following recommendations are made:

- For I-girder superstructures connected integrally with the substructure the following approximations may be used:
  – The girder forces may be determined ignoring the effect of the integral connection (i.e., conventional line girder computer programs may be used for the analysis and design of the girders with integral connections).
  – The longitudinal moments acting on the substructure columns may be determined using 2-dimensional frame analysis. The section properties of the frame members representing the superstructure and those representing intermediate piers or bents should be taken equal to the flexural stiffness of the full cross section of the bridge and the flexural stiffness of the pier column, respectively. In the unlikely case of using

multi-column bents, the stiffness of the member representing the substructure will be taken equal to the sum of the stiffness of all columns in the bent.
  – The transverse moments in the substructure columns may be determined using 2-dimensional frame analysis of the columns and the pier cap. The loads transmitted from the girders to the substructure should be applied as concentrated loads at girder locations.
  – The live load torsional moment in the pier cap on either side of the column of a single-column integral pier may be taken equal to maximum live load moment acting at the top of the column determined using 2-dimensional frame analysis as described above. This moment may be assumed constant along the full length of the pier cap.
  – The maximum torsional moment in the pier cap due to seismic loading may be taken equal to one-half the column overstrength moment at the top. The exterior and the first interior girders may be assumed to transfer 40 and 60 percent of the torsional moment due to seismic load to the pier cap.
  – In most cases the column of a single-column pier will be located at mid-width of the structure. This was the geometry used in this study. However, site geometrical constraints may require offsetting the column from the mid-width of some bridges. The simplifications provided above are recommended to be used if the column is offset by no more than 10 percent of the bridge width. The 10-percent limit is an arbitrary limit based on engineering judgment.
- For other bridges, 3-dimensional refined analysis should be used to determine the forces acting on the components of both the superstructure and the substructure.

3.2.2 Design and Anchoring of the Column-to-Pier Cap Connection

The following were observed during testing of the two test specimens:

- The column design forces may be determined using the AASHTO LRFD Specifications (*1*) supplemented by any specific requirements of the owner agency. According to the AASHTO LRFD Specifications, column design moments and associated shears are taken as the largest calculated forces from all applicable strength limit states and the extreme event limit states. For the extreme event limit state that includes seismic forces, the maximum column moment is determined as the lesser of the moment calculated from elastic analysis and that based on plastic hinging of the column including consideration of the column overstrength effects.
- Filling the pier cap compartment directly above the column (see Figure 17) with concrete and extending the col-
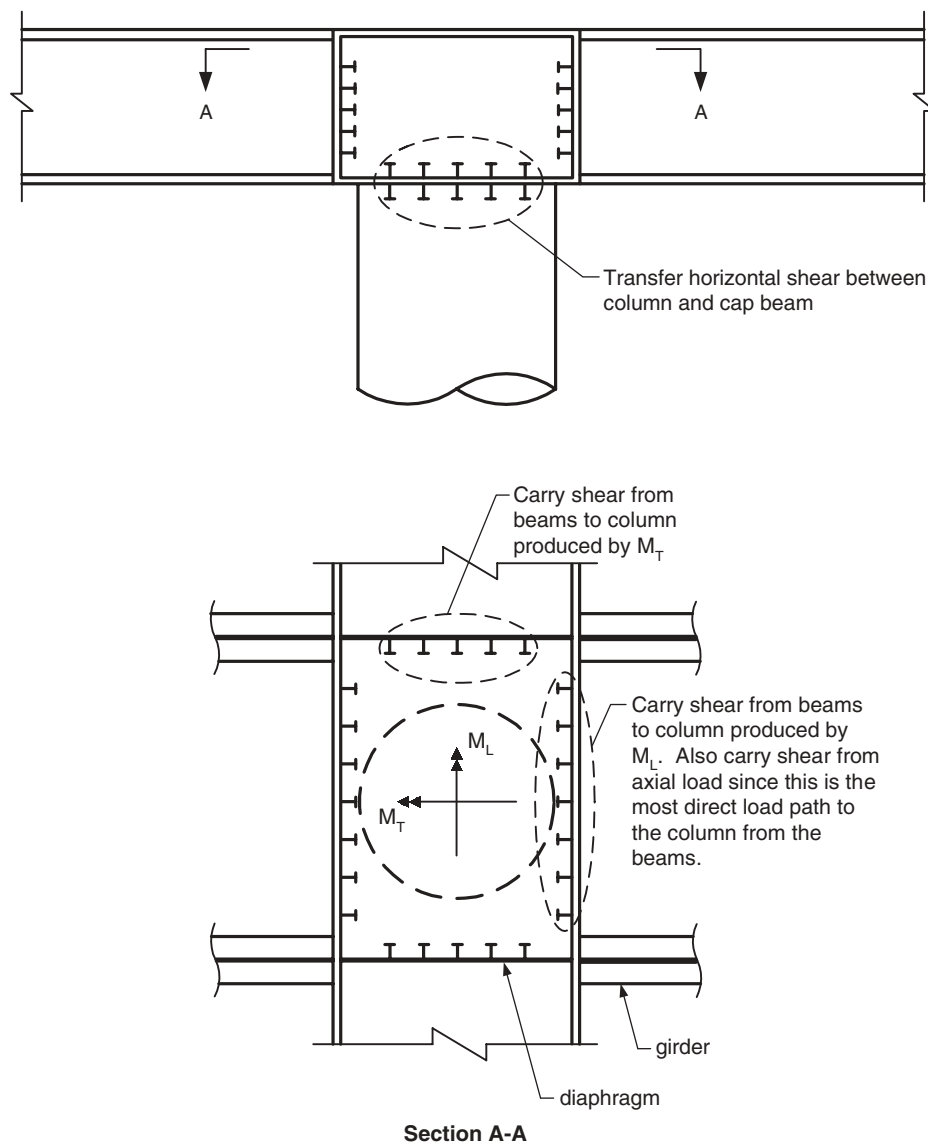
Figure 17.   Shear studs in the integral connection.

umn longitudinal reinforcement into the pier cap provides adequate anchorage to the column. The length of the column longitudinal reinforcement above the bottom flange of the pier cap should be sufficient to develop these bars. If needed, the bars may be extended through the top flange of the pier cap into the deck slab.

- At high levels of inelastic deformation, the column longitudinal reinforcement in the first test specimen appeared to have not been fully confined at the point these bars passed through the bottom pier cap flange. At this point, the column spiral reinforcement was stopped at either side of the pier cap flange plate and was anchored by two extra turns of the spiral as recommended by Sritharan et al. (*15*) which is more than the one and a half turns required by the *AASHTO LRFD Bridge Design Specifications* (*1*). In the second test specimen, the spiral was anchored using

two extra turns and the ends of the spiral bars were bent toward the center of the column and were provided with a seismic hook. The column longitudinal reinforcement in the second specimen did not lose confinement until the end of the test. Unfortunately, the second specimen failed at a lower level of inelastic deformations than the first specimen because of the loss of bond between the longitudinal bars and concrete. It was expected that the performance of the confinement reinforcement in the second specimen would exceed that in the first specimen because of the extra anchorage provided.

- Providing shear studs inside the pier cap (see Figure 17) to transfer the column axial load and moments to the pier cap provided a satisfactory load path. The moment used to design the connection should be taken as the column top design moment, including consideration of the over-

strength effects when analyzing load cases that include seismic loading.

Based on these observations, the following recommendations are made:

- Girder spacing should be selected to eliminate the interference of the girder flanges with the column longitudinal reinforcement extending into the pier cap (i.e., the girder flanges should be located outside the width of the columns). This is of particular importance in seismically active zones. In case one or more girders are placed within the width of the column, the column longitudinal reinforcement bars within the width of the girders need to be terminated below the bottom of the girders. These bars should be ignored when determining the moment resistance of the column top.
- The location of the two girders next to a substructure column should preferably be symmetric with respect to the column.
- The intermediate diaphragms inside the box-beam pier cap divide the interior space of the beam into separate compartments (see Figure 17). A compartment bounded by the webs of the box-beam and two intermediate diaphragms should be centered above the column and, in the unlikely case of multi-column bents, above each substructure column. This compartment should then be filled with concrete to anchor the column longitudinal reinforcement.
- The longitudinal reinforcement of the columns should be extended into the pier cap for at least the development length of the rebar.
- At the end of the spiral on either side of the pier cap bottom flange, two extra turns of spiral bars or wire are required to anchor the spiral reinforcement. Bend the end of the spiral toward the center of the column for a distance equal to 12 times the spiral reinforcement diameter.
- To ensure adequate confinement of the concrete in the connection region, it is necessary to extend the transverse reinforcement of the column in the integral connection region inside the pier cap. The transverse reinforcement ratio inside the pier cap should not be less than the greater of the minimum transverse reinforcement ratio required by the specifications and one-half of that used outside the pier cap.
- Shear connectors should be provided inside the concrete-filled compartment of the pier cap. These shear connectors are required to be designed to transfer the column forces to the pier cap. Column design moments should be converted into shear force acting on the shear connectors. The magnitude of the shear force may be determined by dividing the column top design moment by the distance between the planes of the shear connectors assumed to transfer the moment to the pier cap.
- Shear connectors sufficient to transfer the maximum shear in the column should be installed on either side of the pier cap bottom flange.

3.2.3 Connection Between the Girders and the Pier Cap

Based on the procedures used in designing the test specimens and the successful performance of the specimens during testing, the following recommendations may be made.

- The continuity of the girders over the pier cap may be provided through the use of girder flange splice plates that span the width of the pier cap and are connected to the flanges of the girders on either side of the pier cap (see Figure 18). The splice plates may be assumed to resist the full design moment in the girder. The design force of the splice plates and their connection to the girders may be taken equal to the design moment in the girder divided by the girder depth.
- The connection between the webs of the girders to the webs of the pier cap may be designed to resist the maximum vertical shear in the girders. The effect of the moments on this connection may be ignored when the flange splice plates are designed to resist the full moment on the connection.
- The difference in a girder moment at either face of the pier cap is transferred to the pier cap in the form of torsional moment. This moment is transferred through the shear force acting on the connection between the girder splice plates and the pier cap. It is recommended that the connection between the girder flange splice plates and the pier cap (see Figure 18) be designed to resist a shear force equal to the maximum torsion transferred to the pier cap at the girder location divided by the depth of the girder. It also is recommended that the splice plates and the connection between the splice plates and the girder (see Figure 18) be designed to resist a force equal to the girder moment at the face of the pier cap divided by the depth of the girder.

3.2.4 Box-Beam Pier Cap Design

Once the design forces are determined, box-beam design provisions currently in the AASHTO LRFD Specifications (*1*) are sufficient to design the box-beam pier cap. Bolting spacing and clearance requirements in the specifications should also be satisfied.

3.3 CONSTRUCTION RECOMMENDATIONS

Based on the information collected during this study, the following construction recommendations are made:

- Making the integral connection after the steel members are erected and the deck slab is poured is the favorable construction sequence because it minimizes the dead load locked-in forces in the connection and allows for

Section A-A
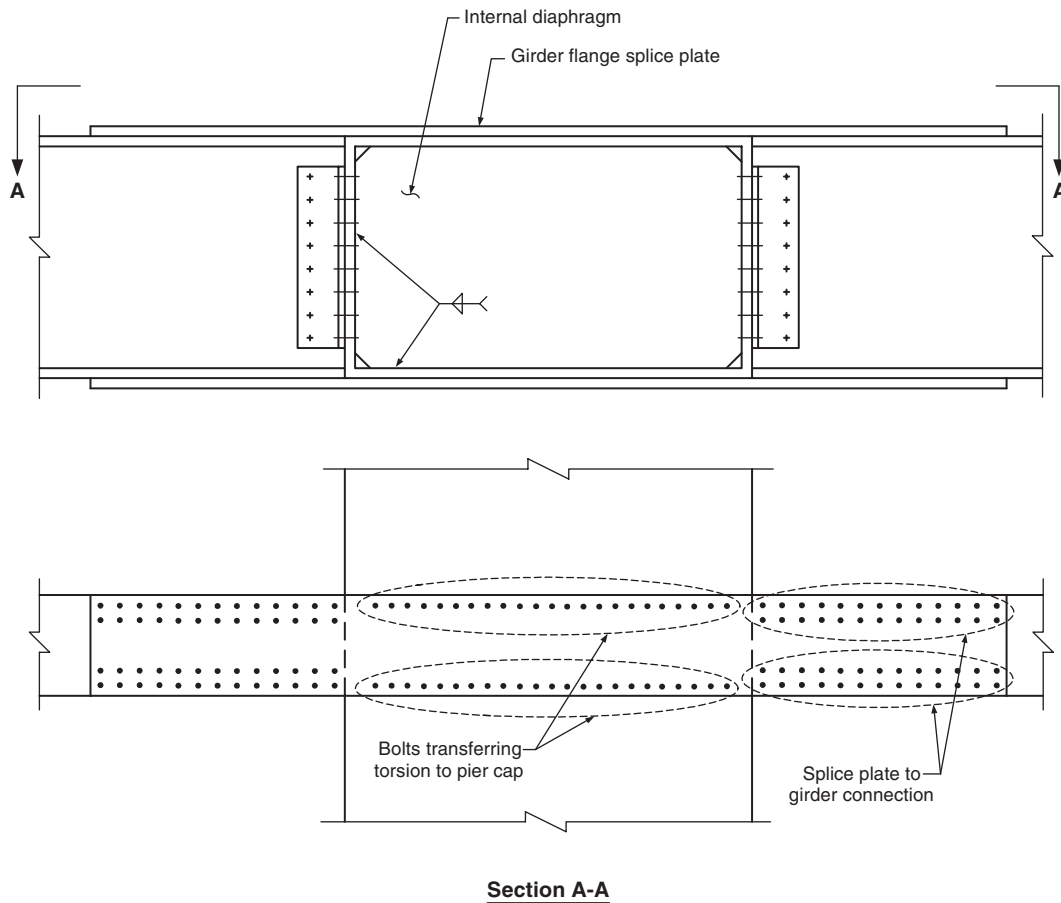
Figure 18.   Girder-to-pier-cap connections.

more liberal construction tolerances. However, where it is desirable to eliminate the need to shore up the superstructure, the integral connection may be made before the superstructure girders are erected. In such cases, tight tolerances on the orientation and elevation of the pier cap are required to allow the superstructure girders to be connected later without undue difficulty. Unbalanced dead loads and the sequence of construction of the superstructure and pouring of the deck may develop permanent locked-in stresses in the connection. These permanent locked-in stresses are required to be accounted for in the design. The designer needs to specify the time

of making the integral connection relative to other construction operations.

• Temperature changes after placement of the concrete of the integral connection cause displacements that produce forces in both the substructure and, due to the integral connection, the superstructure. The movements associated with temperature changes before the connection concrete reaches adequate strength may damage the bond between the pier cap and the connection concrete. To minimize these forces, measures to stabilize the temperature of the girders during, and for adequate time after, placement of the connection concrete should be applied.

CHAPTER **4**

CONCLUSIONS AND SUGGESTED RESEARCH

4.1 CONCLUSIONS

It is feasible to integrally connect reinforced concrete columns to box-beam pier caps by extending the column longitudinal reinforcement through holes in the pier cap flange and filling the pier cap compartment directly above the column with concrete. The resulting connection is sufficient to develop the plastic hinging of the column, given that anchorage adequate to fully develop the column longitudinal reinforcement inside the pier cap is provided. The first test specimen, which had a deeper pier cap and longer anchorage length of the column longitudinal reinforcement, reached a ductility of $\mu\Delta = 6.0$ before failure. The second test specimen, with a shallower pier cap, reached a ductility of $\mu\Delta = 4.0$ before failure. The failure at this lower ductility essentially resulted from the loss of bond between the column bars and the concrete in the integral connection region.

Integral pier connections are most likely to be used for bridges with high skew angles and are supported on single-column piers. The use of the integral pier connections results in lower elevation of the bridge deck and the approaches without reducing the bridge underclearance. The cost of bridges with integral connections is expected to exceed conventional bridges; however, because of the lower approach elevation, the combined cost of the bridge and the approaches is expected to be lower than that of a conventional bridge.

Extending the column spiral reinforcement into the connection region is required to ensure adequate confinement of the connection region. The required spiral reinforcement in the connection region may be taken as the greater of the minimum spiral reinforcement required by the design specifications and one-half the required column spiral reinforcement next to the integral connection region.

The live load distribution factors in the current design specifications, which were developed for use with bridges supported on conventional bearings, may be used for bridges with integral connections.

Using grillage models to analyze bridges with integral connections is expected to yield high accuracy.

4.2 SUGGESTED RESEARCH

Parametric studies to further verify the simplified analysis method for typical structures as included in the proposed design specifications is needed. Some of the parameters that need to be included are the skew angle, variation in adjacent span length, number of continuous spans, and number of the girders in the cross section.

The shear connectors on the outside of the bottom flange of the pier cap may complicate construction. Testing to prove that the column longitudinal reinforcement is sufficient to transfer the column shear force to the connection region is needed.

REFERENCES

1. American Association of State Highway and Transportation Officials, *AASHTO LRFD Bridge Design Specifications*, Second Edition, 1998, and the 1999, 2000, 2001, and 2002 Interim Specifications.

2. Modjeski and Masters, Inc. and Iowa State University. "Integral Connections of Steel Bridge Structures." Interim Report, NCHRP Project 12-54 (December 1999).

3. EERI. "Loma Prieta Earthquake Reconnaissance Report." *Earthquake Spectra*, Special Supplement to Vol. 6 (May 1990).

4. Priestley, M.J.N., F. Seible, and G.M. Calvi. *Seismic Design and Retrofit of Bridges.* New York: John Wiley and Sons (1996).

5. Priestley, M.J.N. "Assessment and Design of Joints for Single-Level Bridges with Circular Columns." Report No. SSRP-93/02, Department of Applied Mechanics and Engineering Sciences, University of California, San Diego (1993).

6. Seible, F., et al. "Full-Scale Bridge Column/Superstructure Connection Tests Under Simulated Longitudinal Seismic Loads." Report No. SSRP-94/14, Department of Applied Mechanics and Engineering Sciences, University of California, San Diego (1994).

7. Sritharan, S., M.J.N. Priestley, and F. Seible. "Seismic Design and Performance of Concrete Multi-Column Bents for Bridges." Report No. SSRP-94/03, Department of Applied Mechanics and Engineering Sciences, University of California, San Diego (1997).

8. Sritharan, S., M.J.N. Priestley, and F. Seible. "Seismic Response of Column/Cap Beam Tee Connections with Cap Beam Prestressing." Report No. SSRP-96/09, Department of Applied Mechanics and Engineering Sciences, University of California, San Diego (1996).

9. Terayama, T., F. Seible, and M.J.N. Priestley. "Flexural Integrity of Cap Column Connections with #18 Bars." Thesis, Report No. SSRP-93/08, Department of Applied Mechanics and Engineering Sciences, University of California, San Diego (1993).

10. Sritharan, S. "Analysis of Concrete Bridge Joints Subjected to Seismic Actions." Ph.D. Dissertation, Department of Applied Mechanics and Engineering Sciences, University of California, San Diego (1998).

11. Holumbo, J., M.J.N. Priestley, and F. Seible. "Longitudinal Seismic Response of Precast Spliced-Girder Bridges." Report No. SSRP-98/05, Department of Applied Mechanics and Engineering Sciences, University of California, San Diego (1998).

12. Sritharan, S., et al. "Seismic Performance of a Concrete Column/ Steel Cap/Steel Girder Integral Bridge System." Presented at the Third National Conference and Workshop on Bridges and Highways, Portland, Oregon (April 2002).

13. Patty, J., F. Seible, and C. Uang. "Seismic Response of Integral Bridge Connections." Report No. SSRP-2000/16, Structural Systems Research Project, University of California, San Diego (June 2001).

14. Patty, J., F. Seible, and C. Uang. "Longitudinal Seismic Response of Concrete Substructure to Steel Superstructure Integral Bridge Connections." Presented at the Sixth Caltrans Seismic Workshop, Sacramento, California (June 2001).

15. Sritharan, S., M.J.N. Priestley, and F. Seible. (2001) "Seismic Design and Experimental Verification of Concrete Multiple Column Bridge Bents," *ACI Structural Journal,* 98(3):335–346.

APPENDIXES A THROUGH H

Appendixes A through H are provided on the accompanying CD-ROM, *CRP-CD-47*. The appendixes are as follows:

- Appendix A: Questionnaire on Past Use of Integral Pier Caps
- Appendix B: Literature Review
- Appendix C: Integral Pier Concepts
- Appendix D: Prototype Bridge Configuration, Loading and General Experimental Configuration
- Appendix E: Test Fixture and Loading System
- Appendix F: Design, Construction, Testing and Results from Specimen SPC1
- Appendix G: Design, Construction, Testing and Results from Specimen SPC2
- Appendix H: Proposed Design Specifications Articles and Commentary

APPENDIX I

DESIGN EXAMPLE

TABLE OF CONTENTS

LIST OF FIGURES

LIST OF TABLES

I1 PROBLEM STATEMENT

A design example for a bridge consisting of a steel I-girder superstructure integral with a steel box-beam pier cap supported on a single reinforced concrete column is presented. The steel box-beam pier cap and the concrete column are integrally connected by extending the longitudinal bars of the column into the pier cap compartment directly above the column and filling this compartment with concrete. The design is in accordance with the 1998 *AASHTO LRFD Bridge Design Specifications,* Second Edition, with 1999 through 2002 Interim Revisions, hereafter collectively referred to as the AASHTO LRFD Specifications. The design example is presented in SI units with equivalent U.S. customary units in parentheses. References to articles, equations, tables, and figures within the AASHTO LRFD Specifications are made throughout the example and have been placed in bold print. Of particular interest and the main focus of this example is the design of the connection of the cap beam to the girders and column. The level of detail provided is that required by practicing engineers for design of such structures.

I2 NOTATIONS

A	= seismic acceleration coefficient
A_b	= area of an individual bar (mm^2); cross-sectional area of a bolt (mm^2)
A_g	= gross cross-sectional area of a member (mm^2)
A_n	= net cross-sectional area of a member (mm^2)
A_o	= enclosed area within a box section (mm^2)
A_{sc}	= cross-sectional area of a stud shear connector (mm^2)
A_{sp}	= cross-sectional area of spiral reinforcing (mm^2)
A_v	= area of shear reinforcement (mm^2)
b	= width of deck represented by a slab element (mm); compression flange width between webs (mm); width of member (mm)
b_v	= effective web width, or for circular sections, the diameter of the section (mm)
C	= ratio of the shear buckling stress to the shear yield strength
C_{sm}	= dimensionless elastic seismic response coefficient
c	= distance from the neutral axis to the outer fiber (mm)
D	= column diameter (mm); web depth (mm); width or depth of plate between webs or flanges (m)
DC	= designation for dead load due to structural components and nonstructural attachments
D_c	= depth of web in compression in the elastic range (mm)
D_r	= diameter of the circle passing through the centers of the longitudinal reinforcement (mm)
DW	= designation for dead load due to wearing surfaces and utilities
d	= nominal diameter of a bolt (mm); depth of pier cap (m); diameter of a shear stud (mm)
d_b	= nominal diameter of a reinforcing bar (mm)
d_c	= outside diameter of spiral (mm)
d_e	= effective depth from extreme compression fiber to the centroid of the tensile force in the tensile reinforcement (mm)
d_o	= stiffener spacing (mm)
d_v	= effective shear depth (mm)
E	= modulus of elasticity (MPa)
E_c	= modulus of elasticity of concrete (MPa)
EI	= flexural stiffness (N-mm^2)
EQ	= designation for earthquake load
F_n	= nominal flexural resistance in terms of stress (MPa)
F_r	= factored flexural resistance in terms of stress of the flange for which f_u was determined (MPa)
F_u	= specified minimum tensile strength of steel (MPa); specified minimum tensile strength of a stud shear connector (MPa)
F_{ub}	= specified minimum tensile strength of a bolt (MPa)
F_y	= specified minimum yield strength of steel (MPa)
F_{yc}	= specified minimum yield strength of the compression flange (MPa)
F_{yw}	= specified minimum yield strength of the web (MPa)
f_c	= stress in the compression flange due to the factored loading under investigation (MPa)
f_c'	= specified compressive strength of concrete at 28 days (MPa)

f_{cf}	=	maximum compressive elastic flexural stress in the compression flange due to the unfactored permanent load and the fatigue load (MPa)
f_{cw}	=	maximum compressive flexural stress in the web (MPa)
f_u	=	flexural stress in the compression or tension flange due to the factored loading, whichever flange has the maximum ratio of f_u to F_r in the panel under consideration (MPa)
f_y	=	specified minimum yield strength of reinforcing bars (MPa)
g	=	acceleration of gravity (m/s^2)
H	=	horizontal shear (kN)
H_{DSGN}	=	design horizontal shear force (kN)
H_{EQ}	=	horizontal shear force due to seismic load (kN)
$H_{EXTR.\ EVENT\ I}$	=	horizontal shear force from Extreme Event I load combination (kN)
H_{LL}	=	horizontal shear force due to live load (kN)
$H_{STR.\ I}$	=	horizontal shear force from Strength I load combination (kN)
h	=	column height (m); height of a shear stud (mm)
I	=	moment of inertia (mm^4)
I_g	=	moment of inertia of the gross concrete section about the centroidal axis (mm^4)
I_{nc}	=	moment of inertia of the non-composite steel section (mm^4)
J	=	torsional inertia (mm^4)
K	=	bridge lateral stiffness (N/mm); effective length factor for compression members
K_h	=	hole size factor for bolted connections
$K\ell_u/r$	=	slenderness ratio
K_s	=	surface condition factor for bolted connections
k	=	plate buckling coefficient; shear buckling coefficient; elastic bend-buckling coefficient for the web
L	=	total length of bridge (mm)
L_c	=	clear distance between holes or between the hole and the end of the member in the direction of the applied bearing force (mm)
LL	=	designation for vehicular live load
ℓ_d	=	development length (mm)
ℓ_{db}	=	basic development length for straight reinforcement to which modification factors are applied to determine ℓ_d (mm)
ℓ_u	=	unsupported length of a compression member (mm)
M	=	moment (kN-m)
$M_{BOTT.}$	=	moment at bottom of column (kN-m)
M_c	=	factored moment, corrected to account for second-order effects (kN-m)
M_{CL}	=	girder moment at centerline of pier cap (kN-m)
M_{DC}	=	unfactored moment due to structural components and nonstructural attachments (kN-m)
M_{DC1}	=	unfactored moment due to DC loads applied to the non-composite steel section (kN-m)
M_{DC2}	=	unfactored moment due to DC loads applied to the long-term composite section (kN-m)
M_{DSGN}	=	design moment for flange splice plates (kN-m)
M_{DW}	=	unfactored moment due to wearing surfaces and utilities (kN-m)
$M_{ELASTIC}$	=	elastic seismic moment (kN-m)
$+M_{ELASTIC}$	=	elastic seismic moment for the positive moment section of a girder (kN-m)
$-M_{ELASTIC}$	=	elastic seismic moment for the negative moment section of a girder (kN-m)
M_{EQ}	=	moment due to seismic load (kN-m)
M_L	=	moment in the longitudinal direction or about the transverse axis of the bridge (kN-m)
M_{LEQ}	=	moment due to longitudinal earthquake load (kN-m)
M_{LL}	=	moment due to live load (kN-m)
$M_{MOD.}$	=	modified design moment (kN-m)
M_n	=	nominal moment resistance (kN-m)
$M_{OVRSTR.}$	=	column overstrength moment resistance associated with plastic hinging of the column (kN-m)
$M_{SERV.\ II}$	=	moment from Service II load combination (kN-m)
M_T	=	moment in the transverse direction or about the longitudinal axis of the bridge (kN-m)
M_{TEQ}	=	moment due to transverse earthquake load (kN-m)
M_{TOP}	=	moment at top of column (kN-m)
M_u	=	factored design moment (kN-m)

M_{2b}	=	moment on compression member due to factored gravity loads that result in no appreciable sidesway calculated by conventional first-order elastic frame analysis; always positive (kN-m)
M_{2s}	=	moment on compression member due to factored lateral or gravity loads that result in sidesway, Δ, greater than $\ell_u/1500$, calculated by conventional first-order elastic frame analysis; always positive (kN-m)
N_s	=	number of slip planes per bolt; number of shear planes per bolt
P	=	axial load (kN)
P_{DC}	=	unfactored axial dead load due to structural components and nonstructural attachments (kN)
P_{DL}	=	axial dead load (kN)
P_{DSGN}	=	design force for flange splice plates (kN)
P_{DW}	=	unfactored axial dead load due to wearing surfaces and utilities (kN)
P_e	=	Euler buckling load (kN)
P_{LL}	=	axial live load (kN)
P_n	=	nominal compressive axial resistance and columns and nominal tensile resistance and splice plates (kN)
$P_{SERV. II}$	=	force from Service II load combination (kN)
P_t	=	minimum required bolt tension (N)
P_u	=	factored axial load (kN)
p_e	=	equivalent uniform static seismic loading per unit length of bridge applied to represent the primary mode of vibration (N/mm)
p_o	=	a uniform load arbitrarily set equal to 1.0 (N/mm)
Q_n	=	nominal shear strength of a shear connector (kN)
q	=	shear flow (kN/m)
R	=	seismic response modification factor; shear interaction factor
R_b, R_h	=	flange stress reduction factors
R_n	=	nominal resistance of bolt, connection, or connected material (kN)
R_u	=	factored force on bolt, connection, or connected material (kN)
r	=	radius of gyration (mm)
S	=	coefficient related to site conditions for use in determining seismic loads; elastic section modulus (mm^3); spacing between interior beams (m)
S_{nc}	=	Section modulus of the non-composite steel section (mm^3)
s	=	spacing of spiral reinforcing (mm); bolt spacing (mm)
T	=	torsion (kN-m)
T_{EQ}	=	torsion due to seismic load (kN-m)
T_{LL}	=	torsion due to live load (kN-m)
T_m	=	period of bridge (s)
T_u	=	factored torsion (kN-m)
t	=	deck thickness (mm); plate thickness (mm); thickness of the thinner outside plate or shape (mm)
t_f	=	compression flange thickness (mm)
$t_{SPLICE PL.}$	=	splice plate thickness (mm)
t_w	=	web thickness (mm)
U	=	reduction factor for shear lag
V	=	shear force (kN)
V_{AXIAL}	=	shear force resulting from column axial load (kN)
V_c	=	nominal shear resistance of the concrete (kN)
V_{DC}	=	unfactored shear due to structural components and nonstructural attachments (kN)
V_{DC1}	=	unfactored shear due to DC loads applied to the non-composite steel section (kN)
V_{DC2}	=	unfactored shear due to DC loads applied to the long-term composite section (kN)
V_{DL}	=	shear due to dead load (kN)
V_{DSGN}	=	design shear force for the connection (kN)
V_{DW}	=	unfactored shear due to wearing surfaces and utilities (kN)
V_{EQ}	=	shear due to seismic load (kN)
$V_{EXTR. EVENT I}$	=	shear from Extreme Event I load combination (kN)
V_f	=	shear due to flexure (kN)
V_{LEQ}	=	shear due to longitudinal earthquake load (kN)
V_{LL}	=	shear due to live load (kN)
$V_{LONG. MOM.}$	=	shear force resulting from column longitudinal moment (kN)

V_n	= nominal shear resistance (kN)
V_p	= plastic shear capacity (kN)
V_s	= shear resistance provided by shear reinforcement (kN)
$V_{SERV. II}$	= shear from Service II load combination (kN)
$V_{s,MAX}$	= maximum displacement corresponding to p_o (mm)
V_{sr}	= shear force range determined for the fatigue limit state (kN)
$V_{STR. I}$	= shear for Strength I load combination (kN)
V_T	= shear due to torsion (kN)
V_{TEQ}	= shear due to transverse earthquake load (kN)
$V_{TRANSV. MOM.}$	= shear force resulting from column transverse moment (kN)
V_u	= factored shear force (kN)
W	= total nominal, unfactored dead load of the bridge superstructure and tributary substructure (N)
w	= width of compression flange between longitudinal stiffeners or distance from the web to the nearest longitudinal stiffener (mm); width of pier cap between web plates (m)
Z_r	= shear fatigue strength of a shear connector (kN)
α	= offset factor
β	= factor indicating ability of diagonally cracked concrete to transmit tension
β_d	= ratio of maximum factored permanent load moments to maximum factored total load moment, always positive
Δ	= sidesway (mm)
$(\Delta F)_n$	= nominal fatigue resistance (MPa)
$(\Delta F)_{TH}$	= constant amplitude fatigue threshold (MPa)
(Δf)	= live load stress range due to the passage of the fatigue load (MPa)
$(\Delta M)_{FATIGUE}$	= range in live load moment due to the passage of the fatigue load (kN-m)
$(\Delta M_L)_{FATIGUE}$	= range in longitudinal column live load moment due to the passage of the fatigue load (kN-m)
$(\Delta M_T)_{FATIGUE}$	= range in transverse column live load moment due to the passage of the fatigue load (kN-m)
$(\Delta P)_{FATIGUE}$	= range in axial live load due to the passage of the fatigue load (kN)
δ_b	= moment magnifier for braced mode deflection
δ_s	= moment magnifier for unbraced mode deflection
γ	= load factor for the fatigue load combination
γ_{EQ}	= load factor for live load in Extreme Event Load Combination I
γ_P	= load factor for permanent loads
φ	= resistance factor
φ_f	= resistance factor for flexure
φ_{sc}	= resistance factor for shear connectors
φ_u	= resistance factor for fracture of tension members
φ_y	= resistance factor for yielding of tension members
λ_b	= coefficient related to b/t ratio
θ	= angle of inclination of diagonal compressive stresses (DEG)
ρ_s	= volumetric ratio of spiral reinforcing

I3 GENERAL OVERVIEW

The primary components of a bridge having girders integral with an intermediate pier are shown in Figures I-1 and I-2. The following is an overview of the design procedure for bridges having girders integral with intermediate piers:

A. Develop general bridge dimensions (e.g., roadway width, span arrangements, girder spacing, and column height).
B. Determine preliminary member sizes.
C. Determine member forces for all applicable loads.
D. Design column for controlling load combinations in accordance with current AASHTO LRFD Specifications and the proposed specifications herein. As discussed previously in the report, intermediate piers will typically consist of single column bents for which the proposed specifications apply. Multi-column bent applications will be rare, except in the case of outriggers; therefore, multi-column bents are not covered by the proposed specifications or within the design example. However, as mentioned in the body of the report and in Appendices A
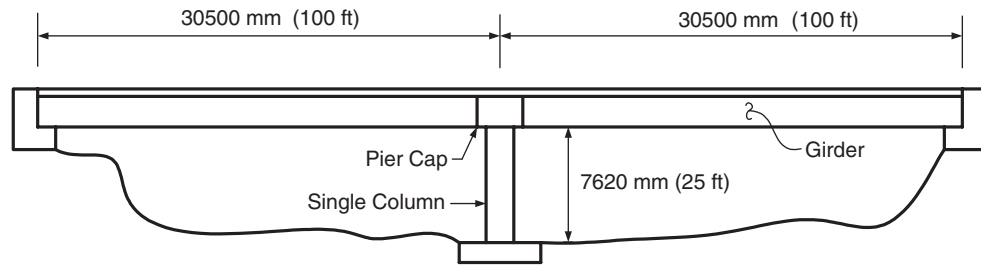
Figure I-1.   Bridge elevation.

through H, which are provided on the accompanying CD-ROM, the design process of the integral connection is applicable to multi-column piers and their integral connections. Once the analyses are completed, the main difference between single-column piers and multi-column piers is that the top regions of the columns in multi-column piers are subjected to significant moments in both the longitudinal and transverse directions while these regions in single-column piers are essentially subjected to longitudinal moments. The column transverse moments may be transferred to the pier cap using the same procedure illustrated in this example for the longitudinal moment of the single-column pier.

E. For bridges located within seismic regions, check preliminary girder sizes for forces from the Strength and Extreme Event I limit states. The design forces due to seismic loading shall be taken as the lesser of the forces from an elastic analysis divided by the applicable response modification factor or those associated with the plastic hinging of the column.

F. Design cap beam in accordance with current box-beam design provisions in the AASHTO LRFD Specifications. For seismic loads, design for the lesser of the elastic forces divided by the applicable response modification factor or those associated with the plastic hinging of the column. Notice that the cap beam is subjected to vertical and horizontal shear forces and the moments associated with them. It is also subjected to torsion. The magnitude of torsion transferred to the pier cap at each girder location is equal to the algebraic difference in girder moment at either face of the pier cap as shown in Figure I-3. The moment at the top of the column is equal to the sum of the torsional moments applied to the pier cap. Figure I-4 shows schematically the torsional moments on the pier cap and the column top moment.

G. Design the girder-to-cap beam connection components shown in Figure I-5.
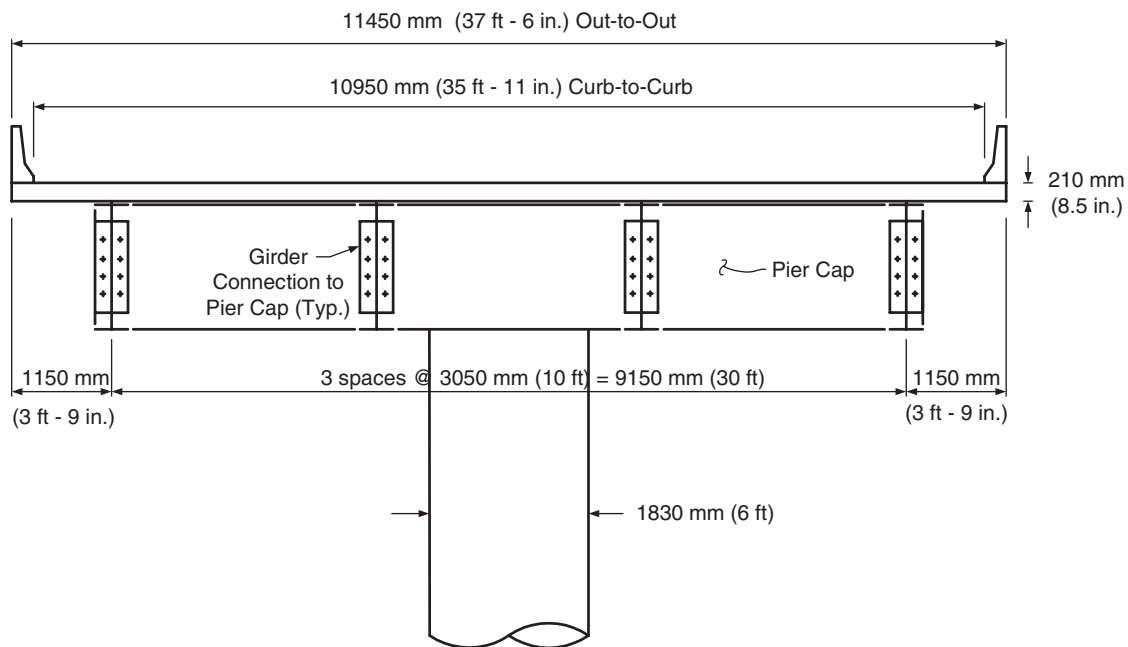
Figure I-2.   Bridge cross section.

Figure I-3. *Girder moments and pier cap torsion.*

Girder Design Moments

Theoretical Moment Diagram

Torsion transferred from girder to pier cap

Pier Cap

Girder

Column

Figure I-3.   Girder moments and pier cap torsion.

Torsion transferred to pier cap at girder location (Typ.)

Longitudinal moment at top of column equal to sum of torsional moments
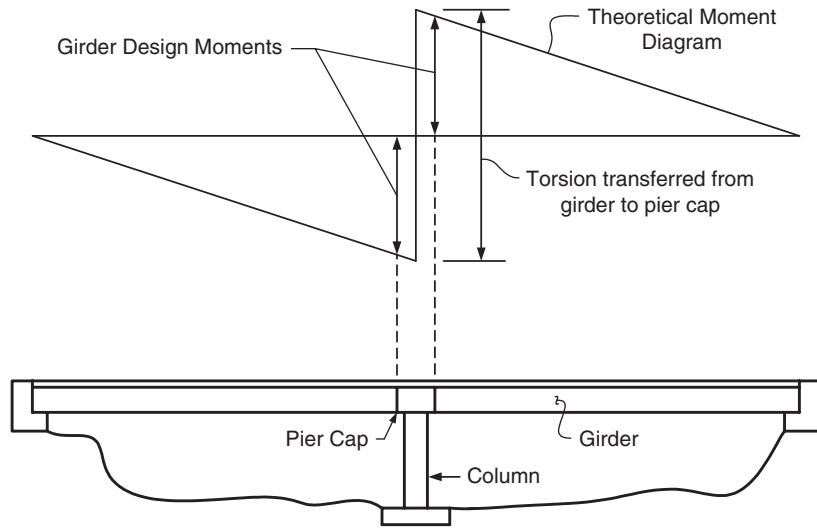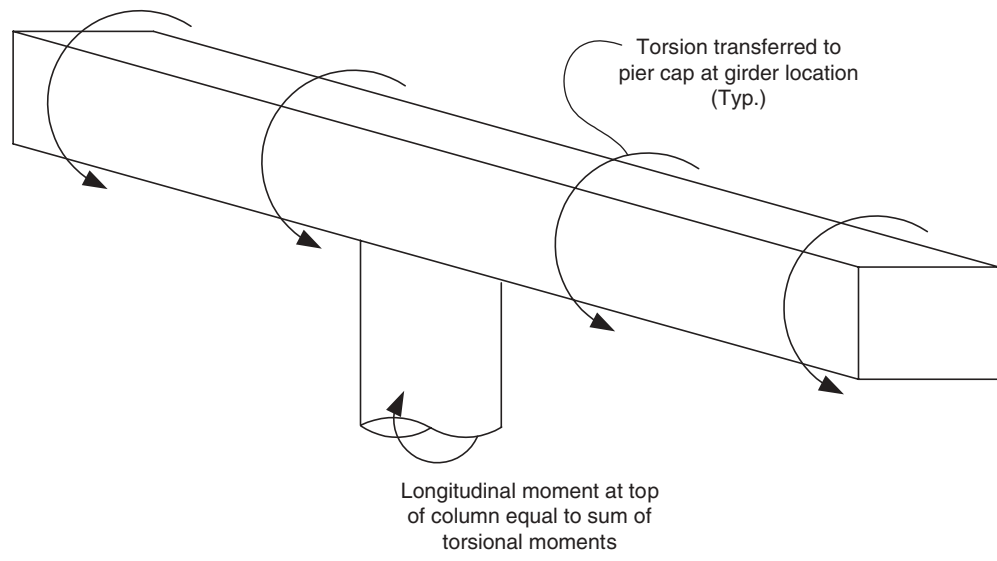
Figure I-4.   Pier cap torsion and column moment.

Intermediate diaphragm

Flange splice plate for moment

Bolted double-angle connection for shear
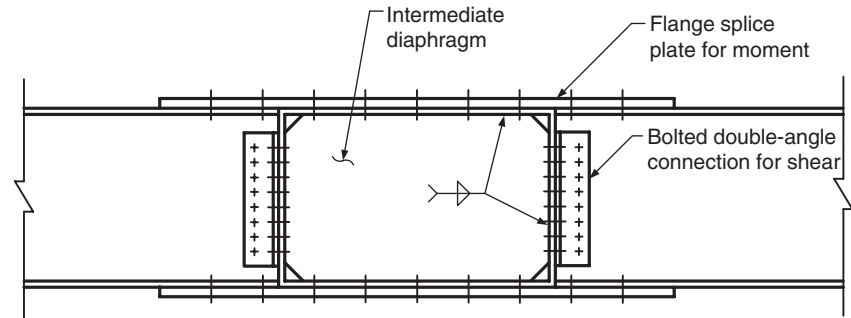
Figure I-5.   Girder-to-cap beam connection.

1. Design double-angle bolted connection for the maximum vertical shear in the girders.
2. Design flange splice plates for the maximum negative moment in the girders. The design force for the splice plates shall be taken equal to the maximum negative girder moment divided by the girder depth as shown in Figure I-6.
3. Design splice plate connection to cap beam. The design shear force for the connection shall be taken equal to the maximum torsion transferred to the pier cap divided by the depth of the pier cap as shown in Figure I-6.

H. Design shear studs for column-to-cap beam connection (see Figure I-7).
1. Design shear studs located on bottom flange plate. Design these studs for the maximum horizontal shear at the top of the column (Figure I-7).
2. Design shear studs located on web plates of cap beam. These studs are designed for the shear produced from the longitudinal moment and axial load at the top of the column as shown in Figure I-8.
3. Design shear studs located on diaphragm plates. These studs shall be designed for the shear originating from the transverse moment at the top of the column as shown in Figure I-9.

I4 DESIGN PARAMETERS

The dimensions of the bridge are as shown in Figures I-1 and I-2. As shown in Figure I-1, the bridge is a two-span continuous structure with 30,500-mm (100-ft) span lengths. As shown in Figure I-2, the superstructure consists of a 210-mm (8.5-in.) thick cast-in-place reinforced concrete deck [10 mm (0.5 in.) of which is assumed nonstructural for an integral wearing surface in accordance with **Article 2.5.2.4**] supported by four steel I-girders spaced at 3,050 mm (10 ft). The girders are integral with a steel box-beam pier cap supported by a single reinforced concrete column. The column is 7,620 mm (25 ft) in height from the bottom of the pier cap to the top of the footing.

Concrete for the deck and column was assumed to have a 28-day strength of 28 MPa (4 ksi). Unless noted otherwise, all structural steel was assumed to be ASTM A 709M (A 709), Grade 345W (50W).

The bridge is located in Seismic Performance Zone 4 and will be designed for the greatest of either Extreme Event I or Strength I limit state forces. Only dead, live, and earthquake loads were considered.

I5 PRELIMINARY DESIGN

I5.1 I-Girders

A conventional line girder design/analysis program was used to obtain preliminary plate sizes for the girders based on dead and live load requirements. The program does not take into account the effect of the integral connection on the girder loads. Initial plate sizes for both an interior and exterior girder were based on a design run for an interior girder of the bridge and are shown in Figure I-10. Final girder design will consist of a check on girder moments obtained

M_{RT} = Girder moment, right side
M_{LT} = Girder moment, left side
P_{RT} = Flange splice plate force, right side = M_{RT} / d
P_{LT} = Flange splice plate force, left side = M_{LT} / d
T = Torsion on pier cap = $M_{RT} + M_{LT}$
V = Splice plate connection force
$V = P_{RT} + P_{LT} = (M_{RT} + M_{LT})/d = T/d$
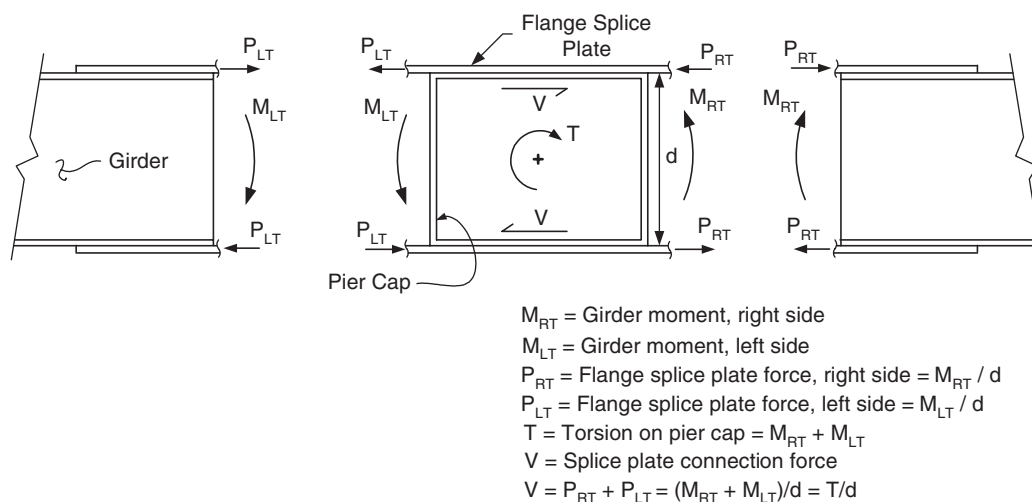
Figure I-6.   Splice plate and splice plate connection forces.

Section A-A
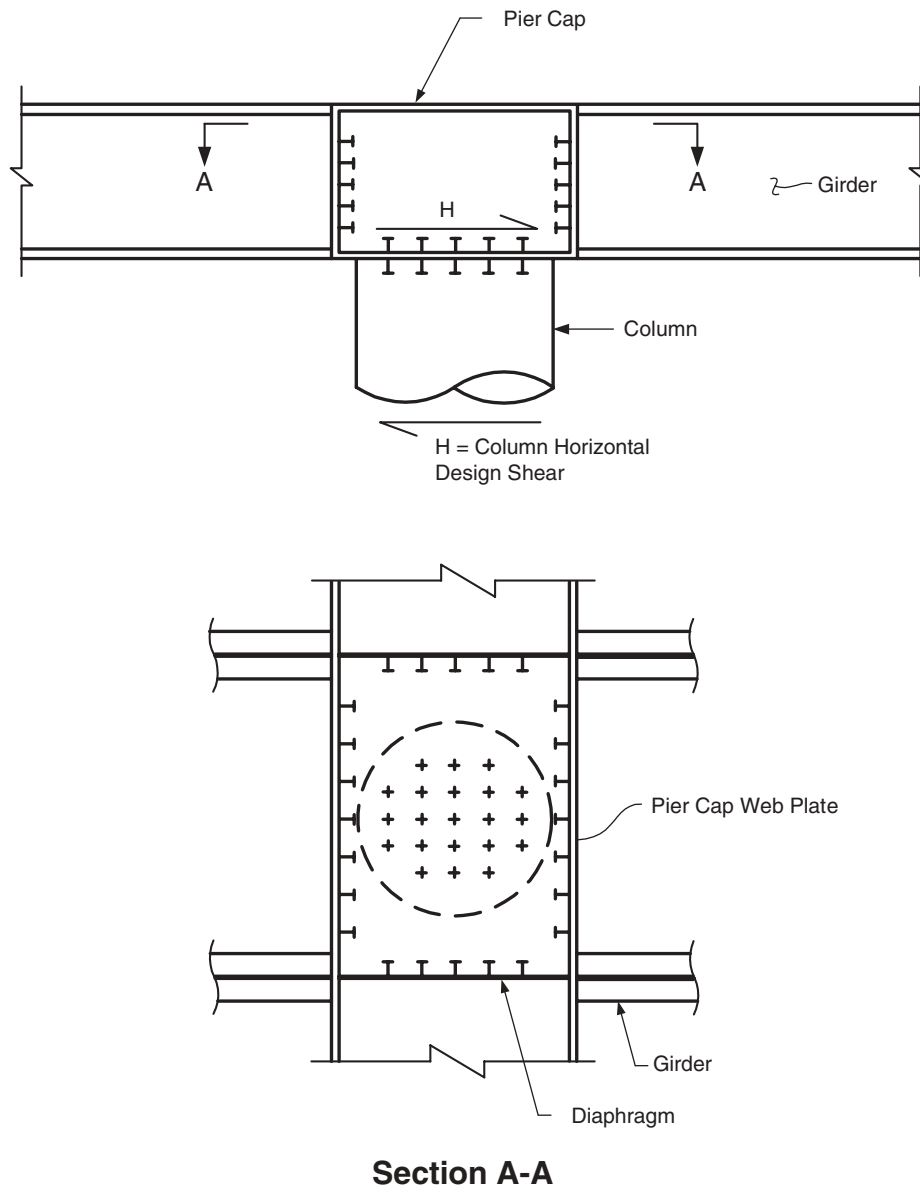
Figure I-7.   Shear studs for column-to-cap beam connection.

from a computer model that incorporates the stiffness of the pier cap and the rigid connection between the cap beam and girders.

I5.2 Column

An initial column diameter of 1,830 mm (6 ft) was selected based on past experience and preliminary design.

I5.3 Pier Cap

The dimensions of the pier cap, as shown in Figure I-11, were controlled by the size of the column and girders. The width of the pier cap is controlled by the diameter of the column and was set equal to the column diameter plus 225 mm (9 in) on each side of the column. The additional width of the cap is required to provide construction tolerance and to provide additional space for the cap beam to column connection steel. The height of the pier cap is set equal to the depth
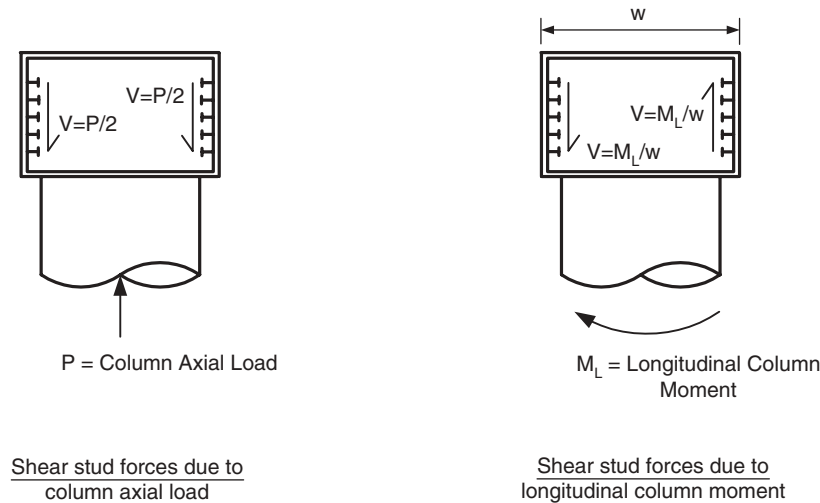
Figure I-8.   Shear forces acting on shear studs located on web plates of cap beam.

of the girders in the negative moment region. This enables the connection of a splice plate to the outside of the girder flanges and to the flange plate of the pier cap for the transfer of moment across the width of the pier cap. The initial plate thickness of the pier cap was selected to prevent buckling of the compression flange under maximum negative moment in accordance with **Article 6.11.2.1.3a** of the AASHTO LRFD Specifications.

I6 COMPUTER MODEL

Under live loading, the vertical movement of the pier cap and the rigid connection between the pier cap and the girders will cause a bridge with an integral pier cap to differ from a conventional structure in three main areas. These areas are: the magnitude and location of maximum positive and negative bending moments in the girders, the maximum negative bending moments and torsion in the pier cap, and the maximum moments in the pier. In addition, the ratio between the moments in the interior and exterior girders will be different compared to this ratio for a conventional structure.
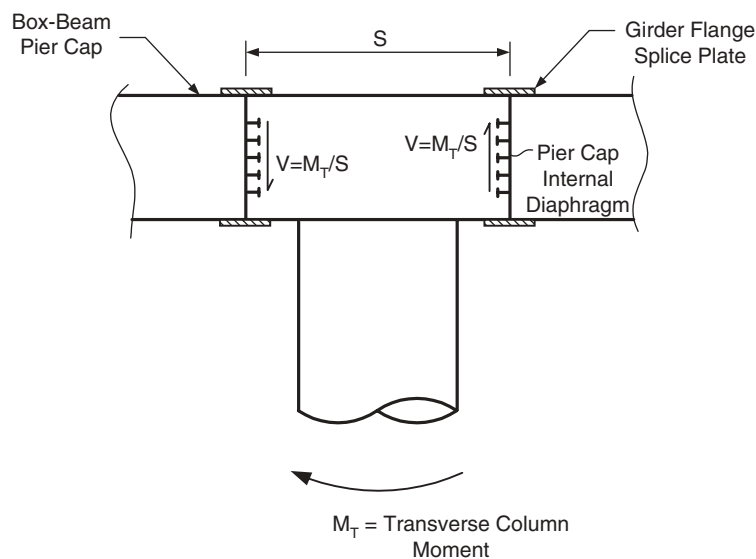
Figure I-9.   Shear forces acting on shear studs located on internal diaphragms of pier cap.

21350 mm (70 ft)   18300 mm (60 ft)   21350 mm (70 ft)

A   B

A   B

305 mm (12 in.)

12 mm (0.5 in.)

12 mm (0.5 in.)

1372 mm (54 in.)

25 mm (1 in.)

Section A-A
Positive Moment Region

380 mm (15 in.)

50 mm (2 in.)

12 mm (0.5 in.)

1372 mm (54 in.)

50 mm (2 in.)

Section B-B
Negative Moment Region
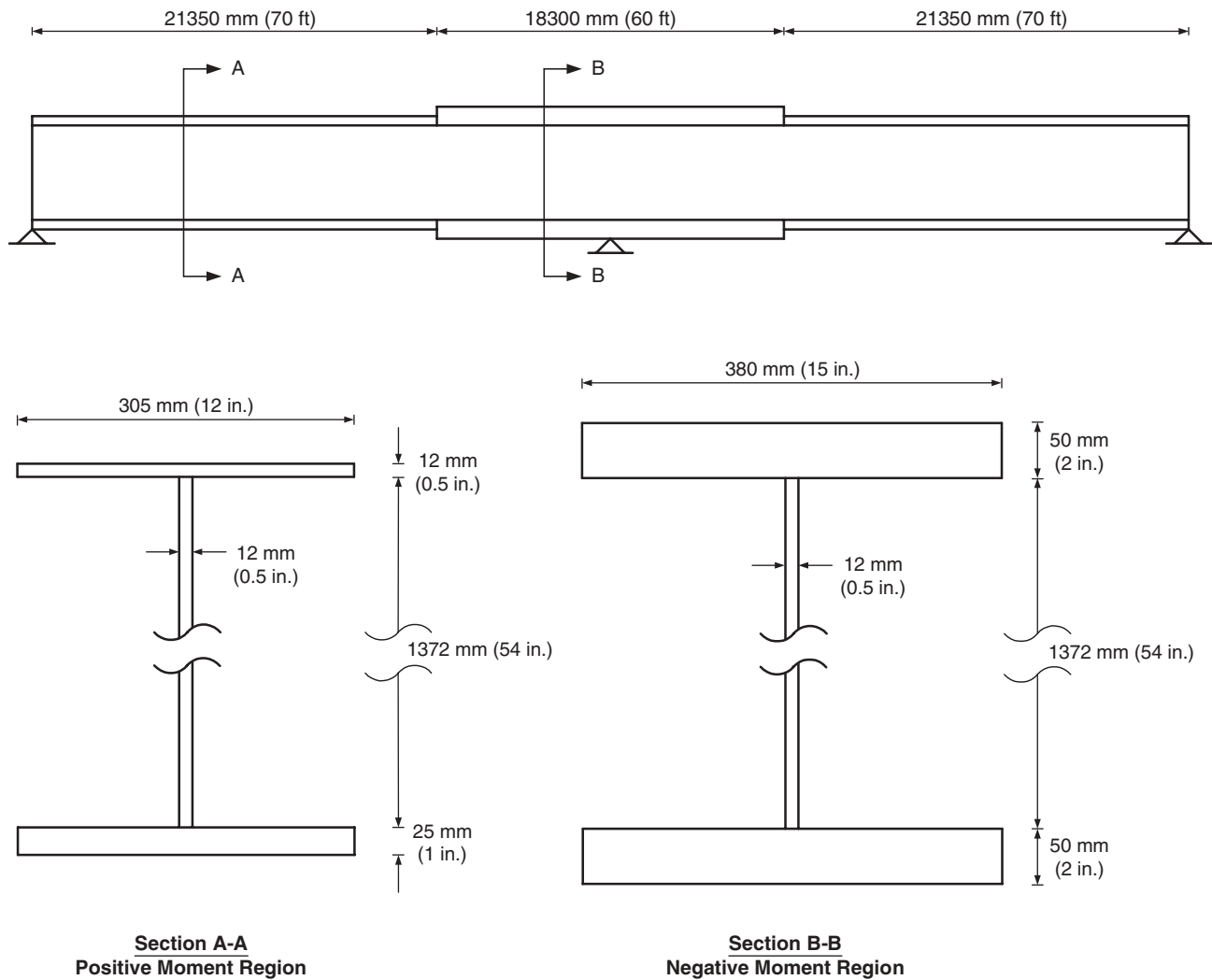
Figure I-10. Preliminary girder dimensions.

For these reasons, a computer model of the structure was created for the purpose of determining the maximum live load forces in the components of the bridge. In addition, the model was also used to determine seismic forces within the bridge, although these forces could have been computed by hand.

I6.1 Description of Model

For the live load analysis of the bridge, a grillage model of the structure was created using the commercial software program SAP2000. In a grillage model, all parts of the bridge are modeled using beam elements. In particular, the structural behavior of the concrete deck is included in the model by placing transverse beams between the main girders with flexural and torsional properties that mimic the action of the deck. This type of approach will give accurate results that are easy to interpret. Figure I-12 provides an overall view of the model. As shown in Figure I-12, roller supports allowing longitudinal movement but restraining transverse movement were assumed for the girders at the abutment locations and the column was assumed fixed at its base. Section properties for elements used in the model are given in Table I-1.

I6.1.1 Girders

Girders were modeled using beam elements positioned at the neutral axis location for the actual composite girder. Per **Article 4.5.2.2** and the corresponding commentary, section properties for the girders were determined assuming

I-16

2280 mm (7 ft - 6 in.)

30 mm
(1.25 in.)

1472 mm
(4 ft - 10 in.)

30 mm
(1.25 in.)
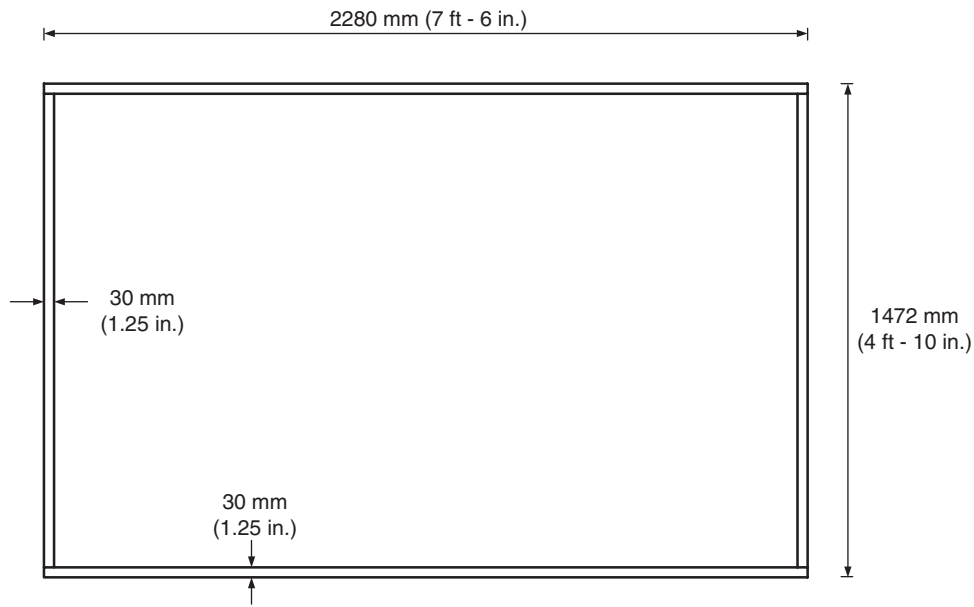
Figure I-11.   Preliminary cap beam dimensions.

uncracked sections and that the girders were composite along their entire length. Since the model is being used for live load analysis, section properties correspond to the short-term composite section (n = 8). Both flexural and torsional properties were included. A haunch thickness equal to zero was assumed in calculating section properties.

Where the girders frame into the pier cap, rigid links were used to account for the difference in neutral axis location between the two elements. Although the steel girders and pier cap have the same depth, the neutral axis of the girders is higher than that for the pier cap due to the composite action of the concrete deck. Thus, an end rotation of the gird-
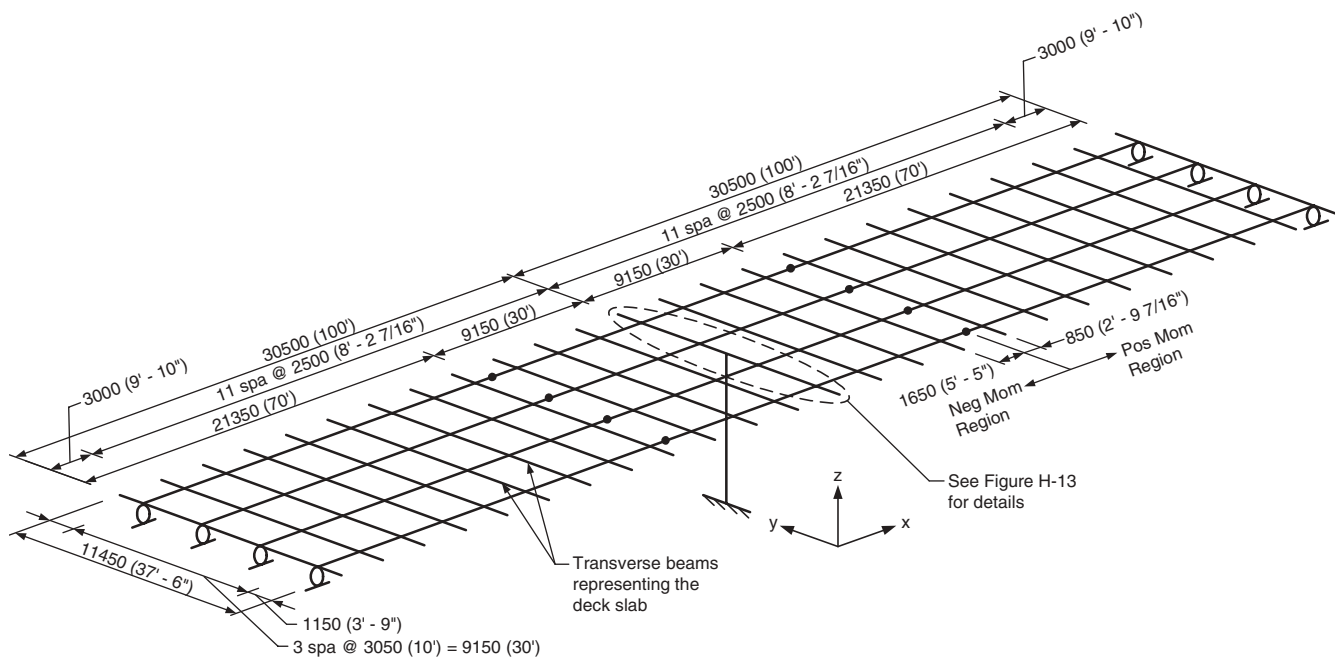
Note: All dimensions are in mm unless noted otherwise.

Figure I-12.   SAP2000 schematic.

TABLE I-1 Element section properties for computer model

Element Type	Material	A mm^2 (in^2)	I$_{vert.}$ x10^9 mm^4 (in^4)	I$_{horiz.}$ x10^9 mm^4 (in^4)	J x10^9 mm^4 (in^4)	Shear Area mm^2 (in^2)
Column	Concrete	2,630,220 (4,077)	550.5 (1,322,582)	550.5 (1,322,582)	1,101 (2,645,163)	----
Int. Bm. – Pos. Mom.	Steel	91,549 (141.9)	34.75 (83,487)	23.60 (56,699)	0.4888 (1,174)	----
Int. Bm. – Neg. Mom.	Steel	119,264 (184.9)	36.65 (88,052)	42.70 (102,587)	0.5046 (1,212)	----
Ext. Bm. – Pos. Mom.	Steel	88,349 (136.9)	30.11 (72,340)	23.34 (56,075)	0.4648 (1,117)	----
Ext. Bm. – Neg. Mom.	Steel	115,664 (179.3)	31.22 (75,006)	42.15 (101,266)	0.4982 (1,197)	----
Pier Cap	Steel	221,520 (343.4)	166.5 (400,018)	85.20 (204,694)	171.1 (411,069)	88,320 (136.9)
Deck	Concrete	500,000 (775.0)	260.4 (625,614)	1.670 (4,012)	3.330 (8,000)	----
Cross Frame	Steel	68,120 (105.6)	260.4 (625,614)	2.760 (6,631)	0.4760 (1,144)	----

ers will introduce a small longitudinal displacement of the pier cap and the pier. The connection between the pier cap and girders is shown in Figure I-13.

I6.1.2 Slab and Cross Frames

The slab was modeled by beam elements spanning transversely across the width of the bridge. Each slab element models the effect of a 2,500 mm (8 ft – 2^7/$_{16}$ in.) wide strip of concrete deck and is rigidly connected to the girder elements. The moment of inertia for the slab elements is taken as the conventional second moment of area. The torsional constant, J, is given by the following equation:

$$J = bt^3/6$$

Where

b = width of the deck represented by the element (mm)
t = thickness of the deck (mm)

The cross frames in the bridge, which occur at 0; 8,000; 15,500; and 23,000 mm (0 ft; 26 ft – 3 in.; 50 ft – 10^1/$_4$ in.; 75 ft – 5^1/$_2$ in.) along the length of each span starting from the abutment, were modeled by using equivalent beams. In determining the moment of inertia for the equivalent beams, the cross frames were analyzed as a truss. The moment of inertia for the equivalent beam was then taken as that which produced the same deflection as the truss when both
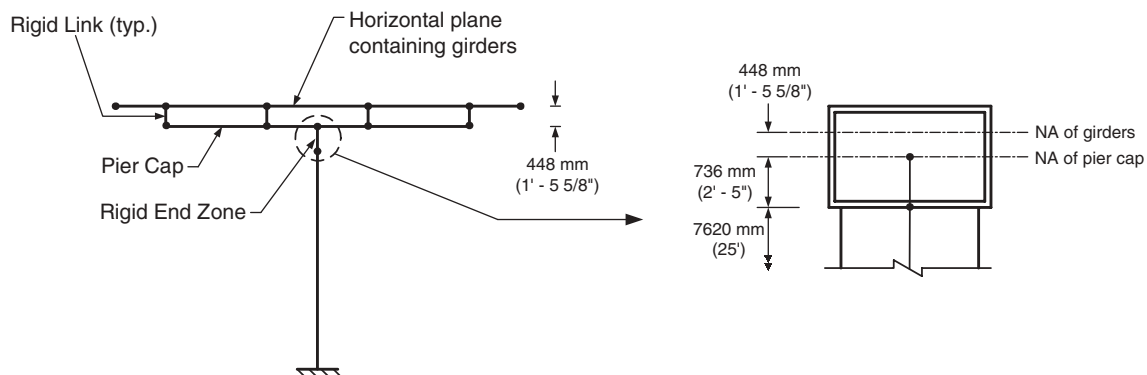
Figure I-13.   Modeling details.

were subjected to the same loading conditions. The torsional constant for the equivalent beam was simply taken as that for the slab contributory to the element.

I6.1.3 Pier Cap and Column

The integral pier cap was modeled with beam elements. The pier cap is short and heavily loaded, therefore, deflections due to shear will be significant and including the effect of shear deformation will improve the accuracy of the results. By entering a value for the shear area of the element, SAP2000 will consider shear deformations in the analysis. The shear area of the pier cap was taken equal to the area of the two side plates.

The reinforced concrete column was modeled using beam elements. The column is assumed fixed at its base and is rigidly connected to the cap beam. A rigid end offset was used at the top of the column to account for the connection region where the column frames into the cap beam as shown in Figure I-13. The column stiffness was calculated based on an uncracked section. However, using a cracked section of the column to reflect the expected cracking under seismic loading is also acceptable. See Appendix D on the accompanying CD-ROM for further discussion regarding the use of cracked sections.

I7 DEAD LOAD ANALYSIS

Since the structure is symmetric under dead loads, the slope of the girders at the pier cap is zero and the column sees no moment. Since the moment in the column is zero, the flexural stiffness of the column and the torsional stiffness of the pier cap do not influence the behavior of the structure. However, the pier cap will deflect vertically and this will affect the distribution of forces between the girders and the magnitude and location of maximum design forces. Since the pier cap is relatively stiff, the deflection will be small and its effect on the behavior of the structure under dead load may be neglected.

To confirm this conclusion, a study was performed to determine the influence of the pier cap deflection on member forces and support reactions. In the study, forces and reactions computed from a line girder analysis program assuming nonyielding supports were compared to the results obtained from a detailed computer model of the structure similar to that discussed in Section I6.1. Since the deflection of the pier cap is greatest at an exterior girder, the study was performed for an exterior girder only. The results of the study are presented in Tables I-2 and I-3 and pertain to dead loads applied to the noncomposite section.

From Table I-2, one can see that the percent difference between the support reactions obtained from the two different types of analyses is small. In addition, except within a small region of the girder, the percent difference between dead load forces is also small, as shown in Table I-3. The location along the girder where the percent difference between dead load forces is high is were the magnitude of the force is small and therefore not critical to the design of the girder. Therefore, in analyzing the structure for dead loads, the influence of the deflection of the pier cap on member forces and reactions can be ignored and the structure can be treated as a conventional two-span structure with nonyielding supports.

For this design example, a conventional line girder analysis program was used to determine dead load forces and reactions. Three separate runs were performed. These runs included: DC1 loads applied to the noncomposite steel section and DC2 and DW loads applied to the long-term composite (3n = 24) section. Dead loads used in the runs are given in Table I-4. DC1 loads consisted of the weight of the girder, miscellaneous steel, slab, and haunch. DC2 loads consisted of the weight of the parapet only. The future wearing surface (FWS) represents the DW load.

For situations where the integral pier connection is not at the axis of symmetry (e.g., bridges with unequal spans) the pier cap will experience torsion and the column will be subjected to moment and shear for any dead loads applied after the joint region above the column has been poured. To determine the forces throughout the structure, a 2-dimensional frame analysis as indicated in the proposed specifications could be performed. Alternatively, a 3-dimensional refined analysis that takes into account the flexural stiffness of the column and the torsional stiffness of the pier cap could be used.

TABLE I-2 Noncomposite dead load reactions

	Line Girder Analysis Program	3-D Computer Model	Percent Difference
Reaction at Abutment, kN (kips)	160.94 (36.18)	167.21 (37.59)	+3.90%
Reaction at Pier, kN (kips)	677.53 (152.32)	668.16 (150.21)	-1.38%

TABLE I-3   Noncomposite dead load forces

Distance from Abut. m (ft)	Moment, kN-m (k-ft)			Shear, kN (kips)		
	Girder Analysis Program	Computer Model	Percent Difference	Girder Analysis Program	Computer Model	Percent Difference
0 (0)	0 (0)	0 (0)	----	160.94 (36.18)	167.21 (37.59)	3.90%
3 (9.8)	411.51 (303.53)	430.31 (317.40)	4.57%	113.39 (25.49)	119.66 (26.90)	5.53%
5.5 (18.0)	645.47 (476.10)	679.93 (501.52)	5.34%	73.77 (16.58)	80.04 (17.99)	8.50%
8 (26.2)	780.36 (575.59)	830.49 (612.57)	6.42%	34.14 (7.67)	40.41 (9.08)	18.37%
10.5 (34.4)	816.19 (602.02)	861.07 (635.12)	5.50%	-5.48 (-1.23)	-7.58 (-1.70)	38.32%
13 (42.7)	752.96 (555.38)	792.58 (584.61)	5.26%	-45.11 (-10.14)	-47.21 (-10.61)	4.66%
15.5 (50.9)	590.66 (435.67)	625.03 (461.02)	5.82%	-84.73 (-19.05)	-86.83 (-19.52)	2.48%
18 (59.1)	329.31 (242.90)	340.90 (251.45)	3.52%	-124.36 (-27.96)	-133.46 (-30.00)	7.32%
20.5 (67.3)	-31.11 (-22.95)	-42.29 (-31.19)	35.94%	-163.98 (-36.87)	-173.09 (-38.91)	5.56%
21.35 (70.05)	-176.22 (-129.98)	-195.14 (-143.94)	10.74%	-177.45 (-39.89)	-186.56 (-41.94)	5.13%
23 (75.5)	-493.02 (-363.65)	-526.97 (-388.69)	6.89%	-206.54 (-46.43)	-215.65 (-48.48)	4.41%
25.5 (83.7)	-1064.47 (-785.15)	-1086.71 (-801.56)	2.09%	-250.62 (-56.34)	-245.93 (-55.29)	1.87%
28 (91.9)	-1746.10 (-1287.92)	-1756.64 (-1295.70)	0.60%	-294.69 (-66.25)	-290.01 (-65.20)	1.59%
30.5 (100.1)	-2537.93 (-1871.97)	-2536.76 (-1871.11)	0.05%	-338.77 (-76.16)	-334.08 (-75.11)	1.38%

For dead loads applied prior to pouring the joint region, there is no means by which forces can be transferred to the column. Since the column sees no moment, the effect of the flexural stiffness of the column and the torsional stiffness of the pier cap on the behavior of the structure can be ignored and the structure can be treated as a conventional structure with nonyielding supports.

I8 SEISMIC ANALYSIS

I8.1 Seismic Design Parameters

For this design example, assume the following parameters:

Acceleration coefficient, A = 0.4
Importance category = essential
Site coefficient, S = 1.2 (Soil Profile Type II)

For an acceleration coefficient greater than 0.29, the bridge is assigned to Seismic Zone 4 in accordance with **Table 3.10.4-1**.

I8.2 Method of Analysis

Per **Table 4.7.4.3.1-2**, the bridge may be taken as regular since it is on tangent and the span length ratio from span to span is less than 3. From **Table 4.7.4.3.1-1**, for a multi-span, essential, regular bridge assigned to Seismic Zone 4, the minimum required method of analysis is the multi-mode spectral method.

Typically, regular bridges will respond principally in their fundamental mode of vibration. Bridges that respond to earthquake ground motion in their fundamental modes of vibration can be analyzed by single mode methods such as

TABLE I-4   Uniform dead loads, N/mm (kip/ft)

	DC1				DC2	DW
	Girder	Misc. Steel[a]	Slab	Haunch[b]	Parapet	FWS[c]
Int. Bm. – Pos. Mom.	2.14 (0.15)	0.21 (0.01)	15.08 (1.03)	0.27 (0.02)	4.74 (0.32)	4.49 (0.31)
Int. Bm. – Neg. Mom.	4.19 (0.29)	0.21 (0.01)	15.08 (1.03)	0.00 (0.00)	4.74 (0.32)	4.49 (0.31)
Ext. Bm. – Pos. Mom.	2.14 (0.15)	0.21 (0.01)	13.23 (0.91)	0.27 (0.02)	4.74 (0.32)	3.18 (0.22)
Ext. Bm. – Neg. Mom.	4.19 (0.29)	0.21 (0.01)	13.23 (0.91)	0.00 (0.00)	4.74 (0.32)	3.18 (0.22)

[a] Taken as 10% of the weight of the interior beam in the positive moment region.
[b] Taken as 38 mm (1.5 in.) in the positive moment region.
[c] Taken equal to 150 kg/^{2} (0.030 ksf) between curbs.

the single-mode spectral method or the uniform load method. Since this bridge is highly regular and quite simple geo-metrically, it will respond predominantly in its fundamental mode of vibration. Therefore, reasonably accurate seismic forces can be obtained from single mode methods of analysis. For this example, seismic analysis was performed using the uniform load method of **Article 4.7.4.3.2c**.

I8.3 Equivalent Transverse Static Earthquake Loading

Calculate the transverse lateral stiffness, K, of the bridge.

$$K = \frac{p_o L}{V_{s,MAX}}$$ **Eq. C4.7.4.3.2c-1**

From the SAP model, the maximum transverse displacement, $V_{s,MAX}$, resulting from a uniform load of 1 N/mm (0.068 kip/ft) is 0.154 mm (0.006 in.).

$$K = \frac{1(61,000)}{0.154} = 396,104 \text{ N/mm } (27,130 \text{ kip/ft})$$

Calculate the total weight, W. The total weight consists of the superstructure, pier cap, and half of the column. Half of the column is assumed tributary to the superstructure and the other half is assumed tributary to the foundation.

$$W = 2(42,700)22.44 + 2(42,700)20.59 + 2(18,300)24.22 + 2(18,300)22.37 + 19.54(9,150) + 61.93(7,620/2) + 61.93(1,412)$$

The quantity 61.93(1,412) accounts for the weight of the concrete in the pier cap above the column.

$$W = 5,882,145 \text{ N } (1,322 \text{ kips})$$

$$T_m = \frac{2\pi}{31.623}\sqrt{\frac{W}{gK}}$$ **Eq. C4.7.4.3.2c-3**

$$T_m = \frac{2\pi}{31.623}\sqrt{\frac{5,882,145}{9.81(396,104)}} = 0.244 \text{ s}$$

$$C_{sm} = \frac{1.2AS}{T_m^{2/3}} \leq 2.5A$$ **Eq. 3.10.6.1-1**

$$2.5A = 2.5(0.4) = 1.0$$

$$C_{sm} = \frac{1.2(0.4)1.2}{(0.244)^{2/3}} = 1.475 > 1.0 \quad \therefore C_{sm} = 1.0$$

$$p_e = \frac{C_{sm}W}{L} \qquad\qquad \textbf{Eq. C4.7.4.3.2c-4}$$

$$p_e = \frac{1.0(5,882,145)}{61,000} = 96.43 \text{ N/mm (6.60 kip/ft)}$$

I8.4 Equivalent Longitudinal Static Earthquake Loading

Calculate the longitudinal stiffness, K, of the bridge.

$$K = \frac{p_o L}{V_{s,MAX}} \qquad\qquad \textbf{Eq. C4.7.4.3.2c-1}$$

From the SAP model, the maximum longitudinal displacement, $V_{s,MAX}$, resulting from a uniform load of 1 N/mm (0.068 kip/ft) is 0.430 mm (0.017 in.).

$$K = \frac{1(61,000)}{0.430} = 141,860 \text{ N/mm (9,716 kip/ft)}$$

W = 5,882,145 N (1,322 kips) (from previous calculations in Section I8.3)

$$T_m = \frac{2\pi}{31.623}\sqrt{\frac{W}{gK}} \qquad\qquad \textbf{Eq. C4.7.4.3.2c-3}$$

$$T_m = \frac{2\pi}{31.623}\sqrt{\frac{5,882,145}{9.81(141,860)}} = 0.408 \text{ s}$$

$$C_{sm} = \frac{1.2AS}{T_m^{2/3}} \leq 2.5A \qquad\qquad \textbf{Eq. 3.10.6.1-1}$$

2.5A = 2.5(0.4) = 1.0

$$C_{sm} = \frac{1.2(0.4)1.2}{(0.408)^{2/3}} = 1.047 > 1.0 \quad \therefore C_{sm} = 1.0$$

$$p_e = \frac{C_{sm}W}{L} \qquad\qquad \textbf{Eq. C4.7.4.3.2c-4}$$

$$p_e = \frac{1.0(5,882,145)}{61,000} = 96.43 \text{ N/mm (6.60 kip/ft)}$$

I8.5 Intermediate Pier Column Seismic Forces

The equivalent uniform loads were applied to the computer model and a second static analysis was performed to obtain the seismic forces shown in Table I-5.

I8.6 Evaluate Slenderness Effects

For unbraced frames, per **Article 5.7.4.3**, slenderness effects may be neglected if the slenderness ratio, $K\ell_u/r$, is less than 22. In computing the slenderness ratio, the unbraced length, ℓ_u, was taken as the distance from the top of

I-22

TABLE I-5 Column seismic forces

Column Location	Longitudinal Earthquake Load					Transverse Earthquake Load				
	Longitudinal Direction			Transverse Direction		Longitudinal Direction			Transverse Direction	
	Axial kN (kips)	Shear kN (kips)	Mom. kN-m (k-ft)	Shear kN (kips)	Mom. kN-m (k-ft)	Axial kN (kips)	Shear kN (kips)	Mom. kN-m (k-ft)	Shear kN (kips)	Mom. kN-m (k-ft)
Top	0 (0)	5883 (1323)	12932 (9539)	0 (0)	0 (0)	0 (0)	0 (0)	0 (0)	948 (213)	904 (667)
Bottom	0 (0)	5883 (1323)	31895 (23526)	0 (0)	0 (0)	0 (0)	0 (0)	0 (0)	948 (213)	8125 (5993)

the foundation to the center of the pier cap. Arguably, this distance could have been taken as the distance from the top of the foundation to the bottom of the pier cap. For the effective length factor, K, use the recommended design values from **Table C4.6.2.5-1**. As specified in **Article C5.7.4.3**, r is taken as 0.25 times the diameter of the column.

Find the slenderness ratio of the column in the transverse direction.

Under the equivalent transverse static earthquake load, the column of a single column pier acts as a cantilever that resembles Case (e) from **Table C4.6.2.5-1**, thus, take K equal to 2.1. The cantilever-type behavior may also be confirmed by checking the deflected shape of the column in the computer output.

$$\frac{Kl_u}{r} = \frac{2.1(8,356)}{0.25(1,830)} = 38.4 > 22 \quad \therefore \text{ consider the effects of slenderness}$$

Find the slenderness ratio of the column in the longitudinal direction.

The rotation of the column is restrained by the connection to the superstructure at the top and the footing at the bottom. This allows the behavior of the column to be represented by Case (c) from **Table C4.6.2.5-1**, thus, take K equal to 1.2. This conclusion may be confirmed by checking the deflected shape of the column in the computer output.

$$\frac{Kl_u}{r} = \frac{1.2(8,356)}{0.25(1,830)} = 21.9 < 22 \quad \therefore \text{ neglect slenderness effects}$$

I8.7 Moment Magnification

Per **Article 5.7.4.3**, for compression members with a slenderness ratio less than 100, the effects of slenderness may be approximated by the moment magnification method, as specified in **Article 4.5.3.2.2b**.

As specified in **Article 3.10.8**, seismic forces from the two static earthquake loadings are combined to form two load cases for design. Load Case 1 is taken equal to 100 percent of the force effects from the longitudinal earthquake load plus 30 percent of the force effects from the transverse earthquake load. Load Case 2 is taken equal to 100 percent of the force effects from the transverse earthquake load plus 30 percent of the force effects from the longitudinal earthquake load. For the moments shown in Table I-5, one can see that Load Case 1 will control the design of the column.

For circular columns, the longitudinal reinforcing is designed for the moment M_u computed as follows:

$$M_u = \sqrt{(M_L)^2 + (M_T)^2}$$

Where

M_L = Moment in longitudinal direction (kN-m)
M_T = Moment in transverse direction (kN-m)

Since 30 percent of either transverse moment shown in Table I-5 is considerably less than the corresponding longitudinal moment, any increase in M_T due to slenderness effects will have a negligible effect on the magnitude of the design moment. Therefore, moment magnification to account for slenderness effects in the transverse direction can be ignored. However, for completeness, calculations for the magnification of the transverse moment have been incorporated within this design example.

Determine the magnified factored moments in the transverse direction.

$$M_c = \delta_b M_{2b} + \delta_s M_{2s}$$

Eq. 4.5.3.2.2b-1

M_{2s} is defined as the moment due to factored lateral loads that result in sidesway, Δ, greater than $\ell_u/1,500$. From the computer model, for the equivalent transverse static earthquake load, $\Delta = 13.7$ mm (0.54 in.).

$\ell_u/1500 = 8,356/1,500 = 5.6$ mm (0.22 in.)

$\Delta > \ell_u/1,500$, therefore,

$M_{2b} = 0$

$(M_{2s})_{TOP} = 904$ kN-m (667 k-ft)

$(M_{2s})_{BOTT} = 8,125$ kN-m (5,993 k-ft)

$$\delta_s = \frac{1}{1 - \dfrac{\sum P_u}{\varphi \sum P_e}}$$

Eq. 4.5.3.2.2b-4

$$P_e = \frac{\pi^2 EI}{(K\ell_u)^2}$$

Eq. 4.5.3.2.2b-5

Since the column reinforcing is not known at this point, use **Equation 5.7.4.3-2** to determine EI.

$$EI = \frac{\dfrac{E_c I_g}{2.5}}{1 + \beta_d}$$

Eq. 5.7.4.3-2

$E_c = 4,800\sqrt{f_c'} = 4,800\sqrt{28} = 25,399$ MPa (3,684 ksi)

$\beta_d = 0$

$I_g = 5.505 \times 10^{11}$ mm⁴ (1,322,582 in.⁴)

$$EI = \frac{\dfrac{25,399(5.505 \times 10^{11})}{2.5}}{1 + 0} = 5.593 \times 10^{15} \text{ N-mm}^2 \left(1.949 \times 10^9 \text{ k-in}^2\right)$$

$$P_e = \frac{\pi^2 (5.593 \times 10^{15})}{1,000[2.1(8,356)]^2} = 179,270 \text{ kN } (40,304 \text{ kips})$$

Use the maximum load factors for dead load in determining the factored axial load since δ_s is maximized when P_u is maximized.

$\sum P_u = 1.25 P_{DC} + 1.5 P_{DW}$

$\sum P_u = 1.25(3,880) + 1.5(608) = 5,762$ kN (1,295 kips)

see Section I9.1 for P_{DC} & P_{DW}

$$\delta_s = \frac{1}{1 - \dfrac{5,762}{0.5(179,270)}} = 1.07$$

I-24

$(M_c)_{TOP} = 1.07(904) = 967$ kN-m (713 k-ft)

$(M_c)_{BOTT} = 1.07(8,125) = 8,694$ kN-m (6,413 k-ft)

Column moments adjusted for the effects of slenderness are given in Table I-6.

I9 COLUMN DESIGN

I9.1 Column Dead Load Forces

Since the bridge is symmetric, the column experiences only axial compression due to dead load. Axial compression in the column is computed from the loading diagrams shown in Figure I-14. Beam reactions applied to the cap beam were taken from a conventional line girder analysis program.

$(P_{DC})_{TOP} = 2(941) + 2(866) + 9.15(19.54) + 1.412(61.93) = 3,880$ kN (872 kips)

The quantity $1.412(61.93)$ accounts for the weight of the concrete in the cap beam above the column.

$(P_{DC})_{BOTT} = 3,880 + 7.62(61.93) = 4,352$ kN (978 kips)

$P_{DW} = 2(126) + 2(178) = 608$ kN (137 kips)

I9.2 Column Live Load Forces

Column live load forces were obtained from the computer model and are shown in Table I-7 for three live load cases. The live load cases are as follows:

Live Load Case 1—maximum transverse moment with corresponding longitudinal moment and axial load.

Live Load Case 2—maximum longitudinal moment with corresponding transverse moment and axial load.

Live Load Case 3—maximum axial load with corresponding longitudinal and transverse moments.

I9.3 Load Cases for Design

Applicable load combinations:

Extreme Event I $- \gamma_P DC + \gamma_P DW + \gamma_{EQ} LL + 1.0EQ$

Strength I $- \gamma_P DC + \gamma_P DW + 1.75LL$

Where

γ_P = Load factor for permanent loads as prescribed in **Table 3.4.1-2.**

γ_{EQ} = Load factor for live load in Extreme Event Load Combination I. As discussed in the commentary to **Article 3.4.1**, an appropriate value for this factor is still unresolved. Based upon past editions of the Standard Specifications, a value of 0.0 was used for this example.

TABLE I-6   Magnified column moments for earthquake load

| Column Location | Longitudinal Earthquake Load | | Transverse Earthquake Load | |
	Long. Moment kN-m (k-ft)	Transv. Moment kN-m (k-ft)	Long. Moment kN-m (k-ft)	Transv. Moment kN-m (k-ft)
Top	12932 (9539)	0 (0)	0 (0)	967 (713)
Bottom	31895 (23526)	0 (0)	0 (0)	8694 (6413)

866 kN
(195 kips)

941 kN
(212 kips)

941 kN
(212 kips)

girder reactions (TYP.)

866 kN
(195 kips)

19.54 N/mm (1.34 kip/ft)

pier cap

61.93 N/mm
(4.24 kip/ft)

a) Unfactored DC Load

Face of column

girder reactions (TYP.)

126 kN
(28 kips)

178 kN
(40 kips)

178 kN
(40 kips)

126 kN
(28 kips)

714 mm
(2' - 4 1/16")

811 mm (2' - 7 15/16")

pier cap

1525 mm (5 ft)

3050 mm (10 ft)

4575 mm (15 ft)
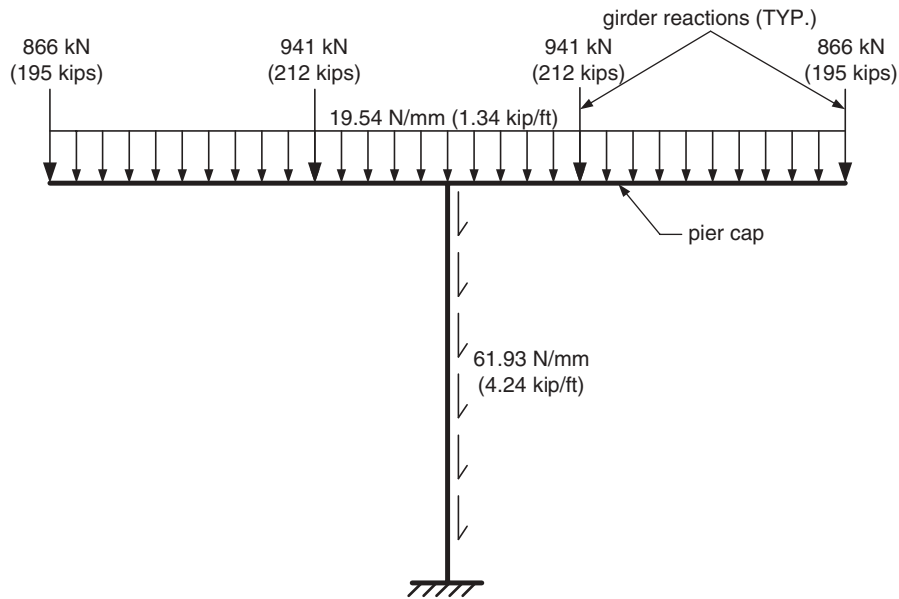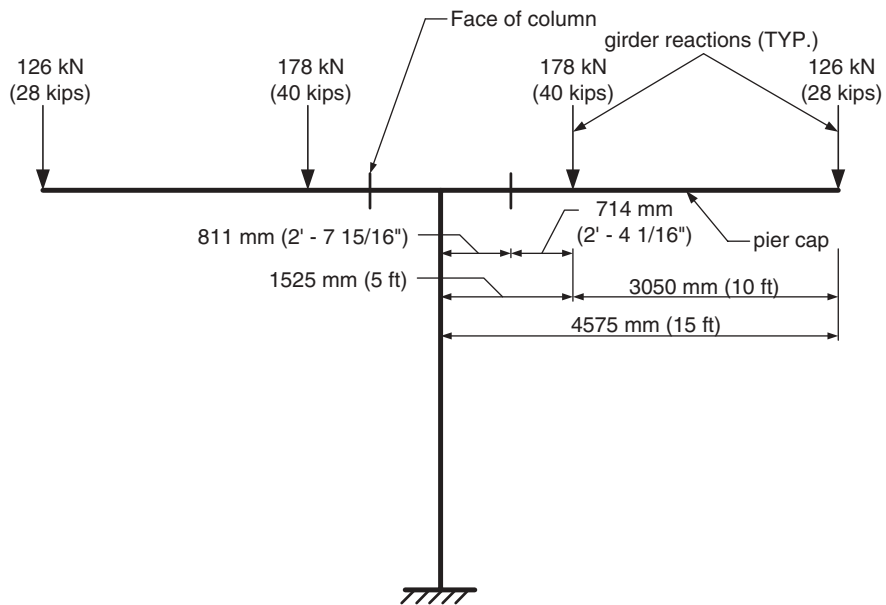
b) Unfactored DW Load

Figure I-14.   Column dead loads.

I9.3.1 Load Cases for Extreme Event I Load Combination

Per **Article 3.10.9.4.1**, design column for the modified design moment was determined in accordance with **Article 3.10.9.4.2**.

$M_{MOD.} = M_u / R$

From **Table 3.10.7.1-1**, for a single column of an essential structure, R = 2.0.

I-26

TABLE I-7 Unfactored column live load forces

	Column Location	P kN (kips)	M_T kN-m (k-ft)	M_L kN-m (k-ft)
Live Load Case 1	Top	1932 (434)	3417 (2520)	19 (14)
	Bottom	1932 (434)	438 (323)	19 (14)
Live Load Case 2	Top	1218 (274)	307 (226)	2489 (1836)
	Bottom	1218 (274)	39 (29)	2489 (1836)
Live Load Case 3	Top	2465 (554)	623 (460)	25 (18)
	Bottom	2465 (554)	80 (59)	25 (18)

For circular columns,

$$M_u = \sqrt{(M_L)^2 + (M_T)^2}$$

As discussed in Section I8.7, the load combination pertaining to 100 percent of the force effects from the longitudinal earthquake load (LEQ) plus 30 percent of the force effects from the transverse earthquake load (TEQ) will control the design of the column. Therefore,

$$M_L = 1.0(M_L)_{LEQ} + 0.3(M_L)_{TEQ}$$

$$M_T = 1.0(M_T)_{LEQ} + 0.3(M_T)_{TEQ}$$

For the values given in Table I-6, the design moments including the response modification factor at the top and bottom of the column are as follows:

$$(M_L)_{TOP} = 1.0(12,932) + 0.3(0.0) = 12,932 \text{ kN-m } (9,539 \text{ k-ft})$$

$$(M_T)_{TOP} = 1.0(0.0) + 0.3(967) = 290 \text{ kN-m } (214 \text{ k-ft})$$

$$(M_u)_{TOP} = \sqrt{(12,932)^2 + (290)^2} = 12,935 \text{ kN-m } (9,541 \text{ k-ft})$$

$$(M_{MOD.})_{TOP} = 12,935/R = 12,935/2 = 6,468 \text{ kN-m } (4,771 \text{ k-ft})$$

$$(M_L)_{BOTT.} = 1.0(31,895) + 0.3(0.0) = 31,895 \text{ kN-m } (23,526 \text{ k-ft})$$

$$(M_T)_{BOTT.} = 1.0(0.0) + 0.3(8,694) = 2,608 \text{ kN-m } (1,924 \text{ k-ft})$$

$$(M_u)_{BOTT.} = \sqrt{(31,895)^2 + (2,608)^2} = 32,001 \text{ kN-m } (23,604 \text{ k-ft})$$

$$(M_{MOD.})_{BOTT.} = 32,001/R = 32,001/2 = 16,001 \text{ kN-m } (11,802 \text{ k-ft})$$

Factored design forces for the load cases of Load Combination Extreme Event I are given in Table I-8.

TABLE I-8 Load cases for extreme Event I load combination

Column Location	Load Case	DC load factor	P_{DC} kN (kips)	DW load factor	P_{DW} kN (kips)	P_{EQ} kN (kips)	P_u kN (kips)	$M_{MOD.}$ kN-m (k-ft)
Top	LC1	1.25	3880 (872)	1.5	608 (137)	0 (0)	5762 (1295)	6468 (4771)
	LC2	0.9	3880 (872)	0.65	608 (137)	0 (0)	3887 (874)	6468 (4771)
Bottom	LC1	1.25	4352 (978)	1.5	608 (137)	0 (0)	6352 (1428)	16001 (11802)
	LC2	0.9	4352 (978)	0.65	608 (137)	0 (0)	4312 (969)	16001 (11802)

I9.3.2 Load Cases for Strength I Load Combination

For the moments in Table I-7, one can see that the design of the column for the Strength I Limit State will be controlled by the moment at the top of the column. For the longitudinal and transverse moments given in Table I-7, factored live load design moments at the top of the column are as follows:

$$M_{LL} = 1.75\sqrt{(M_L)^2 + (M_T)^2}$$

$$(M_{LL})_{LC1} = 1.75\sqrt{(19)^2 + (3,417)^2} = 5,980 \text{ kN-m } (4,411 \text{ k-ft})$$

$$(M_{LL})_{LC2} = 1.75\sqrt{(2,489)^2 + (307)^2} = 4,389 \text{ kN-m } (3,237 \text{ k-ft})$$

$$(M_{LL})_{LC3} = 1.75\sqrt{(25)^2 + (623)^2} = 1,091 \text{ kN-m } (805 \text{ k-ft})$$

Factored design forces at the top of the column for the load cases of Load Combination Strength I are given in Table I-9.

I9.4 Longitudinal Reinforcing

I9.4.1 Controlling Load Case

Typically, load cases for the design of columns on highway bridges fall below the balance point on the interaction diagram for the column. Investigating the load cases for the Strength I load combination in Table I-9, one can see that Load Cases 1a and 2a will control for the Strength I limit state. Comparing Load Cases 1a and 2a to those for the Extreme Event I load combination in Table I-8 and considering that the resistance factor, φ, for the extreme event limit state is less than that for the strength limit state ($\varphi = 0.5$ compared to 0.75 for the strength limit state), one can see that the extreme event limit state will control the design of the column. It can also be seen that the bottom of the column will control the design.

Size column based on the design forces at the bottom of the column. Limit maximum bar size to #36 (#11 USCU) to keep development lengths reasonable. Try a 1,830 mm (6 ft) diameter column with sixty-eight #36 (#11 USCU) bars bundled in groups of two for a total of thirty-four bundles. The interaction diagram for the factored resistance at the bottom of the column is plotted in Figure I-15. From the figure, one can see that the load cases given in Table I-8 for the bottom of the column plot inside the interaction diagram, therefore, okay.

Terminate one bar in each bundle around two-thirds the column height leaving thirty-four #36 (#11 USCU) bars for strength at the top of the column. The interaction diagram for the factored resistance at the top of the column is plotted in Figure I-16. From the figure, one can see that the load cases given in Table I-8 for the top of the column plot inside the interaction diagram, therefore, okay.

TABLE I-9   Load cases for Strength I load combination

Load Case	DC load factor	P_{DC} kN (kips)	DW load factor	P_{DW} kN (kips)	LL load factor	P_{LL} kN (kips)	P_u kN (kips)	M_u kN-m (k-ft)
LC1	1.25	3880 (872)	1.5	608 (137)	1.75	1932 (434)	9143 (2056)	5980 (4411)
LC1a	0.9	3880 (872)	0.65	608 (137)	1.75	1932 (434)	7268 (1634)	5980 (4411)
LC2	1.25	3880 (872)	1.5	608 (137)	1.75	1218 (274)	7894 (1775)	4389 (3237)
LC2a	0.9	3880 (872)	0.65	608 (137)	1.75	1218 (274)	6019 (1353)	4389 (3237)
LC3	1.25	3880 (872)	1.5	608 (137)	1.75	2465 (554)	10076 (2265)	1091 (805)
LC3a	0.9	3880 (872)	0.65	608 (137)	1.75	2465 (554)	8201 (1844)	1091 (805)

I-28
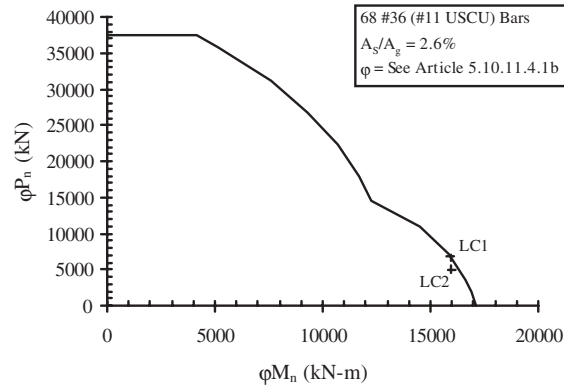
Figure I-15.   Interaction diagram for factored resistance at bottom of column.

I9.4.2 Development Length

Check that the required development length for a straight #36 (#11 USCU) bar can be accommodated within the joint region atop the column shown in Figure I-17.

As specified in **Article 5.11.2.1.1**, the tension development length, ℓ_d, shall not be less than the basic tension development length, ℓ_{db}, modified by any applicable modification factors that increase or decrease ℓ_{db}.

For #36 (#11 USCU) bar and smaller,

$$\ell_{db} = \frac{0.02A_bf_y}{\sqrt{f_c'}} = \frac{0.02(1,006)420}{\sqrt{28}} = 1,597 \text{ mm (62.87 in.)} \quad \textbf{controls}$$

but not less than

$0.06d_bf_y = 0.06(35.8)420 = 902$ mm (35.51 in.)

Modify the basic development length by 0.75 for reinforcement enclosed within a spiral composed of bars of not less than 6 mm (0.25 in.) in diameter and spaced at not more than a 100 mm (4 in.) pitch per **Article 5.11.2.1.3**. In addition, increase the basic development length by 1.25 to account for the overstrength capacity of the reinforcing, as specified in **Article 5.10.11.4.3**.

$\ell_d = 0.75(1.25)\ell_{db} = 0.75(1.25)1,597 = 1,497$ mm (58.94 in.)
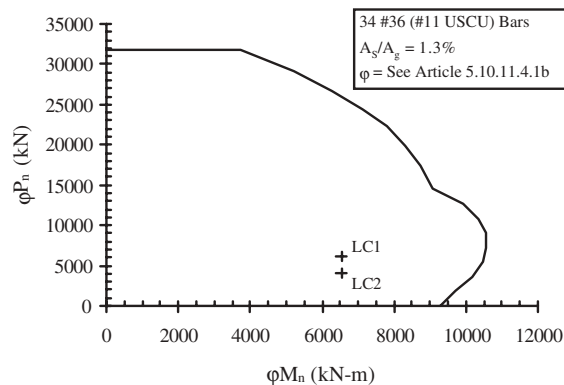
Figure I-16.   Interaction diagram for factored resistance at top of column.
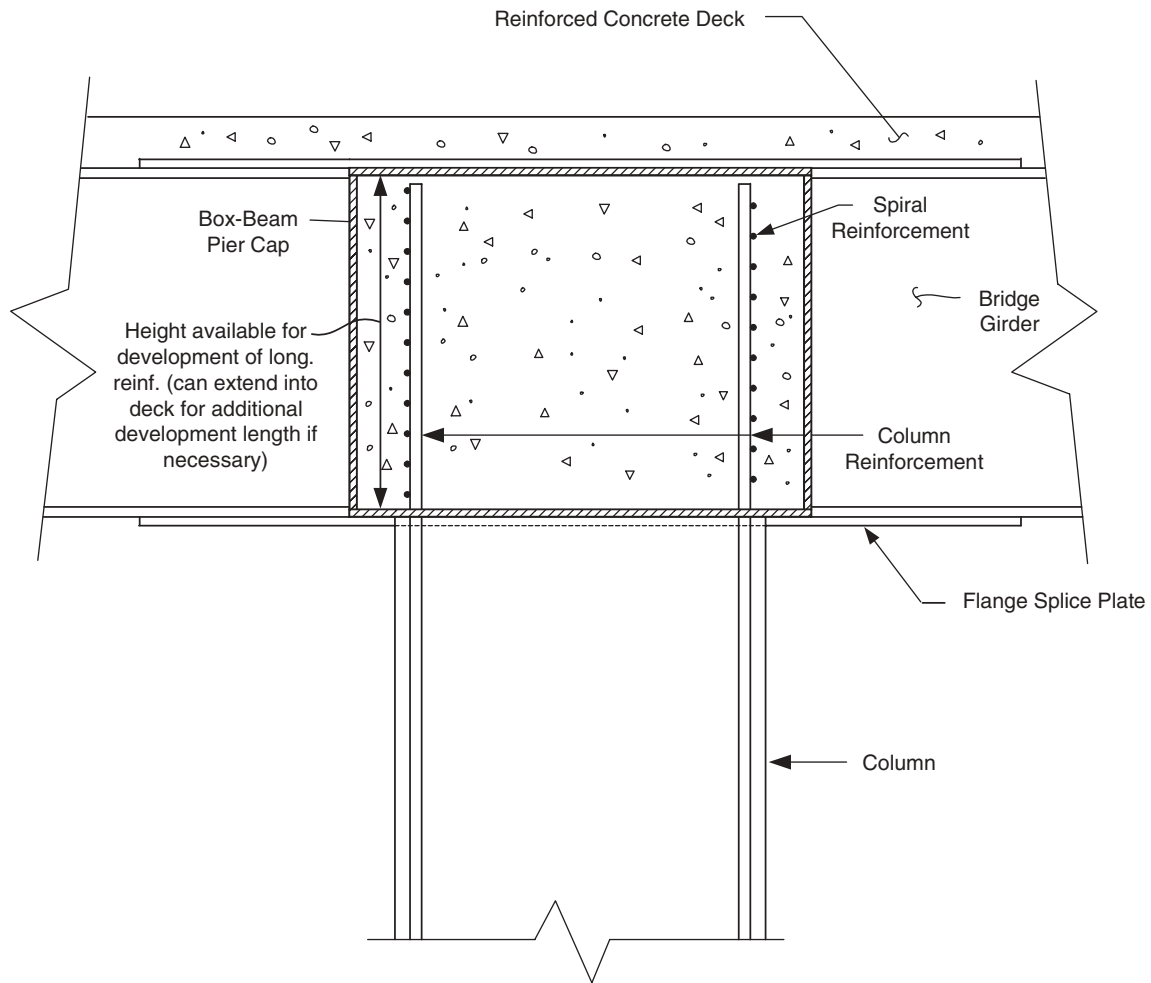
Figure I-17.   Development length for column longitudinal reinforcement.

Length available within pier cap (see Figure I-11).

$\ell_{available} = 1{,}472 - 60 = 1{,}412$ mm (55.59 in.) $< 1{,}497$ mm (58.94 in.) $\therefore$ No Good

Extend bars through the top of the pier cap and into the deck 85 mm (3.35 in.).

$\ell_{available} = 1{,}412 + 85 = 1{,}497$ mm (58.94 in.) $= 1{,}497$ mm (58.94 in.) $\therefore$ OK

The design of the column-to-footing connection is not addressed in this example; therefore, a check on the development length for the bundled bars at the bottom of the column is not presented

I9.5 Column Overstrength

Determine column overstrength moments in accordance with **Article 3.10.9.4.3b**.
For reinforced concrete columns,

$M_{OVRSTR.} = 1.3M_n$

Interaction diagrams for the nominal resistance at the top and bottom of the column, for the assumed column diameter and reinforcing, are plotted in Figures I-18 and I-19. From Figure I-18, the nominal moment resistance at the top of the column for the axial loads given in Table I-8, with $P_u = P_n$ is as follows:
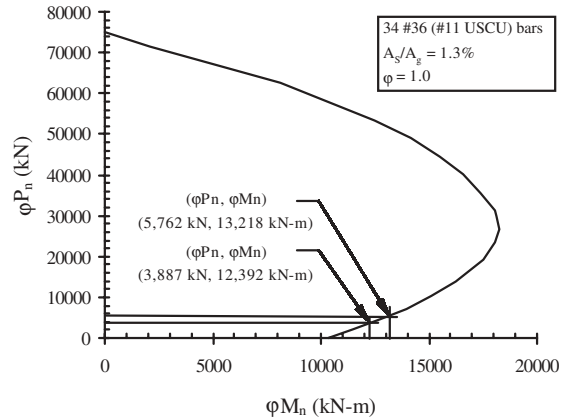
Figure I-18.   Interaction diagram for nominal resistance at top of column.

LC1: $(M_n)_{TOP} = 13,218$ kN-m (9,750 k-ft)

LC2: $(M_n)_{TOP} = 12,392$ kN-m (9,140 k-ft)

From Figure I-19, the nominal moment resistance at the bottom of the column for the axial loads given in Table I-8 with $P_u - P_n$ is as follows:

LC1: $(M_n)_{BOTT.} = 21,406$ kN-m (15,789 k-ft)

LC2: $(M_n)_{BOTT.} = 20,712$ kN-m (15,277 k-ft)

Calculate the column overstrength moment at the top of the column.

LC1: $(M_{OVRSTR.})_{TOP} = 1.3(13,218) = 17,184$ kN-m (12,675 k-ft)

LC2: $(M_{OVRSTR.})_{TOP} = 1.3(12,392) = 16,109$ kN-m (11,882 k-ft)

Calculate the column overstrength moment at the bottom of the column.
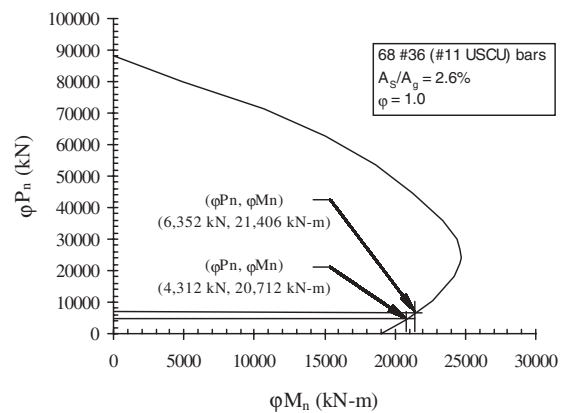
Figure I-19.   Interaction diagram for nominal resistance at bottom of column.

LC1: $(M_{OVRSTR.})_{BOTT.} = 1.3(21,406) = 27,828$ kN-m (20,526 k-ft)

LC2: $(M_{OVRSTR.})_{BOTT.} = 1.3(20,712) = 26,925$ kN-m (19,860 k-ft)

I9.6 Spiral Reinforcing

I.9.6.1 Design Shear Force

Determine the design shear force for the column in accordance with **Articles 3.10.9.4.1** and **3.10.9.4.3d**.
For the free body diagram of the column shown in Figure I-20, the shear force V equals the sum of the moments at the top and bottom of the column divided by the column height.

$V = (M_{TOP} + M_{BOTT.})/h$

The moment at the top and bottom of the column is taken as the lesser of the design moment including a response modification factor of 1.0, rather than the value of 2.0 used to determine M or the moment associated with plastic hinging of the column ($M_{OVRSTR.}$).
Since the shear resistance of the concrete decreases for axial loads less than $0.1f'_cA_g$ in the end regions of the column per **Article 5.10.11.4.1c**, shear forces associated with both the minimum and maximum axial loads on the column need to be investigated.
Shear force for Load Case 1 (maximum axial load)

$M_{TOP} = $ lesser of $(M_{MOD.})_{TOP}$ or $(M_{OVRSTR.})_{TOP}$

$(M_{MOD.})_{TOP} = M_u/R = 12,935/1.0 = 12,935$ kN-m (9,541 k-ft)

see Section I9.3.1 for M_u

$(M_{OVRSTR.})_{TOP} = 17,184$ kN-m (12,675 k-ft)   (see Section I9.5)

$M_{TOP} = $ lesser of 12,935 and 17,184 = 12,935 kN-m (9,541 k-ft)

$M_{BOTT.} = $ lesser of $(M_{MOD.})_{BOTT.}$ or $(M_{OVRSTR.})_{BOTT.}$

$(M_{MOD.})_{BOTT.} = M_u/R = 32,001/1.0 = 32,001$ kN-m (23,604 k-ft)

see Section I9.3.1 for M_u
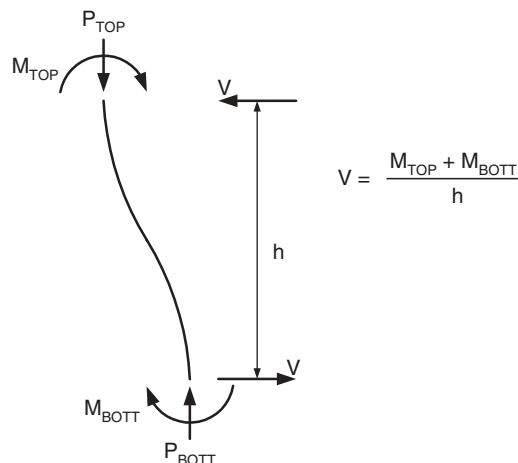
Figure I-20.   Free body diagram of column.

I-32

$(M_{OVRSTR.})_{BOTT.} = 27,828$ kN-m (20,526 k-ft)   (see Section I9.5)

$M_{BOTT.}$ = lesser of 32,001 and 27,828 = 27,828 kN-m (20,526 k-ft)

$(V_u)_{LC1} = (12,935 + 27,828)/7.62 = 5,349$ kN (1,203 kips)

    Since the shear resistance of the concrete is less for smaller axial loads, take the corresponding axial load in the column for shear design as that at the top of the column (as opposed to the axial load at the bottom of the column). Therefore,

$(P_u)_{LC1} = 5,762$ kN (1,295 kips)   (see Table I-8)

    Shear force for Load Case 2 (minimum axial load)

M_{TOP} = lesser of $(M_{MOD.})_{TOP}$ or $(M_{OVRSTR.})_{TOP}$

$(M_{MOD.})_{TOP} = M_u / R = 12,935/1.0 = 12,935$ kN-m (9,541 k-ft)

see Section I9.3.1 for M_u

$(M_{OVRSTR.})_{TOP} = 16,109$ kN-m (11,882 k-ft)   (see Section I9.5)

M_{TOP} = lesser of 12,935 and 16,109 = 12,935 kN-m (9,541 k-ft)

$M_{BOTT.}$ = lesser of $(M_{MOD.})_{BOTT.}$ or $(M_{OVRSTR.})_{BOTT.}$

$(M_{MOD.})_{BOTT.} = M_u / R = 32,001/1.0 = 32,001$ kN-m (23,604 k-ft)

see Section I9.3.1 for M_u

$(M_{OVRSTR.})_{BOTT.} = 26,925$ kN-m (19,860 k-ft)   (see Section I9.5)

$M_{BOTT.}$ = lesser of 32,001 and 26,925 = 26,925 kN-m (19,860 k-ft)

$(V_u)_{LC2} = (12,935 + 26,925)/7.62 = 5,231$ kN (1,176 kips)

$(P_u)_{LC2} = 3,887$ kN (874 kips)   (see Table I-8)

I.9.6.2 Shear Resistance of the Concrete

$V_c = 0.083\beta\sqrt{f_c'}\, b_v d_v$ **Eq. 5.8.3.3-3**

    Per **Article C5.8.2.9**, d_v can be taken as $0.9d_e$, where

$d_e = D/2 + D_r/\pi$ **Eq. C5.8.2.9-2**

Where

  D = diameter of the column (mm)
  D_r = diameter of the circle passing through the centers of the longitudinal reinforcement (mm)
  $d_e = 1,830/2 + [1,830-2(50)-36]/\pi = 1,454$ mm (57.24 in.)
  $d_v = 0.9d_e = 0.9(1,454) = 1,309$ mm (51.54 in.)

    Per the simplified procedure of **Article 5.8.3.4.1**, take β equal to 2.0.

$$V_c = \frac{0.083(2.0)\sqrt{28}(1,830)1,309}{1,000} = 2,104 \text{ kN (473 kips)}$$

In end regions, for axial loads below $0.1f_c'A_g$, reduce shear resistance in accordance with **Article 5.10.11.4.1c**.

$0.1f_c'A_g = 0.1(28)\pi(1,830)^2/[4(1,000)] = 7,365 \text{ kN (1,656 kips)}$

End region shear resistance for Load Case 1.

$(V_c)_{LC1} = V_c (P_u)_{LC1}/(0.1f_c'A_g) = 2,104(5,762)/7,365 = 1,646 \text{ kN (370 kips)}$

End region shear resistance for Load Case 2.

$(V_c)_{LC2} = V_c (P_u)_{LC2}/(0.1f_c'A_g) = 2,104(3,887)/7,365 = 1,110 \text{ kN (250 kips)}$

I.9.6.3 Spacing of Spiral Reinforcing

An equation giving the required spacing for the spiral reinforcing can be obtained as follows:

$\varphi V_n \geq V_u$

$V_n = V_c + V_s$ **Eq. 5.8.3.3-1**

Substituting **Equation 5.8.3.3-1** for V_n and rearranging gives

$\varphi V_s \geq V_u - \varphi V_c$

$V_s = A_v f_y d_v \cot\theta/s$ **Eq. C5.8.3.3-1**

Substituting **Equation C5.8.3.3-1** for V_s and solving for s gives

$s \leq \varphi A_v f_y d_v \cot\theta/(V_u - \varphi V_c)$

Per the simplified procedure of **Article 5.8.3.4.1**, take θ equal to 45 degrees. For the Extreme Event limit state, $\varphi = 1.0$ per **Article 1.3.2.1**.
Determine the required spacing of the spiral reinforcing within the end regions of the column.

Load Case 1: $V_u - \varphi V_c = 5,349 - 1.0(1,646) = 3,703 \text{ kN (833 kips)}$

Load Case 2: $V_u - \varphi V_c = 5,231 - 1.0(1,110) = 4,121 \text{ kN (926 kips)}$ $\leftarrow$ **controls**

Try #16 (#5 USCU) bar for spiral reinforcing, $A_v = 400 \text{ mm}^2 (0.62 \text{ in}^2)$.

$s \leq 1.0(400)420(1,309)\cot 45°/[4,121(1,000)]$

$s \leq 53 \text{ mm (2.09 in.)}$ $\rightarrow$ say $s = 50 \text{ mm (2 in.)}$

Check clear spacing between bars of spiral.

clr. spacing $= 50 - 16 = 34 \text{ mm (1.34 in.)} > 25 \text{ mm (1 in.)}$ per **Article 5.10.6.2** $\therefore$ OK

Use #16 (#5 USCU) bar for spiral with spacing not to exceed 53 mm (2.09 in.) within the end regions of the column.
Determine required spacing of spiral reinforcing between the end regions of the column.

I-34

Between the end regions of the column the shear resistance of the concrete is not reduced for axial loads less than $0.1f'_c A_g$; therefore, Load Case 1 will control the spacing of the spiral reinforcing.

$V_u - \varphi V_c = 5349 - 1.0(2104) = 3,245$ kN (730 kips)

$s \leq 1.0(400)420(1,309)\cot 45°/[3,245(1,000)]$

$s \leq 68$ mm (2.68 in.)

Check the volumetric ratio of the spiral reinforcing as specified in **Article 5.10.11.4.1d**.

$\rho_s \geq 0.12 f'_c / f_y$ 　　　　　　　　　　　　　　　　　　　　　　　**Eq. 5.10.11.4.1d-1**

$$(\rho_s)_{provided} = \frac{4A_{sp}}{d_c s}$$

Where,

　A_{sp} = cross-sectional area of spiral reinforcing (mm²)
　A_{sp} = 200 mm² (0.31 in²) for #16 (#5 USCU) bar
　d_c = outside diameter of spiral (mm)
　d_c = 1,830-2(50)+2(16) = 1,762 mm (69.37 in.)

The critical value for the volumetric ratio occurs for the spacing between the end regions of the column.

$$(\rho_s)_{provided} = \frac{4(200)}{1,762(68)} = 0.0067$$

$0.12 f'_c / f_y = 0.12(28)/420 = 0.008$

$(\rho_s)_{provided} < 0.12 f'_c / f_y$, therefore,

decrease spiral pitch between the end regions of the column.
　　Find the spacing of the spiral reinforcing that satisfies **Equation 5.10.11.4.1d-1**.

$$\frac{4A_{sp}}{d_c s} \geq 0.12 f'_c / f_y$$

Solving for s gives

$$s \leq \frac{4A_{sp}f_y}{0.12 f'_c d_c}$$

$$s \leq \frac{4(200)420}{0.12(28)1,762}$$

$s \leq 57$ mm (2.24 in.)　　$\rightarrow$　say 50 mm (2 in.)

In addition, provide spiral reinforcing within the center compartment of the pier cap according to the proposed design specifications. Within the connection region, the required spiral reinforcement shall be greater than half the amount provided in the plastic hinge region.

I9.7 Column Reinforcing Details

Refer to Figure I-21 for final column reinforcing details.
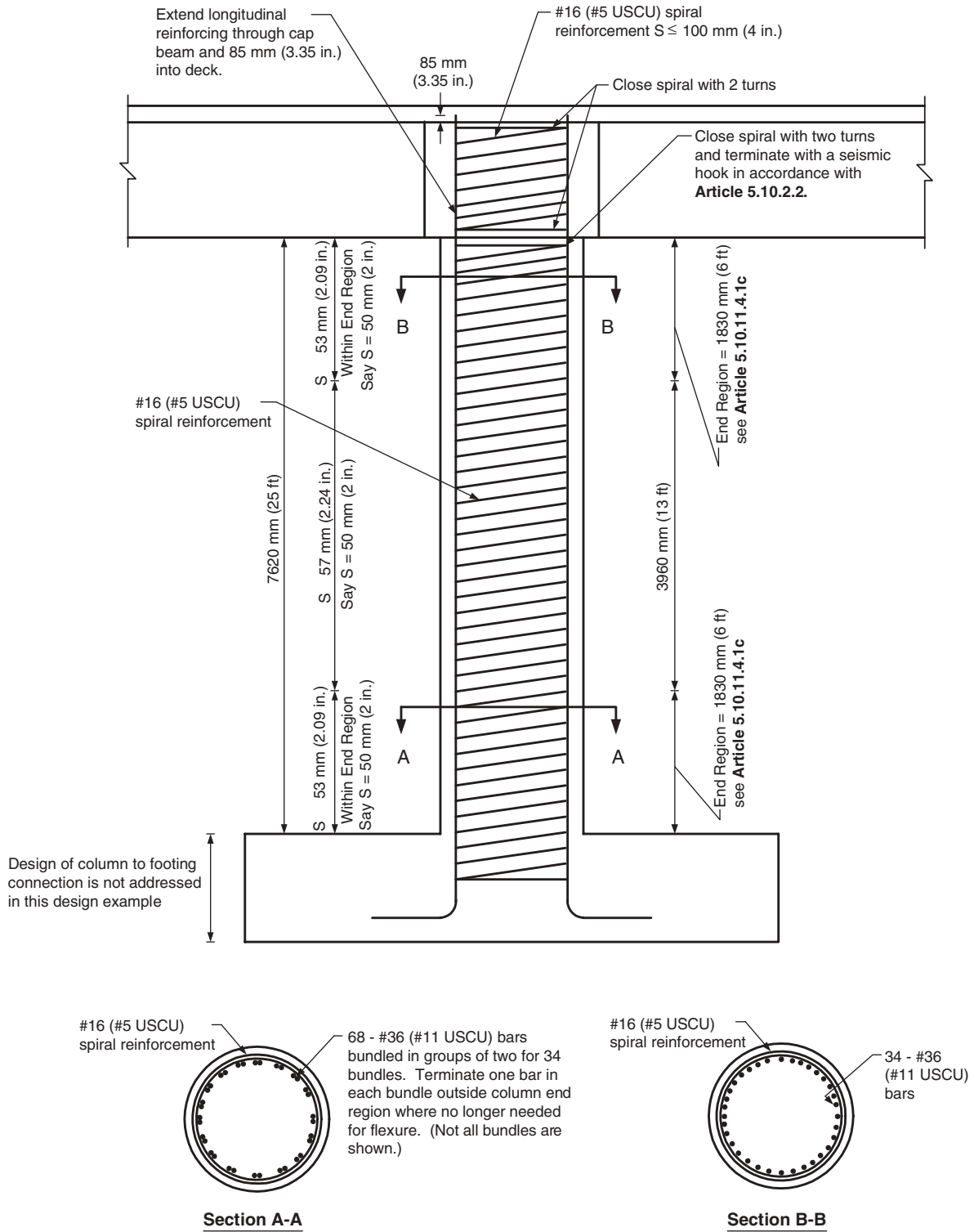
Figure I-21.   Column reinforcement details.

I10 BEAM DESIGN

The girders are rigidly connected to the pier cap, therefore, the column top moment is transferred to the girders.

I10.1 Earthquake Loading

Check preliminary girder size for moments developed during a seismic event.

Design girders for the lesser of the elastic moments computed in accordance with **Article 3.10.8** or the moments associated with the plastic hinging of the column. Maximum elastic moments within the positive and negative moment sections of the girders for the earthquake loads computed in Sections I8.3 and I8.4 are given in Table I-10.

From Table I-10, one can see that load combinations consisting of 100 percent of the moment from the longitudinal earthquake load (M_{LEQ}) plus 30 percent of the moment from the transverse earthquake load (M_{TEQ}) will produce the largest elastic design moments. In addition, elastic design moments will be greatest for the interior girder. Interior girder moments due to 30 percent of the transverse earthquake load are small and can be ignored; therefore, elastic design moments for the positive and negative moment sections of the girder are as follows:

$$+ M_{ELASTIC} = 1,851 \text{ kN-m } (1,365 \text{ k-ft})$$

$$- M_{ELASTIC} = 3,242 \text{ kN-m } (2,391 \text{ k-ft})$$

Since girder moments from the transverse earthquake load are negligible, compare moments at the top of the column from the longitudinal earthquake load, including a response modification factor of 1.0 rather than the value of 2.0 used to determine $M_{MOD.}$, and the moment associated with plastic hinging to determine the controlling condition for design.

$$(M_L)_{TOP} = 12,932 \text{ kN-m } (9,539 \text{ k-ft}) \hspace{3cm} \text{(see Section I9.3.1)}$$

$$(M_{OVRSTR.})_{TOP} = 17,184 \text{ kN-m } (12,675 \text{ k-ft}) \hspace{3cm} \text{(see Section I9.5)}$$

$$(M_L)_{TOP} < (M_{OVRSTR.})_{TOP}$$

Since the elastic moment at the top of the column from the longitudinal earthquake load is less than the moment resulting from plastic hinging, use the elastic moments computed above for the seismic design of the girders.

Table I-11 compares the factored seismic girder moments to the factored live load moments used in the preliminary design of the girders. As seen in Table I-11, seismic moments are less than corresponding live load moments; therefore, girder dimensions from the design for the Strength I limit state are adequate to resist the seismic moments developed within the girders.

TABLE I-10 Maximum elastic seismic moments within the girders

		Max. M_{LEQ} kN-m (k-ft)	Max. M_{TEQ} kN-m (k-ft)
Interior Girder	Pos. Mom. Section	± 1851 (1365)	± 58 (43)
	Neg. Mom. Section	± 3242 (2391)	± 85 (63)
Exterior Girder	Pos. Mom. Section	± 1631 (1203)	± 167 (123)
	Neg. Mom. Section	± 1741 (1284)	± 263 (194)

TABLE I-11 Maximum factored girder moments

	γM_{EQ} kN-m (k-ft)	γM_{LL} kN-m (k-ft)
Pos. Mom. Section	+1851 (1365)	+3866 (2852)
Neg. Mom. Section	-3242 (2391)	-4914 (3625)

I10.2 Live Loading

Check preliminary girder dimensions for the live load moments obtained from the computer model discussed in Section I6.1.

Table I-12 compares the maximum unfactored live load girder moments obtained from the 3-dimensional computer model to those obtained from a line girder analysis program. As seen in Table I-12, the maximum moments from the computer model are less than the corresponding moments obtained from the line girder analysis program, therefore, the girder design for the Strength I limit state may be based on line girder analysis. This will allow the use of existing conventional computer programs to design the girders.

I11 CAP BEAM DESIGN

Initial dimensions of the pier cap were determined in Section I5.3 and are shown in Figure I-11.

I11.1 Flexure

I11.1.1 Factored Design Moment

Design for the moment at the face of the column. Per **Article 5.13.3.4**, in the case of columns that are not rectangular, the critical section shall be taken at the side of the concentric rectangle of equivalent area.

Column area = 2,630,220 mm² (4,077 in²)

Equivalent square column = $\sqrt{2,630,220}$ = 1,622 mm × 1,622 mm (63.85 in. × 63.85 in.)

From the loading diagrams shown in Figure I-14, calculate the dead load moments at the face of the equivalent column.

M_{DC} = 866(3.764) + 941(0.714) + 19.54(3,764)²/[2(1,000)²] = 4,070 kN-m (3,002 k-ft)

M_{DW} = 126(3.764) + 178(0.714) = 601 kN-m (443 k-ft)

From the 3-dimensional computer model, the unfactored live load moment and corresponding torsion in the cap beam at the face of the column are given as follows:

M_{LL} = 3,201 kN-m (2,361 k-ft)

T_{LL} = 21 kN-m (15 k-ft)

Factored moment and torsion

M_u = 1.25(4,070) + 1.5(601) + 1.75(3,201) = 11,591 kN-m (8,550 k-ft)

T_u = 1.75(21) = 37 kN-m (27 k-ft)

The corresponding factored torsion is small and therefore can be neglected.

TABLE I-12   Maximum unfactored live load girder moments, kN-m (k-ft)

		3-D Computer Model	Line Girder Analysis
Interior Girder	Pos. Mom. Section	+1844 (1360)	+2209 (1629)
	Neg. Mom. Section	-2634 (1943)	-2808 (2071)
Exterior Girder	Pos. Mom. Section	+2226 (1642)	+2577 (1901)
	Neg. Mom. Section	-3025 (2231)	-3275 (2416)

I-38

I11.1.2 Nominal Flexural Resistance

Determine the nominal flexural resistance of the compression flange in accordance with **Article 6.11.2.1.3a**. For compression flanges without longitudinal stiffeners,

$w = b = 2{,}280 - 2(30) = 2{,}220$ mm (87.40 in.)

$k = 4$

$$\frac{w}{t_f} = \frac{2{,}220}{30} = 74$$

$$0.57\sqrt{\frac{kE}{F_{yc}}} = 0.57\sqrt{\frac{4(200{,}000)}{345}} = 27.4$$

$$1.23\sqrt{\frac{kE}{F_{yc}}} = 1.23\sqrt{\frac{4(200{,}000)}{345}} = 59.2$$

Since $\dfrac{w}{t_f} > 1.23\sqrt{\dfrac{kE}{F_{yc}}}$

$F_n = 181{,}000\, R_b R_h k (t_f / w)^2$ **Eq. 6.11.2.1.3a-3**

Determine R_b from **Article 6.10.4.3.2a**.
For box symmetrical about the horizontal axis,

$D_c = D/2 = 1{,}412/2 = 706$ mm (27.80 in.)

$$\frac{2D_c}{t_w} > \frac{1{,}412}{30} = 47$$

$f_c = M_u/S$

$S = I / c = 8.520 \times 10^{10}/(1{,}472/2) = 1.157 \times 10^8$ mm³ (7,060 in³)

$$f_c = \frac{11{,}591(1{,}000)^2}{1.157 \times 10^8} = 100.2 \text{ MPa (14.5 ksi)}$$

$$\lambda_b\sqrt{\frac{E}{f_c}} = 5.76\sqrt{\frac{200{,}000}{100.2}} = 257$$

$$\frac{2D_c}{t_w} < \lambda_b\sqrt{\frac{E}{f_c}} \quad \therefore \ R_b = 1.0$$ **Eq. 6.10.4.3.2a-1**

Per **Article 6.10.4.3.1a**, $R_h = 1.0$ for homogeneous sections,

$F_n = 181{,}000(1.0)1.0(4)(30/2{,}220)^2 = 132.2$ Mpa (19.2 ksi)

$\varphi F_n = 1.0(132.2) = 132.2$ MPa (19.2 ksi) > 100.2 MPa (14.5 ksi) applied stress $\therefore$ OK

Tension flange is OK by inspection.

I11.1.3 Web Slenderness

Check web slenderness in accordance with **Article 6.11.2.1.3b**. Per **Article 6.10.2.2**, webs shall be proportioned such that

$$\frac{2D_c}{t_w} \le 6.77\sqrt{\frac{E}{f_c}} \le 200 \qquad \qquad \textbf{Eq. 6.10.2.2-1}$$

$$\frac{2D_c}{t_w} = 47$$

$$6.77\sqrt{\frac{E}{f_c}} = 6.77\sqrt{\frac{200,000}{100.2}} = 302.5$$

$$\frac{2D_c}{t_2} < 6.77\sqrt{\frac{E}{f_c}} \quad \therefore \ \ OK$$

I11.2 Shear

Design for the maximum shear force in the flange and web plates of the cap beam from either the Extreme Event I or Strength I load combinations.

I11.2.1 Shear Forces for the Extreme Event I Load Combination

Shear forces in the flange and web plates of the cap beam result from both flexure and torsion. Web plates experience both flexural and torsional shears while flange plates see only torsional shear as shown in Figure I-22.

$$V_u = V_f + V_T$$

For earthquake loads, design for the lesser of the elastic forces computed in accordance with **Article 3.10.8** or the forces associated with the plastic hinging of the column. Maximum elastic forces in the pier cap for the earthquake loads computed in Sections I8.3 and I8.4 are given in Table I-13.

Shear in the pier cap from the transverse earthquake load is small, therefore, design for the load combination consisting of 100 percent of the shear due to the forces from the longitudinal earthquake load plus 30 percent of the shear due to the forces from the transverse earthquake load. Thirty percent of the shear from the transverse earthquake load is small and can be ignored; therefore, the maximum elastic shear in the pier cap can be taken as that due to the torsion from the longitudinal earthquake load.

Torsional Shear   Flexural Shear
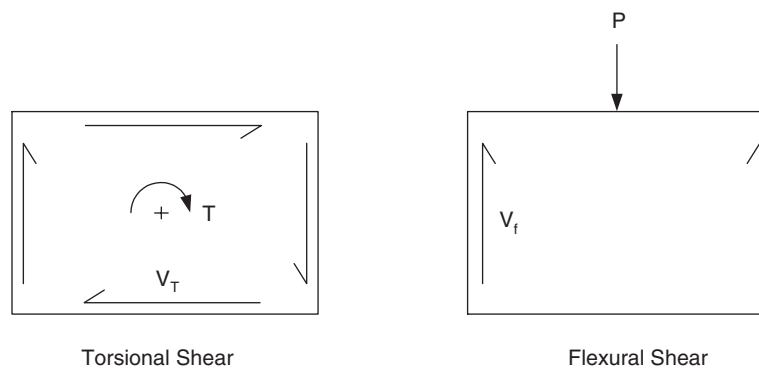
Figure I-22.   Cap beam shear forces.

TABLE I-13 Maximum elastic seismic pier cap forces

Longitudinal Earthquake Load		Transverse Earthquake Load	
Torsion	Flexural Shear	Torsion	Flexural Shear
kN-m (k-ft)	kN (kips)	kN-m (k-ft)	kN (kips)
8632 (6,367)	0 (0)	0 (0)	26 (6)

Since the torsion in the cap beam at the face of the column is equal to half of the longitudinal moment in the column at the centerline of the pier cap, compare moments at the top of the column from the longitudinal earthquake load and plastic hinging to determine the controlling condition for design.

$(M_L)_{TOP} = 12{,}932$ kN-m (9,539 k-ft)   (see Section I9.3.1)

$(M_{OVRSTR.})_{TOP} = 17{,}184$ kN-m (12,675 k-ft)   (see Section I9.5)

$(M_L)_{TOP} < (M_{OVRSTR.})_{TOP}$

Since the elastic moment at the top of the column from the longitudinal earthquake load is less than the moment resulting from plastic hinging, design for the elastic shear due to the torsion from the longitudinal earthquake load.
    Calculate shear forces due to torsion.

$V_T = qD$

Where,

q = shear flow = $T/(2A_o)$ (kN/m)
A_o = enclosed area within the box section (mm^2)
D = width or depth of plate between webs or flanges (m)
    = 2.22 m (7.28 ft) for calculation of force in flange plates
    = 1.412 m (4.63 ft) for calculation of force in web plates
$T_u = T_{EQ} = 8{,}632$ kN-m (6,367 k-ft)
$A_o = (2{,}280 - 30)(1{,}472 - 30) = 3{,}244{,}500$ mm^2 (5,029 in^2)
$q = \dfrac{8{,}632(1{,}000)^2}{2(3{,}244{,}500)} = 1{,}330$ kN/m (91 kip/ft)
$(V_T)_{FLANGE\ PLS.} = qD = 1{,}330(2.220) = 2{,}953$ kN (664 kips)
$(V_T)_{WEB\ PLS.} = qD = 1{,}330(1.412) = 1{,}878$ kN (422 kips)

Calculate shear forces per web plate due to dead load flexure, V_f. See Figure I-14 for dead loads.

$(V_f)_{DC} = 1.25[866 + 941 + 19.54(4{,}575)/1{,}000]/2 = 1{,}185$ kN (266 kips)

$(V_f)_{DW} = 1.5(178 + 126)/2 = 228$ kN (51 kips)

$V_f = (V_f)_{DL} = 1{,}185 + 228 = 1{,}413$ kN (318 kips)

See Figure I-23 for the shear forces in the flange and web plates for the Extreme Event I load combination (i.e., due to seismic load plus dead load).

I11.2.2 Shear Forces for the Strength I Load Combination

As permitted in **Article 6.11.2.2.1**, maximum shear will be taken as the sum of the absolute values of the shears due to maximum flexure and maximum torsion.
    Calculate shear forces due to torsion.
    From the 3-dimensional computer model, the maximum unfactored live load torsion in the pier cap is 2,484 kN-m (1,832 k-ft).

Extreme Event I

2953 kN (664 kips)

1413 - 1878 = -465 kN (-105 kips)

1413 + 1878 = 3291 kN (740 kips)

2953 kN (664 kips)

Strength I

1487 kN (334 kips)

2731 - 946 = 1785 kN (401 kips)

2731 + 946 = 3677 kN (827 kips)
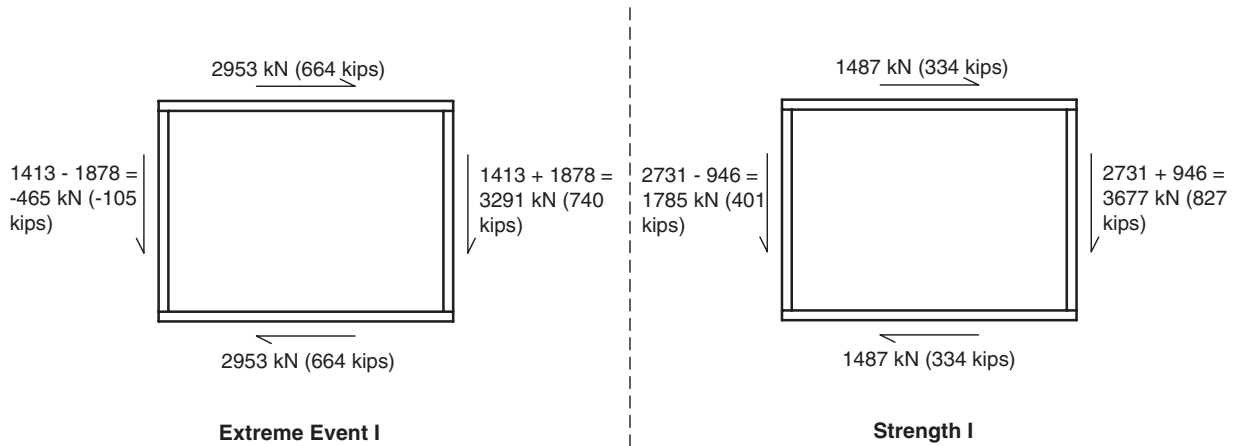
1487 kN (334 kips)

Figure I-23.   Shear forces on cap beam.

$T_u = 1.75(2,484) = 4,347$ kN-m (3,206 k-ft)

$$q = \frac{4,347(1,000)^2}{2(3,244,500)} = 670 \text{ kN/m (46 kip/ft)}$$

$(V_T)_{\text{FLANGE PLS.}} = 670(2.220) = 1,487$ kN (334 kips)

$(V_T)_{\text{WEB PLS.}} = 670(1.412) = 946$ kN (213 kips)

Calculate factored shear forces in the web plates due to flexure.

From the 3-dimensional computer model, the maximum unfactored live load shear in the pier cap is 1,506 kN (339 kips). Therefore, the vertical shear per web plate from dead plus live load, not including torsion, is as follows:

$V_f = 1.75(1,506)/2 + 1,185 + 228 = 2,731$ kN (614 kips)

See Figure I-23 for the shear forces in the flange and web plates for the Strength I load combination including torsion.

I11.2.3 Nominal Shear Resistance

Determine the nominal shear resistance for the plates of the cap beam in accordance with **Articles 6.11.2.2.1** and **6.10.7.2**. Interior diaphragm plates are present within the cap beam and have a stiffening effect on the plates of the pier cap. Since these diaphragm plates are spaced relatively wide with respect to the depth of the pier cap, any stiffening effect on the plates of the cap beam will be ignored. Therefore, treat the plates of the cap beam as unstiffened.

$V_n = CV_p$ **Eq. 6.10.7.2-1**

$V_p = 0.58F_{yw}Dt_w$ **Eq. 6.10.7.2-2**

For the flange plates,

$$\frac{D}{t_w} = 2,220/30 = 74$$

For unstiffened web panels, the buckling coefficient, k, may be taken equal to 5 (**Equation 6.10.7.3.3a-8** with $d_o \gg D$).

$$1.10\sqrt{\frac{Ek}{F_{yw}}} = 1.10\sqrt{\frac{200,000(5)}{345}} = 59.2$$

I-42

$$1.38\sqrt{\frac{Ek}{F_{yw}}} = 1.38\sqrt{\frac{200,000(5)}{345}} = 74.3$$

Since $1.10\sqrt{\frac{Ek}{F_{yw}}} < \frac{D}{t_w} < 1.38\sqrt{\frac{Ek}{F_{yw}}}$,

$$C = \frac{1.10}{\frac{D}{t_w}}\sqrt{\frac{Ek}{F_{yw}}}$$ **Eq. 6.10.7.3.3a-6**

$$C = \frac{1.10}{74}\sqrt{\frac{200,000(5)}{345}} = 0.8$$

$$V_n = CV_p = \frac{0.8(0.58)(345)(2,220)(30)}{1,000} = 10,661 \text{ kN } (2,397 \text{ kips})$$

$\varphi V_n = 1.0(10,661) = 10,661$ kN (2,397 kips) $> 2,953$ kN (664 kips) $\therefore$ OK

For the web plates,

$$\frac{D}{t_w} = 1,412/30 = 47.1$$

$$\frac{D}{t_w} < 1.10\sqrt{\frac{Ek}{F_{yw}}} \quad \therefore \quad C = 1.0$$ **Eq. 6.10.7.3.3a-5**

$$\varphi V_n = \frac{1.0(1.0)(0.58)(345)(1,412)(30)}{1,000} = 8,476 \text{ kN } (1,906 \text{ kips}) > 3,677 \text{ kN } (827 \text{ kips}),$$

therefore, OK

I11.3 Check of Box-Beam Flanges for Combined Moment and Torsional Shear

Evaluate the bottom flange plate of the cap beam for the interaction between moment and torsion for the Extreme Event I and Strength I limit states by investigating the ratio of the factored force to the factored resistance for both moment and torsion.

I11.3.1 Extreme Event I Limit State

Maximum factored torsion.

$T_u = 8,632$ kN-m (6,367 k-ft) (see Section I11.2.1)

Shear in bottom flange plate due to the maximum factored torsion.

$V_u = 2,953$ kN (664 kips) (see Section I11.2.1)

Corresponding factored moment at the face of the column.

$M_u = 1.25(4,070) + 1.5(601) = 5,989$ kN-m (4,417 k-ft) (see Section I11.1.1)

Compute the nominal moment resistance of the bottom flange plate.

$\varphi M_n = \varphi F_n S$

Where,

$\varphi F_n = 132.2$ MPa (19.2 ksi) (see Section I11.1.2)
$S = 1.157 \times 10^8$ mm³ (7,060 in³) (see Section I11.1.2)

$\varphi M_n = \dfrac{1.0(132.2)(1.157 \times 10^8)}{(1,000)^2} = 15,296$ kN-m (11,282 k-ft)

$\dfrac{M_u}{\varphi M_n} = \dfrac{5,989}{15,296} = 0.39$

$$\dfrac{V_u}{\varphi V_n} = \dfrac{2,953}{10,661} = 0.28$$

Since the ratio of the factored force to the factored resistance for both moment and shear is low, moment-torsion interaction will not be critical for the Extreme Event I limit state.

I11.3.2 Strength I Limit State

Maximum factored torsion.

$T_u = 4,347$ kN-m (3,206 k-ft) (see Section I11.2.2)

Shear in bottom flange plate due to the maximum factored torsion.

$V_u = 1,487$ kN (334 kips) (see Section I11.2.2)

From the 3-dimensional computer model, the unfactored live load moment corresponding to the live loading producing the maximum factored torsion is 1,098 kN-m (810 k-ft). Therefore, the corresponding factored moment is as follows:

$M_u = 1.25(4,070) + 1.5(601) + 1.75(1,098) = 7,911$ kN-m (5,835 k-ft)

$\dfrac{M_u}{\varphi M_n} = \dfrac{7,911}{15,296} = 0.52$

$\dfrac{V_u}{\varphi V_n} = \dfrac{1,487}{10,661} = 0.14$

Since the ratio of the factored force to the factored resistance for both moment and shear is low, moment-torsion interaction will not be critical for the Strength I limit state.

I11.4 Fatigue Requirements for Webs

Per **Article 6.11.1**, check the fatigue requirements for webs according to the provisions specified in **Article 6.10.6**. Check requirements for flexure in accordance with **Article 6.10.6.3**.

$\dfrac{D}{t_w} = 1,412/30 = 47$

$k = 9\left(\dfrac{D}{D_c}\right)^2 = 9(2)^2 = 36$

$0.95\sqrt{\dfrac{kE}{F_{yw}}} = 0.95\sqrt{\dfrac{36(200,000)}{345}} = 137$

I-44

$$\frac{D}{t_w} < 0.95 \sqrt{\frac{kE}{F_{yw}}}, \text{ therefore,}$$

$$f_{cf} \le F_{yw} \qquad\qquad \text{Eq. 6.10.6.3-1}$$

The factored flexural stress of the cap beam under the Strength I limit state does not exceed yield, therefore, the compressive stress in the flange under unfactored dead load plus fatigue load will be less than yield. This means that **Equation 6.10.6.3-1** will be satisfied and there is no need for further calculations.

Since the web is unstiffened, the shear requirement of **Article 6.10.6.4** does not apply.

I11.5 Constructability

Per **Article 6.11.1**, check the constructability of the cap beam according to the provisions specified in **Article 6.11.5**. Check the webs of the cap beam in accordance with **Article 6.11.5.2**.

$$f_{cw} \le \frac{0.9E\alpha k}{\left(\dfrac{D}{t_w}\right)^2} \le F_{yw} \qquad\qquad \text{Eq. 6.10.3.2.2-1}$$

$$\frac{0.9E\alpha k}{\left(\dfrac{D}{t_w}\right)^2} = \frac{0.9(200,000)(1.25)(36)}{(47)^2} = 3,667 \text{ MPa (532 ksi)} > F_{yw}, \text{ therefore,}$$

$$f_{cw} \le F_{yw}$$

The factored flexural stress of the cap beam under the Strength I limit state does not exceed yield, therefore, the compressive flexural stress in the web due to factored dead loads acting on the noncomposite section during construction will be less than yield. This means that **Equation 6.10.3.2.2-1** will be satisfied and there is no need for further calculations.

I11.6 Service Limit State Control of Permanent Deflections

Per **Article 6.11.1**, check the Service limit state control of permanent deflections as specified in **Article 6.11.7**. Per **Article C6.11.7**, this check does not apply since the pier cap is a single box section.

I11.7 Fatigue

Check fatigue resistance of details in accordance with **Article 6.6.1.2**.

$$\gamma(\Delta f) \le (\Delta F)_n \qquad\qquad \text{Eq. 6.6.1.2.2-1}$$

Detail categories for the various details of the pier cap are given in Figure I-24. For simplification of calculations, provide infinite fatigue life for details.

$$(\Delta F)_n = \frac{1}{2}(\Delta F)_{TH} \qquad\qquad \text{Eq. 6.6.1.2.5-1}$$

For infinite life, Detail Category C controls. From **Table 6.6.1.2.5-3**, for Detail Category C, $(\Delta F)_{TH} = 69$ MPa (10 ksi).

$$(\Delta F)_n = \frac{1}{2}(69) = 34.5 \text{ MPa (5.0 ksi)}$$

$$\gamma(\Delta f) = 0.75(\Delta M)_{FATIGUE}/S$$
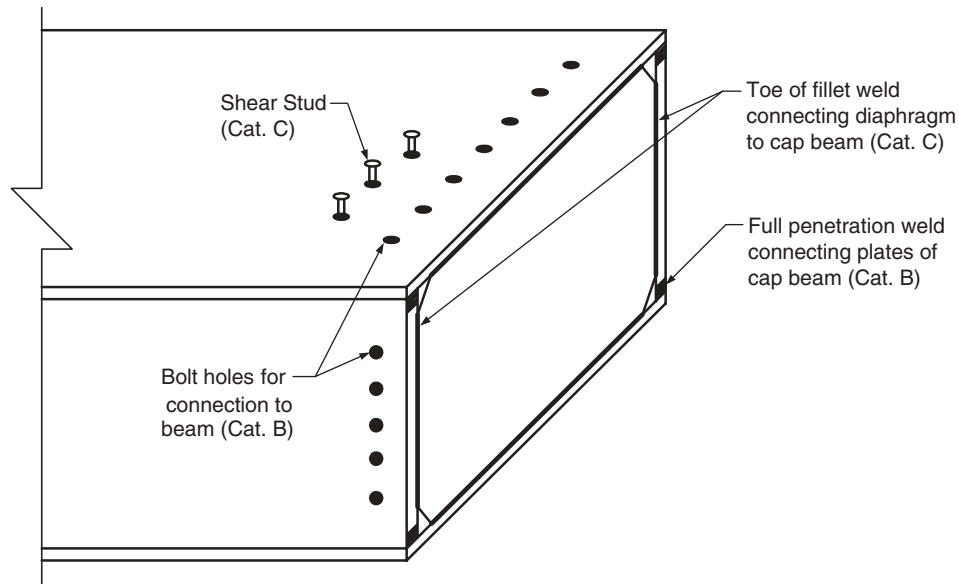
Figure I-24. Detail categories for fatigue.

From the computer model, the range in moment experienced by the pier cap due to the passage of the fatigue load, $(\Delta M)_{FATIGUE}$, is 1,095 kN-m (808 k-ft). This value is computed at the centerline of the column and does not include impact.

$$\gamma(\Delta f) = 0.75(1.15)1,095(1,000)^2/1.157 \times 10^8 = 8.2 \text{ MPa (1.2 ksi)}$$

$$\gamma(\Delta f) < (DF)_n \quad \therefore \quad OK$$

I12 GIRDER-TO-CAP BEAM CONNECTION

Figure I-5 shows the components of the girder-to-cap beam connection. They include a bolted double-angle connection for the transfer of shear from the web of the girder to the web of the box-beam pier cap and flange splice plates for the transfer of girder moments across the width of the pier cap. The flange splice plates also transfer the difference between the moment on either side of the pier cap to the pier cap in the form of torsional moment.

I12.1 Bolted Double-Angle Connection

Design the connection for the shear transferred from the web of the girder to the web of the cap beam. Per **Article 6.13.2.1.1**, design the connection as slip-critical since the connection is subject to impact and the reversal of forces.

I12.1.1 Shear Forces Due to Unfactored Loadings

Unfactored shear forces are greatest for the interior beam and are as follows:

$$V_{DC} = V_{DC1} + V_{DC2} = 376 + 94 = 470 \text{ kN (106 kips)} \qquad \text{(from line girder analysis)}$$

$$V_{DW} = 89 \text{ kN (20 kips)} \qquad \text{(from line girder analysis)}$$

$$V_{LL} = 517 \text{ kN (116 kips)} \qquad \text{(from computer model)}$$

For seismic loading, design the connection for the lesser of the elastic shear including the response modification factor or the shear associated with the plastic hinging of the column. From **Table 3.10.7.1-2**, the response modification factor for the connection is 1.0, therefore, the modified design shear is simply equal to the elastic shear from the earthquake

I-46

loading. Shear in the girder webs at the edge of the pier cap resulting from the earthquake loads computed in Sections I8.3 and I8.4 are given in Table I-14.

From Table I-14, shear is greatest in the interior girder. In addition, shear due to the transverse earthquake load is small and can be ignored. Since the shear due to the transverse earthquake load is negligible, the magnitude of the shear force in the web of the girder is directly related to the longitudinal moment at the top of the column resulting from the longitudinal earthquake load. Therefore, compare longitudinal moments at the top of the column from the longitudinal earthquake load and plastic hinging to determine the controlling condition for seismic design.

$(M_L)_{TOP} = 12,932$ kN-m (9,539 k-ft)   (see Section I9.3.1)

$(M_{OVRSTR.})_{TOP} = 17,184$ kN-m (12,675 k-ft)   (see Section I9.5)

$(M_L)_{TOP} < (M_{OVRSTR.})_{TOP}$

Since the longitudinal moment at the top of the column from the longitudinal earthquake load is less than the moment resulting from plastic hinging, use the elastic shear from the longitudinal earthquake load for the seismic design of the connection.

$V_{EQ} = V_{LEQ} = 165$ kN (37 kips)

I12.1.2 Slip Resistance

Per **Article 6.13.2.1.1**, slip-critical connections shall be proportioned to prevent slip under Load Combination Service II.

$V_{SERV. II} = V_{DC} + V_{DW} + 1.3V_{LL}$

$V_{SERV. II} = 470 + 89 + 1.3(517) = 1,231$ kN (277 kips)

In accordance with **Article 6.13.2.8**, the nominal slip resistance of a bolt in a slip-critical connection shall be taken as:

$R_n = K_h K_s N_s P_t$ **Eq. 6.13.2.8-1**

Assuming 24 mm (1 in.) diameter ASTM A 325M (A 325) bolts in standard holes, double shear, and Class B surface conditions,

$$R_n = \frac{1.0(0.5)(2)(205 \times 10^3)}{1,000} = 205 \text{ kN/bolt (46 kips/bolt)}$$

$$\text{No. of Bolts} = \frac{1,231}{205} = 6 \text{ bolts}$$

I12.1.3 Shear Resistance

I12.1.3.1 Design Force. Per **Article 6.5.5**, since seismic forces within the girders are based on the elastic moment at the top of the column and not on the formation of a plastic hinge, the connection may be assumed to behave as a bearing-type connection at the extreme event limit state.

TABLE I-14 Elastic seismic girder shears

	V_{LEQ} kN (kips)	V_{TEQ} kN (kips)
Interior Girder	165 (37.1)	2 (0.4)
Exterior Girder	2 (0.4)	11 (2.5)

$V_{EQ} < V_{LL}$, therefore, the extreme event limit state will not control.

As specified in **Article 6.13.2.1.1**, slip-critical connections shall also be designed for shear and bearing at the strength limit state. In accordance with **Article 6.13.1**, design the connection at the strength limit state for not less than the larger of

$$\frac{V_u + \varphi V_n}{2}$$

or

$$0.75\varphi V_n$$

$V_u = 1.25(470) + 1.5(89) + 1.75(517) = 1,626$ kN (366 kips)

In accordance with **Article 6.10.7.3.3b**, the nominal shear resistance for the interior web panel of a noncompact section is determined as follows:

From the preliminary design of the girders,

$f_u = \varphi_f F_y$, therefore,

$$V_n = RV_p \left[C + \frac{0.87(1-C)}{\sqrt{1 + \left(\frac{d_o}{D}\right)^2}} \right] \geq CV_p$$

Eq. 6.10.7.3.3b-2

for which,

$$R = \left[0.6 + 0.4 \left(\frac{F_r - f_u}{F_r - 0.75\varphi_f F_y} \right) \right]$$

Eq. 6.10.7.3.3b-3

$f_u = \varphi_f F_y$, therefore, $R = 0.6$

$$k = 5 + \frac{5}{\left(\frac{d_o}{D}\right)^2}$$

Eq. 6.10.7.3.3a-8

Since the design of the transverse stiffeners is not presented, take $d_o = 1,350$ mm (53.15 in.) for this example.

$$k = 5 + \frac{5}{\left(\frac{1,350}{1,372}\right)^2} = 10.16$$

$$1.10\sqrt{\frac{Ek}{F_y}} = 1.10\sqrt{\frac{200,000(10.16)}{345}} = 84.4$$

$$1.38\sqrt{\frac{Ek}{F_y}} = 1.38\sqrt{\frac{200,000(10.16)}{345}} = 105.9$$

$$\frac{D}{t_w} = \frac{1,372}{12} = 114.3$$

I-48

$$\frac{D}{t_w} > 1.38\sqrt{\frac{Ek}{F_y}}$$

Therefore,

$$C = \frac{1.52}{\left(\dfrac{D}{t_w}\right)^2}\left(\frac{Ek}{F_y}\right)$$

Eq. 6.10.7.3.3a-7

$$C = \frac{1.52}{(114.3)^2}\left[\frac{200,000(10.16)}{345}\right] = 0.685$$

$$\varphi V_n = 1.0(0.6)(0.58)(345)(1,372)(12)\left[0.685 + \frac{0.87(1-0.685)}{\sqrt{1+\left(\dfrac{1,350}{1,372}\right)^2}}\right] / 1,000$$

$\varphi V_n = 1,740$ kN (391 kips)

$$\frac{V_u + \varphi V_n}{2} = \frac{1,626 + 1,740}{2} = 1,683 \text{ kN (378 kips)}$$

$0.75\varphi V_n = 0.75(1,740) = 1,305$ kN (293 kips)

$$V_{DSGN} = \text{larger of } \frac{V_u + \varphi V_n}{2} \text{ and } 0.75\varphi V_n = 1,683 \text{ kN (378 kips)}$$

I12.1.3.2 Nominal Bolt Resistance. In accordance with **Article 6.13.2.7**, the nominal shear resistance of a high-strength bolt at the strength limit state in joints whose length between extreme fasteners measured parallel to the line of action of the force is less than 1,270 mm (50 in.) shall be taken as follows.
   Conservatively assuming bolt threads are included in the shear plane,

$$R_n = 0.38 A_b F_{ub} N_s$$

Eq. 6.13.2.7-2

$$R_n = \frac{0.38\pi(24)^2(830)(2)}{4(1,000)} = 285 \text{ kN/bolt (64 kips/bolt)}$$

$\varphi R_n = 0.8(285) = 228$ kN/bolt (51 kips/bolt)

$$\text{No. of bolts} = \frac{1,683}{228} = 7.4 \text{ bolts} \rightarrow \text{ use 8 bolts}$$

I12.1.4 Bearing Resistance

   Check bearing on the connected material in accordance with **Article 6.13.2.9**.
   Bearing on web of girder controls.

Minimum spacing = 3d = 3(24) = 72 mm (2.83 in.)

$L_c = 72 - 26 = 46$ mm (1.81 in.)

2d = 2(24) = 48 mm (1.89 in.)

$L_c < 2d$, therefore,

$R_n = 1.2L_ctF_u$ **Eq. 6.13.2.9-2**

$$R_n = \frac{1.2(46)(12)(485)}{1,000} = 321 \text{ kN/bolt (72 kips/bolt)}$$

$\varphi R_n = 0.8(321) = 257 \text{ kN/bolt (58 kips/bolt)}$

$$R_u = \frac{V_{DSGN}}{\text{No. of bolts}} = \frac{1,683}{8} = 210 \text{ kN/bolt (47 kips/bolt)}$$

$\varphi R_n > R_u \quad \therefore \text{ OK}$

I12.1.5 Size Angles

Assume $F_y = 250$ MPa (36 ksi) for angles.

With the aid of design tables or through a series of short hand calculations, one can determine that an angle thickness of 12.7 mm ($^1/_2$ in.) will satisfy design requirements. In order to meet minimum edge distance requirements and still satisfy entering and tightening clearances, provide 127-mm (5-in.) angle legs.

Space bolts at the maximum spacing allowed for sealing bolts as specified in **Article 6.13.2.6.2**, but do not exceed a connection length of 1,270 mm (50 in.), otherwise, the bolt resistance should be reduced in accordance with **Article 6.13.2.7**.

$s \le (100 + 4.0t) \le 175$ **Eq. 6.13.2.6.2-1**

$s \le [100 + 4(12.7)] = 150.8$ mm (6.03 in.)

$s \le 150.8$ mm (6.03 in.) $\rightarrow$ say $s = 150$ mm (6 in.)

connection length $= 150(8 - 1) = 1,050$ mm (42 in.) $< 1,270$ mm (50 in.) $\quad \therefore \text{ OK}$

I12.2 Flange Splice Plates

Flange splice plates provide moment continuity for the girders. These plates also transfer torsion to the pier cap produced by the difference in moments in the girders at either side of the pier cap.

I12.2.1 Girder Moments Due to Unfactored Loadings

Unfactored moments in the girders at the centerline of the pier cap are given in Table I-15.

TABLE I-15   Unfactored girder moments at centerline of pier

	M_{DC1}[a] kN-m (k-ft)	M_{DC2}[a] kN-m (k-ft)	M_{DW}[a] kN-m (k-ft)	M_{LL}[b] kN-m (k-ft)	M_{EQ}[b] kN-m (k-ft)
Interior Girder	2827 (2085)	663 (489)	628 (463)	2634 (1943)	3242 (2391)
Exterior Girder	2538 (1872)	663 (489)	445 (328)	3025 (2231)	1733 (1278)

[a] From line girder analysis
[b] From computer model

I-50

I12.2.2 Size Flange Plates

I12.2.2.1 Design Force. Design flange splice plates for the Extreme Event I or Strength I limit state.

$M_{EQ} < 1.75M_{LL}$, therefore, extreme event limit state will not control.

Since the bolted double-angle connection to the web of the girder is assumed to possess little-to-no rotational restraint, moments at the point of splice are resisted entirely by the flange splice plates. Therefore, in accordance with **Article 6.13.1**, design splice plates at the strength limit state for a moment not less than the larger of

$$\frac{M_u + \varphi M_n}{2}$$

or

$$0.75\varphi M_n$$

Since moments are greatest at the centerline of the cap beam, it is conservative to design for the factored moment at the centerline of the pier cap instead of for the moments in the girders at the face of the pier cap.

$(M_{CL})_{\text{INT. BM.}} = 1.25(2,827 + 663) + 1.5(628) + 1.75(2,634) = 9,914$ kN-m (7,313 k-ft)

$(M_{CL})_{\text{EXT. BM.}} = 1.25(2,538 + 663) + 1.5(445) + 1.75(3,025) = 9,963$ kN-m (7,349 k-ft)

$(M_{CL})_{\text{EXT. BM.}} > (M_{CL})_{\text{INT. BM.}}$ $\therefore$ $M_u = 9,963$ kN-m (7,349 k-ft)

Slab reinforcing has been neglected in computing section properties for the design of the girders for negative moment. Therefore,

$$\varphi M_n = \varphi F_n S_{nc}$$

Where

S_{nc} = section modulus for noncomposite steel section (mm³) = I_{nc}/c
$I_{nc} = 2.180 \times 10^{10}$ mm⁴ (52,375 in⁴) (conservatively calculated for the gross section)
$$\varphi M_n = \varphi F_n S_{nc} = \left[\frac{(1.0)345(2.180 \times 10^{10})}{(1472/2)}\right] / 1,000^2 = 10,219 \text{ kN-m (7,538 k-ft)}$$

Compute design moment.

$$\frac{M_u + \varphi M_n}{2} = \frac{9,963 + 10,219}{2} = 10,091 \text{ kN-m (7,443 k-ft)}$$

$0.75\varphi M_n = 0.75(10,219) = 7,664$ kN-m (5,653 k-ft)

$$M_{DSGN} = \text{larger of } \frac{M_u + \varphi M_n}{2} \text{ and } 0.75\varphi M_n = 10,091 \text{ kN-m (7,443 k-ft)}$$

To find the force in the flange splice plates, divide the design moment by the distance between the centers of the splice plates. Since the thickness of the plates is not yet known, divide the design moment by the cap beam depth to determine the force in the flange splice plates.

$P_{DSGN} = 10,091/1.472 = 6,855$ kN (1,541 kips)

I12.2.2.2 Plate Thickness. Design for tension in accordance with **Article 6.13.5.2**.
For gross section yield,

$$\phi P_n = \phi_y F_y A_g = \phi_y F_y bt \qquad \text{Eq. 6.8.2.1-1}$$

$$\phi P_n \geq P_{DSGN}$$

Substituting **Equation 6.8.2.1-1** for ϕP_n and solving for t gives

$$t \geq \frac{P_{DSGN}}{\phi_y F_y b} = \frac{6,855(1,000)}{0.95(345)(380)} = 55 \text{ mm (2.17 in.)}$$

$$t \geq 55 \text{ mm (2.17 in.)}$$

For net section fracture,

$$\phi P_n = \phi_u F_u A_n U \qquad \text{Eq. 6.8.2.1-2}$$

Per **Article 6.13.5.2**,

$$A_n \leq 0.85 A_g$$

Assuming four 24-mm (1-in.) diameter bolts per section,

$$A_n = [b - 4(28)]t \leq 0.85bt$$

Dividing both sides of the inequality by t gives

$$[380 - 4(28)] = 268 \text{ mm (10.55 in.)} < 0.85(380) = 323 \text{ mm (12.72 in.)},$$

therefore, A_n controls

$$\phi P_n = \phi_u F_u [b - 4(28)] t U$$

$$\phi P_n \geq P_{DSGN}$$

Substituting for ϕP_n and solving for t gives

$$t \geq \frac{P_{DSGN}}{\phi_u F_u [b - 4(28)]U} = \frac{6,855(1,000)}{0.8(485)[380 - 4(28)]1.0} = 65.9 \text{ mm (2.59 in.)}$$

$$t \geq 65.9 \text{ mm (2.59 in.)} \rightarrow \text{use } t = 70 \text{ mm (2.75 in.)}$$

I12.2.3 Design Connection to Girder Flanges

As specified in **Article 6.13.6.1.4a**, bolted splices for flexural members shall be designed using slip-critical connections.

I12.2.3.1 Slip Resistance. Per **Article 6.13.2.1.1**, slip-critical connections shall be proportioned to prevent slip under Load Combination Service II.

$$(M_{SERV. II})_{INT. BM.} = 2,827 + 663 + 628 + 1.3(2,634) = 7,542 \text{ kN-m (5,563 k-ft)}$$

$$(M_{SERV. II})_{EXT. BM.} = 2,538 + 663 + 445 + 1.3(3,025) = 7,579 \text{ kN-m (5,590 k-ft)}$$

$$(M_{SERV. II})_{EXT. BM.} > (M_{SERV. II})_{INT. BM.} \quad \therefore \ M_{SERV. II} = 7,579 \text{ kN-m (5,590 k-ft)}$$

$$P_{SERV. II} = 7,579/1.472 = 5,149 \text{ kN (1,158 kips)}$$

In accordance with **Article 6.13.2.8**, the nominal slip resistance of a bolt in a slip-critical connection shall be taken as:

$$R_n = K_h K_s N_s P_t$$ **Eq. 6.13.2.8-1**

Assuming 24-mm (1-in.) diameter ASTM A 325M (A 325) bolts in standard holes, single shear, and Class B surface conditions,

$$R_n = \frac{1.0(0.5)(1)(205 \times 10^3)}{1,000} = 102.5 \text{ kN/bolt (23.0 kips/bolt)}$$

$$\text{No. of Bolts} = \frac{5,149}{102.5} = 50.2 \text{ bolts} \rightarrow \text{ use 13 rows of 4 bolts} = 52 \text{ bolts}$$

I12.2.3.2 Shear Resistance. In accordance with **Article 6.13.2.7**, the nominal shear resistance of a high-strength bolt at the strength limit state in joints whose length between extreme fasteners measured parallel to the line of action of the force is less than 1,270 mm (50 in.) shall be taken as follows.

For a 50-mm (2-in.) thick girder flange, bolt threads will be excluded from the shear plane. Therefore,

$$R_n = 0.48 A_b F_{ub} N_s$$ **Eq. 6.13.2.7-1**

$$R_n = \frac{0.48 \pi (24)^2 (830)(1)}{4(1,000)} = 180.2 \text{ kN/bolt (40.5 kips/bolt)}$$

$$\varphi R_n = 0.8(180.2) = 144.2 \text{ kN/bolt (32.4 kips/bolt)}$$

$$\text{No. of bolts} = \frac{6,855}{144.2} = 47.5 \text{ bolts} \rightarrow \text{ say 48 bolts} < 52 \text{ bolts} \quad \therefore \text{ does not control}$$

I12.2.3.3 Bearing Resistance. Check bearing on the connected material in accordance with **Article 6.13.2.9**.

Bearing on flange of girder controls.

From **Table 6.13.2.6.6-1**, for a 24-mm (1-in.) diameter bolt and a rolled- or gas-cut edge, minimum end distance equals 30 mm (1.25 in.). Therefore,

$$L_c = 30 - 26/2 = 17 \text{ mm (0.67 in.)}$$

$$2d = 2(24) = 48 \text{ mm (1.89 in.)}$$

$L_c < 2d$, therefore,

$$R_n = 1.2 L_c t F_u$$ **Eq. 6.13.2.9-2**

$$R_n = \frac{1.2(17)(50)(485)}{1,000} = 494.7 \text{ kN/bolt (111.2 kips/bolt)}$$

$$\varphi R_n = 0.8(494.7) = 395.8 \text{ kN/bolt (89.0 kips/bolt)}$$

$$R_u = \frac{P_{DSGN}}{\text{No. of bolts}} = \frac{6,855}{52} = 132 \text{ kN/bolt (29.7 kips/bolt)}$$

$$\varphi R_n > R_u \quad \therefore \text{ OK}$$

I12.2.4 Design Connection to Cap Beam

I12.2.4.1 Design Force. Design the connection for the transfer of torsion to the cap beam resulting from the difference in girder moments. Torsion is transferred to the pier cap through the flange splice plates and their connection to the pier cap as shown in Figure I-6. From Figure I-6, the design force for the connection can be taken as follows.

$V = T/d$

Where

   d = depth of pier cap (m)

   The torsion transferred to the pier cap through the flange splice plates can be taken as the change in torque at the girder location from the torsion diagram for the pier cap. Unfactored torsion diagrams for the pier cap for earthquake loading and the live load case that produces the maximum difference in girder moment (and, consequentially, maximum torsion transfer to the pier cap) from one side to another of the pier cap are given in Figure I-25. The pier cap sees no torsion from the transverse earthquake load or dead load, therefore, torsion diagrams are not shown in Figure I-25 for these loads.
   For the Extreme Event I limit state,

$V_{EXTR.\ EVENT\ I} = T_{EQ}/d = 5,493/1.472 = 3,732$ kN (839 kips)

   In accordance with **Article 6.13.1**, at the strength limit state, the connection shall be designed for not less than the larger of

$$\frac{V_u + \varphi V_n}{2}$$

a) Longitudinal Earthquake Load

b) Live Load
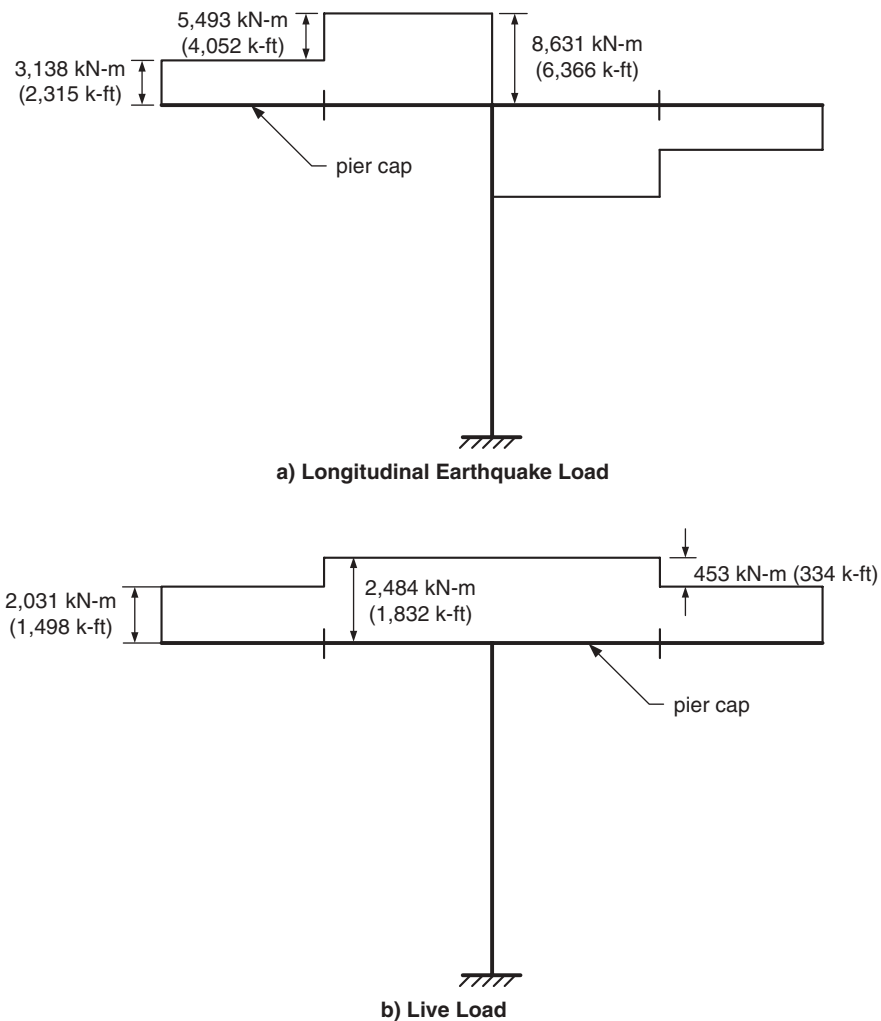
Figure I-25.   Unfactored torsion diagrams for pier cap.

I-54

or

$0.75\varphi V_n$

$V_u = 1.75T_{LL}/d = 1.75(2,031)/1.472 = 2,415$ kN (543 kips)

Base the factored resistance on the tensile strength of the flange splice plates in accordance with **Article 6.13.5.2**. For gross section yield,

$\varphi P_n = \varphi_y F_y A_g$ **Eq. 6.8.2.1-1**

$\varphi P_n = \dfrac{0.95(345)(380)(70)}{1,000} = 8,718$ kN (1,960 kips)

For net section fracture,

$\varphi P_n = \varphi_u F_u A_n U$ **Eq. 6.8.2.1-2**

$\varphi P_n = \dfrac{0.8(485)[380 - 4(28)](70)(1.0)}{1,000} = 7,279$ kN (1,636 kips) $\leftarrow$ **controls**

The girder moment corresponding to the factored resistance of the flange splice plates is as follows:

$M = \varphi P_n(d + t_{SPLICE\ PL.}) = 7,279(1.472 + 0.070) = 11,224$ kN-m (8,279 k-ft)

For the loading that produced the live load torsion diagram shown in Figure I-25, the maximum unfactored negative moment in the exterior girder is 2,224 kN-m (1,640 k-ft). This corresponds to an increase in moment at the exterior girder of

$11,224/2,224 = 5.047$

Since the torsion in the pier cap results from the moments in the girder, the torsion in the pier cap at this location is increased by the same factor. Therefore, when the factored resistance of the flange splice plates is reached, the corresponding torsion in the pier cap will be as follows:

$T = 5.047(2,031) = 10,250$ kN-m (2,304 k-ft)

$\varphi V_n = T/d = 10,250/1.472 = 6,963$ kN (1,565 kips)

$\dfrac{V_u + \varphi V_n}{2} = \dfrac{2,415 + 6,963}{2} = 4,689$ kN (1,054 kips)

$0.75\varphi V_n = 0.75(6,963) = 5,222$ kN (1,174 kips)

$V_{STR.\ I} =$ larger of $\dfrac{V_u + \varphi V_n}{2}$ and $0.75\varphi V_n = 5,222$ kN (1,174 kips)

$V_{EXTR.\ EVENT\ I} = 3,732$ kN (839 kips) $< V_{STR.\ I} = 5,222$ kN (1,174 kips),

therefore, $V_{DSGN} = 5,222$ kN (1,174 kips)

I12.2.4.2 Shear Resistance. For a 24-mm (1-in.) diameter ASTM A 325M (A 325) bolt and a connection length less than 1,270 mm (50 in.),

$\varphi R_n = 144.2$ kN/bolt (32.4 kips/bolt) (see Section I12.2.3.2)

However, since the width of the pier cap is 2,280 mm (89.76 in.), the connection length will be greater than 1,270 mm (50 in.). Therefore, in accordance with **Article 6.13.2.7**, reduce the bolt resistance by a factor of 0.80.

$\varphi R_n = 0.8(144.2) = 115.4$ kN/bolt (25.9 kips/bolt)

No. of Bolts $= \dfrac{1,794}{102.5} = 17.5$ bolts $\rightarrow$ say 18 bolts < 46 bolts $\therefore$ does not control

I12.2.4.3 Slip Resistance. Per **Article 6.13.2.1.1**, slip-critical connections shall be proportioned to prevent slip under Load Combination Service II.

$V_{SERV. II} = 1.3 T_{LL}/d = 1.3(2,031)/1.472 = 1,794$ kN (403 kips)

Assuming 24-mm (1-in.) diameter ASTM A 325M (A 325) bolts in standard holes and Class B surface conditions,

$R_n = 102.5$ kN/bolt (23.0 kips/bolt)   (see Section I12.2.3.1)

No. of Bolts $= \dfrac{1,794}{102.5} = 17.5$ bolts $\rightarrow$ say 18 bolts < 46 bolts $\therefore$ does not control

I12.2.4.4 Bearing Resistance. Bearing on flange plate of cap beam controls.

Minimum spacing $= 3d = 3(24) = 72$ mm (2.83 in.)

$L_c = 72 - 26 = 46$ mm (1.81 in.)

$2d = 2(24) = 48$ mm (1.89 in.)

$L_c < 2d$, therefore,

$R_n = 1.2 L_c t F_u$ **Eq. 6.13.2.9-2**

$R_n = \dfrac{1.2(46)(30)(485)}{1,000} = 803$ kN/bolt (181 kips/bolt)

$\varphi R_n = 0.8(803) = 642$ kN/bolt (144 kips/bolt)

$R_u = \dfrac{V_{DSGN}}{\text{No. of bolts}} = \dfrac{5,222}{46} = 113.5$ kN/bolt (25.5 kips/bolt)

$\varphi R_n > R_u$ $\therefore$ OK

I12.3 Girder-to-Cap Beam Connection Details

Refer to Figure I-26 for final girder-to-cap beam connection details.

I13 COLUMN-TO-CAP BEAM CONNECTION

The transfer of forces between the column and cap beam is achieved through the use of shear studs located as shown in Figure I-27.
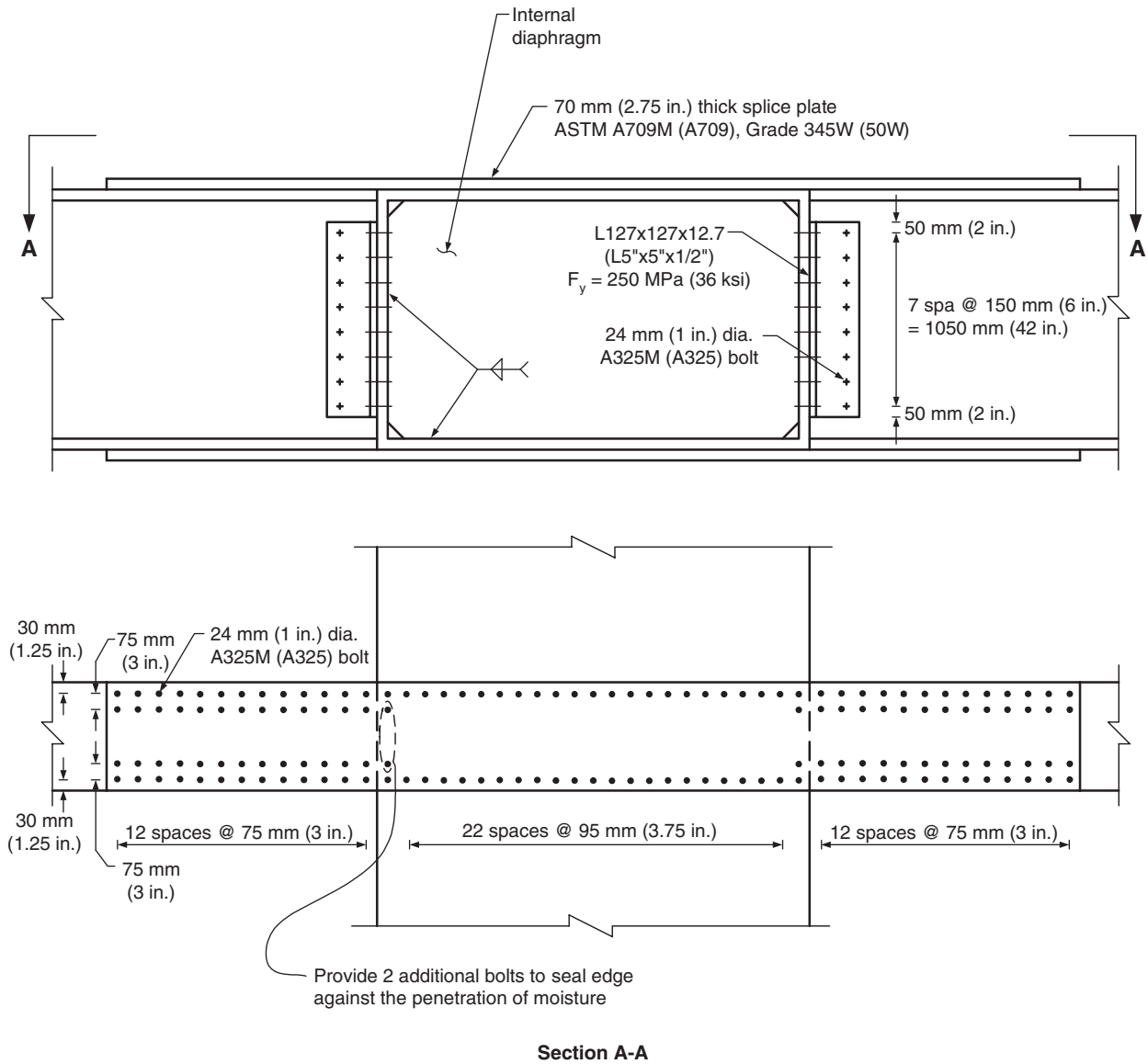
Figure I-26.   Girder-to-cap beam connection details.

I13.1 Shear Studs on Bottom Flange Plate

Shear studs located on the bottom flange plate of the cap beam shall be designed to transfer horizontal shear between the column and cap beam.

I13.1.1 Strength Design

I13.1.1.1 Design Force. Design these studs for the maximum horizontal shear, H, developed at the top of the column.

$H_{\text{EXTR. EVENT I}} = H_{EQ} = 5,349$ kN (1,203 kips)   (see Section I9.6.1)

$H_{\text{STR. I}} = 1.75(H_{LL}) = 1.75(506) = 886$ kN (199 kips)   (from computer model)

$H_{\text{EXTR. EVENT I}} > H_{\text{STR. I}}$ ∴ $H_{DSGN} = 5,349$ kN (1,203 kips)
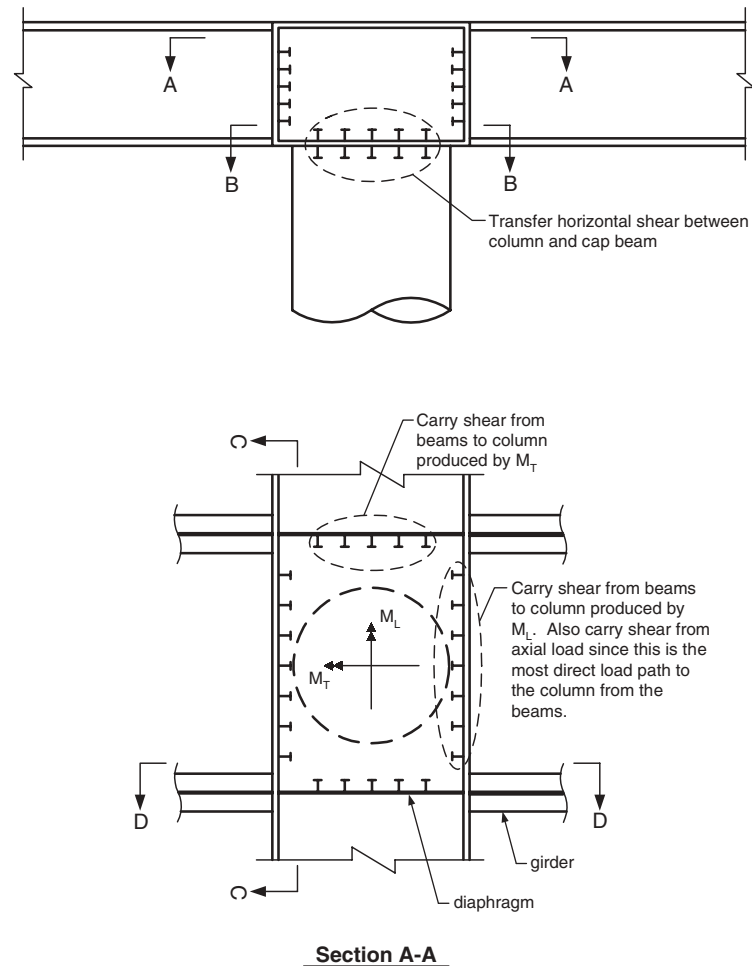
Section A-A
See Figures I-28, I-29, and I-30 for Sections B-B, C-C, and D-D, respectively.

Figure I-27.   Column-to-cap beam connection.

Notice that due to the symmetric geometry of the structure, dead loads do not produce shear in the column.

I13.1.1.2 Nominal Shear Resistance. In accordance with **Article 6.10.7.4.4c**, the nominal shear resistance for one shear stud shall be taken as

$$Q_n = 0.5A_{sc}\sqrt{f'_c E_c} \le A_{sc}F_u$$

<div align="right">**Eq. 6.10.7.4.4c-1**</div>

Assuming 25-mm (1-in.) diameter studs,

$A_{sc} = \pi(25)^2/4 = 491$ mm^2 (0.76 in^2)

$E_c = 4,800\sqrt{f'_c} = 4800\sqrt{28} = 25,399$ MPa (3,684 ksi)

$A_{sc}F_u = 491(415)/1,000 = 203.8$ kN/stud (45.8 kips/stud)

$Q_n = \dfrac{0.5(491)\sqrt{28(25,399)}}{1,000} = 207$ kN/stud (46.5 kips/stud) > 203.8 kN/stud (45.8 kips/stud), therefore,

$Q_n = 203.8$ kN/stud (45.8 kips/stud)

As specified in **Article 1.3.2.1**, $\varphi_{sc} = 1.0$ for extreme event limit states.

I-58

$\varphi_{sc}Q_n = 1.0(203.8) = 203.8$ kN/stud (45.8 kips/stud)

No. of studies = 5,349/203.8 = 26.2 studs $\rightarrow$ use 27 studs

Per **Article 6.10.7.4.1a**, the ratio of the height to the diameter of a shear stud shall not be less than 4.

h/d $\geq$ 4

h $\geq$ 4d = 4 (25) = 100 mm (4 in.)

I13.1.2 Fatigue Design

Fatigue of the shear studs is not a concern since the live load shear is considerably less than the design level shear force due to the earthquake load.

I13.1.3 Shear Stud Layout

For strength, provide a minimum of twenty-seven 25-mm (1-in.) diameter shear studs at least 100 mm (4 in.) in length on both the top and bottom side of the bottom flange plate of the cap beam. Refer to Figure I-28 for the shear stud layout on the bottom flange plate of the cap beam.
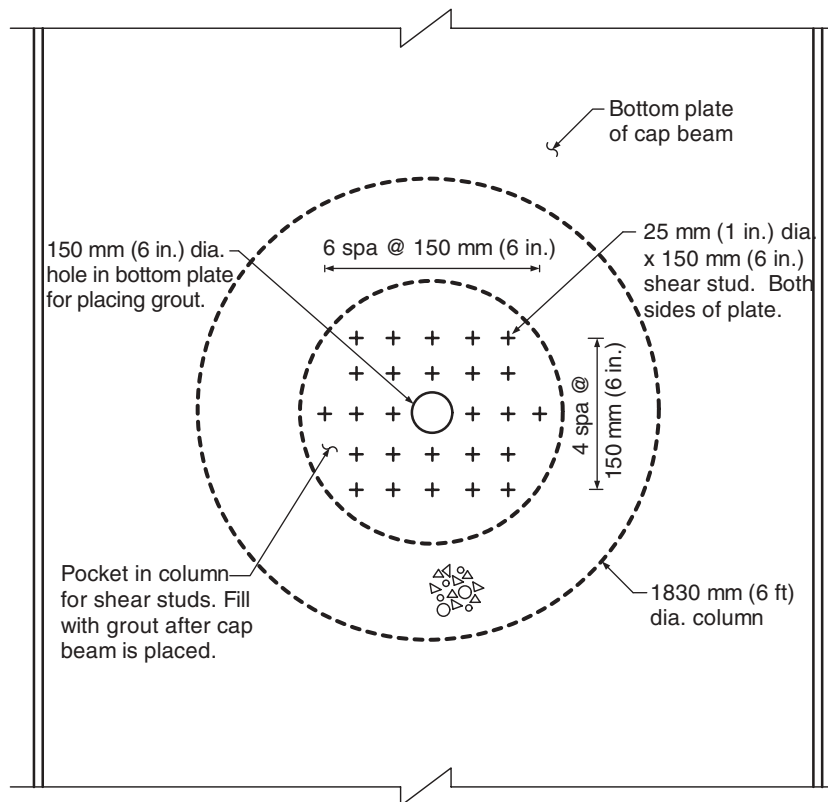
Section B-B
See Figure I-27 for location

Figure I-28.   Stud layout for bottom flange plate of cap beam.

I13.2 Shear Studs on Web Plates of Cap Beam

Shear studs located on the web plates of the cap beam shall be designed to transfer shear from the girder webs to the top of the column. These studs shall be designed for the shear originating from the longitudinal moment at the top of the column. In addition, since the most direct load path from the beams to the column is through the web plates of the cap beam (as opposed to the diaphragm plates), these studs shall also be designed to carry the shear resulting from the axial load in the column. These shear forces are shown in Figure I-8 and their magnitude per web plate is determined as follows:

$$V_{AXIAL} = P / 2$$

$$V_{LONG.\ MOM.} = M_L / w$$

Where

w = width of pier cap less web plates (m) = 2.220 m (7.28 ft)

I13.2.1 Strength Design

I13.2.1.1 Shear Forces for Extreme Event I Limit State. Shear due to axial dead load.

$$V_{DL} = P_{DL} / 2$$

$$P_{DL} = 1.25P_{DC} + 1.5P_{DW}$$

$$P_{DL} = 1.25(3,880) + 1.5(608) = 5,762 \text{ kN (1,295 kips)}$$

see Section I9.1 for P_{DC} & P_{DW}

$$V_{DL} = 5,762/2 = 2,881 \text{ kN (648 kips)}$$

Shear due to longitudinal moment at the top of the column from earthquake loading.

$$V_{EQ} = (M_L)_{EQ} / w$$

In accordance with **Article 3.10.9.4.1**, $(M_L)_{EQ}$ shall be taken as the lesser of

$$M_{MOD.} = M_{ELASTIC} / R$$

or

$$M_{OVRSTR.}$$

Per **Article 3.10.8**,

$$M_{ELASTIC} = 1.0(12,932) + 0.3(0.0) = 12,932 \text{ kN-m (9,539 k-ft)}$$

See Table I-6 for values.
From **Table 3.10.7.1-2**, for a column-to-cap beam connection, R = 1.0.

$$M_{MOD.} = 12,932/1.0 = 12,932 \text{ kN-m (9,539 k-ft)}$$

$$M_{OVRSTR.} = 17,184 \text{ kN-m (12,675 k-ft)} \qquad \text{(see Section I9.5)}$$

$(M_L)_{EQ}$ = lesser of $M_{MOD.}$ and $M_{OVRSTR.}$ = 12,932 kN-m (9,539 k-ft)

$V_{EQ} = 12,932/2.220 = 5,825$ kN (1,310 kips)

$V_{EXTR.\ EVENT\ I} = V_{DL} + V_{EQ} = 2,881 + 5,825 = 8,706$ kN (1,957 kips)

I13.2.1.2 Shear Forces for Strength I Limit State. Shear force for Load Case 1 (maximum axial load)

$P_{LL} = 1.75(2,465) = 4,314$ kN (970 kips)   (from Table I-7)

   Corresponding longitudinal moment at the top of the column

$(M_L)_{LL} = 1.75(25) = 44$ kN-m (32 k-ft)   (from Table I-7)

$(V_{STR.\ 1})_{LC1} = (5,762 + 4,314)/2 + (44/2.220) = 5,058$ kN (1,137 kips)

   Shear force for Load Case 2 (maximum longitudinal moment)

$(M_L)_{LL} = 1.75(2,489) = 4,356$ kN-m (3,213 k-ft)   (from Table I-7)

   Corresponding axial load at the top of the column

$P_{LL} = 1.75(1,218) = 2,132$ kN (479 kips)   (from Table I-7)

$(V_{STR.\ 1})_{LC2} = (5,762 + 2,132)/2 + (4,356/2.220) = 5,909$ kN (1,328 kips) **controls**

   Determine controlling limit state for strength design.

$\varphi_{sc} = 0.85$ for strength limit state

$V_{STR.\ I} / \varphi_{sc} = 5,909/0.85 = 6,952$ kN (1,563 kips) $< V_{EXTR.\ EVENT\ I} = 8,706$ kN (1,957 kips), therefore,

$V_{DSGN} = V_{EXTR.\ EVENT\ I} = 8,706$ kN (1,957 kips)

I13.2.1.3 Nominal Shear Resistance. Assuming 25-mm (1-in.) diameter shear studs,

$\varphi_{sc}Q_n = 203.8$ kN/stud (45.8 kips/stud)   (see Section I13.1.1.2)

No. of studs = 8,706/203.8 = 42.7 studs $\rightarrow$ use 43 studs

I13.2.2 Fatigue Design

I13.2.2.1 Live Load Shear Force Range. Shear force range for Load Case 1 (maximum axial load)

$(\Delta P)_{FATIGUE} = 0.75(1.15)(314) = 271$ kN (61 kips)   (from computer model)

   Corresponding longitudinal moment at the top of the column

$(\Delta M_L)_{FATIGUE} = 0.75(1.15)(52) = 45$ kN-m (33 k-ft)   (from computer model)

$(V_{sr})_{LC1} = (271)/2 + (45/2.220) = 156$ kN (35 kips)

   Shear force range Load Case 2 (maximum longitudinal moment)

$(\Delta M_L)_{FATIGUE} = 0.75(1.15)(461) = 398$ kN-m (294 k-ft)   (from computer model)

Corresponding axial load at the top of the column

$(\Delta P)_{FATIGUE} = 0.75(1.15)(203) = 175$ kN (39 k-ft)   (from computer model)

$(V_{sr})_{LC2} = (175)/2 + (398/2.220) = 267$ kN (60 k-ft) $\leftarrow$ **controls**

I13.2.2.2 Fatigue Resistance. In accordance with **Article 6.10.7.4.2**, the fatigue resistance of an individual shear con-
nector, Z_r, shall be taken as

$Z_r = \alpha d^2 \geq 38d^2/2$ **Eq. 6.10.7.4.2-1**

For simplification of calculations,

$$Z_r = \frac{38d^2}{2} = \frac{38(25)^2}{2(1,000)} = 11.9 \text{ kN/stud (2.7 kips/stud)}$$

No. of studs $= 267/11.9 = 22.4$ studs $\rightarrow$ say 23 studs < 43 provided, therefore, does not control.

I13.2.3 Shear Stud Layout

For strength, provide a minimum of forty-three 25-mm (1-in.) diameter shear studs at least 100 mm (4 in.) in length
on each web plate of the cap beam within the joint region of the pier cap. Refer to Figure I-29 for the shear stud lay-
out on the web plates of the cap beam.

I13.3 Shear Studs on Diaphragm Plates

Shear studs located on the diaphragm plates adjacent to the joint region within the cap beam shall be designed to
transfer shear from the girder webs to the top of the column. These studs shall be designed for the shear originating
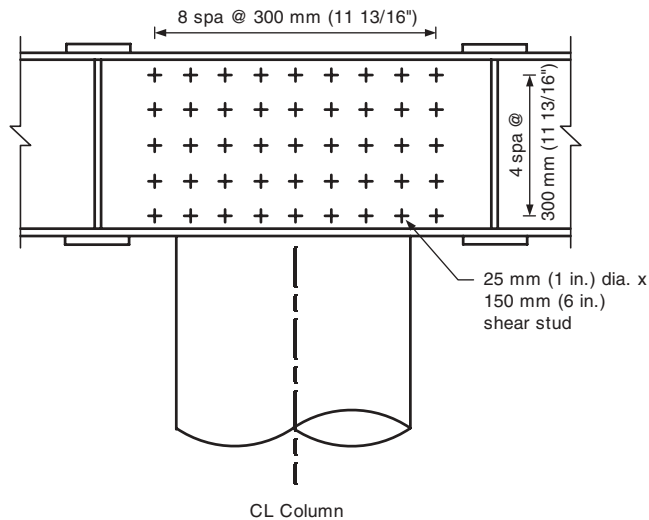
Section C-C
See Figure I-27 for location

Figure I-29.   Stud layout for web plates of cap beam.

from the transverse moment at the top of the column. This shear force is shown in Figure I-9 and can be determined as follows:

$V_{\text{TRANSV. MOM.}} = M_T / S$

Where

   S = spacing between interior beams (m) = 3.050 m (10 ft)

I13.3.1 Strength Design

I13.3.1.1 Shear Force for Extreme Event I Limit State. Shear due to transverse moment at the top of the column from earthquake loading.

$V_{EQ} = (M_T)_{EQ} / S$

$(M_T)_{EQ} = $ lesser of $M_{\text{MOD.}}$ and $M_{\text{OVRSTR.}}$

$M_{\text{MOD.}} = M_{\text{ELASTIC}} / R$

$M_{\text{MOD.}} = [1.0(967) + 0.3(0.0)]/1.0$ (moment values from Table I-6)

$M_{\text{MOD.}} = 967$ kN-m (713 k-ft)

$M_{\text{OVRSTR.}} = 17,184$ kN-m (12,675 k-ft)   (see Section I9.5)

$(M_T)_{EQ} = $ lesser of $M_{\text{MOD.}}$ and $M_{\text{OVRSTR.}} = 967$ kN-m (713 k-ft)

$V_{EQ} = 967/3.05 = 317$ kN (71 kips)

$V_{\text{EXTR. EVENT I}} = V_{EQ} = 317$ kN (71 kips)

I13.3.1.2 Shear Force for Strength I Limit State.

$(M_T)_{LL} = 1.75(3,417) = 5,980$ kN-m (4,411 k-ft)   (from Table I-7)

$V_{\text{STR. I}} = V_{LL} = 5,980 / 3.05 = 1,961$ kN (441 kips) ← **controls**

I13.3.1.3 Nominal Shear Resistance. Assuming 25-mm (1-in.) diameter shear studs,

$Q_n = 203.8$ kN/stud (45.8 kips/stud)   (see Section I13.1.1.2)

$\varphi_{sc}Q_n = 0.85(203.8) = 173.2$ kN/stud (38.9 kips/stud)

No. of studs = 1,961/173.2 = 11.3 studs   →   say 12 studs

I13.3.2 Fatigue Design

   Live Load Shear Force Range.

$(\Delta M_T)_{\text{FATIGUE}} = 0.75(1.15)(1,037) = 894$ kN-m (659 k-ft)   (from computer model)

$V_{sr} = 894 / 3.05 = 293$ kN (66 kips)

Fatigue Resistance

Z_r = 11.9 kN/stud (2.7 kips/stud)   (see Section I13.2.2.2)

No. of studs = 293/11.9 = 24.6 studs → use 25 studs

I13.3.3 Shear Stud Layout

For fatigue, provide a minimum of twenty-five 25-mm (1-in.) diameter shear studs at least 100 mm (4 in.) in length on each diaphragm on each side of the joint region. Refer to Figure I-30 for the shear stud layout on the diaphragm plates adjacent to the joint region within the pier cap.
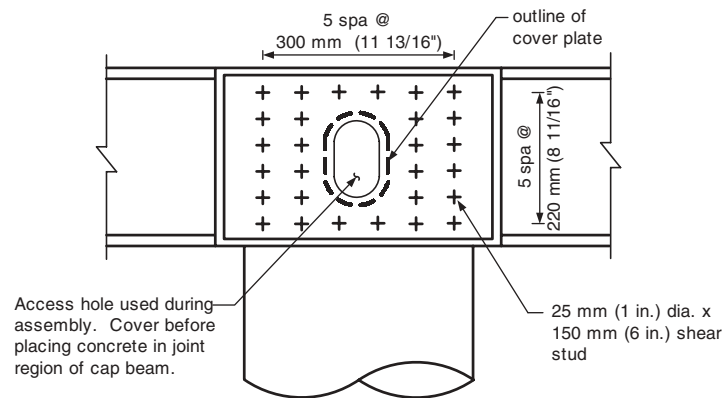
Section D-D
See Figure I-27 for location

Figure I-30.   Shear stud layout for diaphragm plates adjacent to joint region.

Abbreviations used without definitions in TRB publications:

AASHO   American Association of State Highway Officials
AASHTO   American Association of State Highway and Transportation Officials
APTA   American Public Transportation Association
ASCE   American Society of Civil Engineers
ASME   American Society of Mechanical Engineers
ASTM   American Society for Testing and Materials
ATA   American Trucking Associations
CTAA   Community Transportation Association of America
CTBSSP   Commercial Truck and Bus Safety Synthesis Program
FAA   Federal Aviation Administration
FHWA   Federal Highway Administration
FMCSA   Federal Motor Carrier Safety Administration
FRA   Federal Railroad Administration
FTA   Federal Transit Administration
IEEE   Institute of Electrical and Electronics Engineers
ITE   Institute of Transportation Engineers
NCHRP   National Cooperative Highway Research Program
NCTRP   National Cooperative Transit Research and Development Program
NHTSA   National Highway Traffic Safety Administration
NTSB   National Transportation Safety Board
SAE   Society of Automotive Engineers
TCRP   Transit Cooperative Research Program
TRB   Transportation Research Board
U.S.DOT   United States Department of Transportation